Improvement of Strength and Quality of Sheared Edge in Punching of High Strength Steel Sheets

March 2014

DOCTOR OF ENGINEERING

Purwo Kadarno

Toyohashi University of Technology

Abstract

In order to achieve better global environment, the reduction of CO_2 emission of automobiles is intensively required. It is convinced that the body mass has a strong influence to CO_2 emission of the automobiles, therefore the reduction of weight of the body components has become a high priority in vehicle development. Although the application of aluminium and magnesium alloy sheets to the automobile parts is attractive for the reduction of the automobile weight, high cost and small formability are crucial problems, and thus the industry still has a great interest in steel sheets. The strength of high tensile strength steel sheets remarkably increases and ultra-high tensile strength steel sheets more than 1 GPa have been developed.

Body-in-white parts are generally punched to make many holes for joining, paint removing, attachment, reduction in weight, etc. In the punching of the high strength steel sheets, large tool wear and rough sheared edges becomes problems. Although the static strength of high strengths steel sheets is almost proportional with the strength of the sheet, the increase in fatigue strength becomes gradually small. In addition, onset and progress of fatigue cracks of the punched high strength steel sheets are accelerated around holes due to concentration of stress, particularly for rough fracture surface and sharp burr of the sheared edge. Therefore, the improvement of the quality of the sheared edge of punched sheets is useful for increasing the fatigue life.

In the present study, the special shape of the punch was developed and the clearance ratio was adjusted for improving the quality of the sheared edge in punching of ultra-high strength steel sheets. By the slight clearance punching, the tensile stress during the punching was reduced, and thus the onset of cracks was delayed. However, sharp edges of the punch and die tend to chip. The punch having a small round edge was developed to prevent the chipping of the tools and delay the onset of crack by relaxing concentration of deformation, thus the burnished surfaces became considerably large. The delayed fracture was prevented and the fatigue strength was improved by the increase in compressive residual stress for the punch having the small round edge.

The effect of punch shape and clearance ratio on the quality of the sheared edge in the punching of inclined ultra-high strength steel was also investigated. In the punching of the inclined sheet, the contact between the sheet and punch becomes gradual because of touch from the bottom edge of the punch, and thus the sheared portion tends to bend in the latter half of punching. Punches having taper and curved head were developed to improve the quality of the sheared edge in the punching of inclined ultra-high strength steel sheet. The asymmetric punching clearance ratio was also applied to eliminate the burr and the secondary burnished in the sheared edge. The quality of the sheared edge in the punching process of inclined ultra-high strength steel sheet was improved by adjusting the punching clearance ratio and the eccentricity of the punch.

Although the fatigue strength was improved by the quality of the sheared edge, the improvement was not enough to extend the applicable range of ultra-high strength steel sheets. The concentration of stress around the punched hole was retrieved by increasing the thickness around the hole edge, and thus the fatigue strength might be improved. In the present study, the effect of thickening of hole edge on the fatigue strength of the punched high strength steel sheets was examined. A hole flanging process using a step die was performed to thickened one side of the hole edge, whereas a two-stage plate forging process using upper and lower punches was developed to thicken the both sides of the hole edge. The fatigue strength for the punched sheets with the thickened hole edge was improved by the thickness increases, the smooth sheared surface and the harder the surface around the hole edge.

Furthermore, a punching process including thickening of a hole edge of ultra-high strength steel sheets was developed. In this process, the pair of punch and die was designed so as to have both functions of punching and thickening in one stroke process and easily install in conventional die sets. The taper angle of the punch and the step height of the die were optimised to increase the amount of thickening. As the step height of the die increases, the fatigue strength increases. The delayed fracture was prevented by thickening due to the large compressive residual stress and the small surface roughness. It was found that the present approach was effective in improving the fatigue strength and in preventing occurrence of delayed fracture of the punched ultra-high strength steel sheet.

Acknowledgments

First and foremost, I thank God who ordained this entire journey and let me through it. For providing support, courage, and faith throughout it, I praise His name.

I would like to express my deepest and sincere gratitude to Prof. Ken-chiro Mori for his guidance, expertise, time and patience throughout the course of my studies. His supports helped me tremendously in every stage of the research work. This dissertation is immeasurably better as a result of his valuable comments.

I am deeply grateful to Associate Professor Dr. Yohei Abe and Dr. Tomoyoshi Maeno who always support and enrich my perspective on research. I also want to thank my fellow students at Frontier Forming System Laboratory for sharing their knowledge, wisdom, and inspiration.

I also would like to thanks for JICA for their financial support for my studies. Numerous thanks I appreciate to the staff of JICA, Academic Affair and International Affair Division of Toyohashi University of Technology for their sympathy, kindness, and help. An immeasurable debt of gratitude also goes to my colleagues in Toyohashi University of Technology for their advices and helping me on the difficult moments.

Finally, I would like to describe my deepest love and sincere gratitude to my lovely mother, father, and brother who always there for me when I need them, and to my wife, who sacrificed her time, energy, and career because of her love and our dreams, and also to my little angles, who always brighten my days and provide the source of my motivation.

Table of Contents

List of Figures

List of Tables

Chapter 1

Introduction

1.1. Punching of lightweight and high strength materials – An overview

In order to achieve better global environment, the reduction of CO_2 emission of automobiles is intensively required [1,2]. Several major car technologies for reduction of CO_2 emission have been developed, such as battery-electric, hybrid-electric, plug-in hybrid-electric and hydrogen vehicles [3-5]. In the battery-electric vehicle, the electricity is supplied from outside electric source, stored in a battery on the vehicle and used in electric motor. The hybrid-electric vehicles have the combination of a conventional gas engine and electronic motors in its drive system, whereas the plug-in hybrid-electric vehicles are hybrid which can be recharged from external electric sources. In the hydrogen vehicle, the electricity is generated by a fuel cell combining hydrogen stored in a fuel tank with oxygen from the air, and then is used to power the electric motor.

Each system still needs the improvement of the basic performance, as shown in Fig. 1.1 [6]. The required improvement is including reduction in frictional resistance of the engine and the power train, reduction in the tyre rolling resistance, better aerodynamics of body shapes, and also the reduction in car body weight.

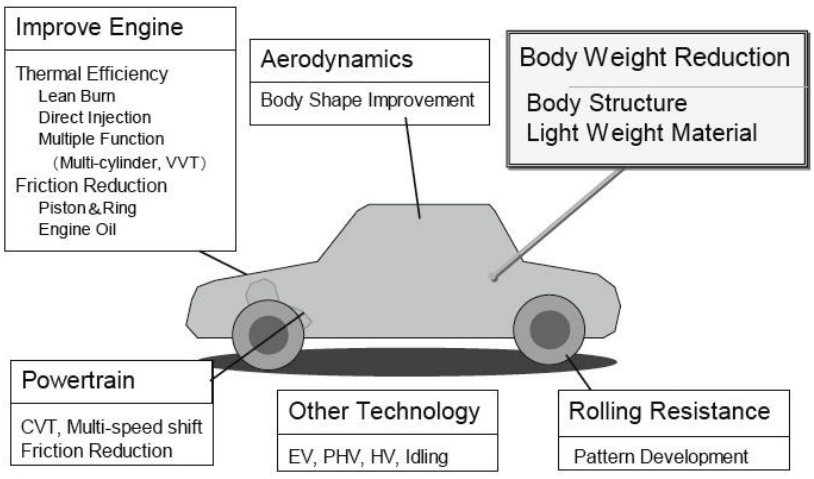

Fig. 1.1. Lightweight car technology [6].

As the increasing demands for higher comfort, better collision safety and high performance of the automobiles, the body mass has increased. It is convinced that the body mass has a strong influence to CO_2 emission of the automobiles [6,7]. Referring to the weight ratio of each car component as shown in Fig. 1.2, body components have a large portion of the vehicle mass. Therefore the reduction of weight of the body components has become a high priority in vehicle development for improving the CO_2 emission of automobile, and forming processes of lightweight materials have been actively developed [8-10].

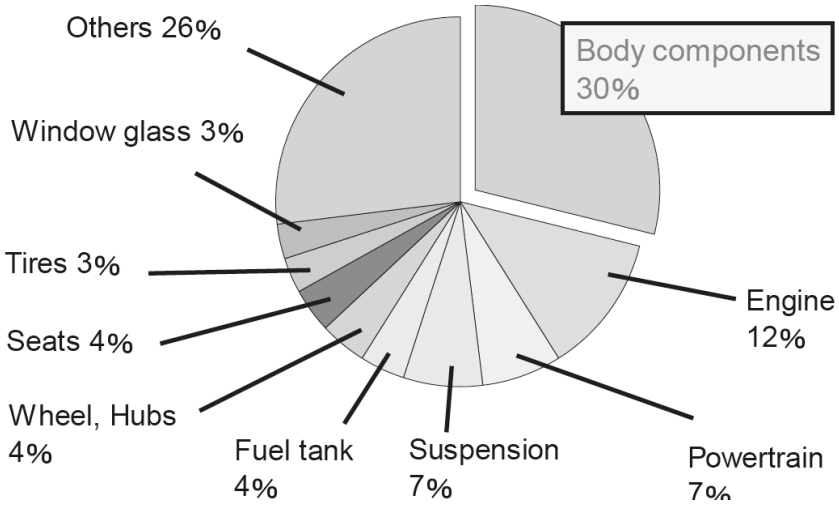

Fig. 1.2. Car component part weight ratio [6].

1.1.1. Lightweight materials

Aluminium and magnesium alloys offer a high potential for the reduction in weight of the automobile due to lightweight and high specific strength [11-13]. The density of the magnesium and aluminium alloys is 1/4 and 3/8 time of the mild steels, respectively, whereas the specific strength is 2.5 times more than that for the mild steels.

Although the application of aluminium and magnesium alloy sheets to the automobile parts is attractive for the reduction of the automobile weight, high cost and small formability are crucial problems [14,15], and thus the industry still has a great interest in steel sheets. The strength of high tensile strength steel sheets remarkably increases and ultra-high tensile strength steel sheets more than 1 GPa have been developed. As shown in Table 1.1, the strength of the ultra-high tensile strength sheets is 3 or 4 times higher than

that of mild steel sheets, and the strength-to-specific gravity ratio exceeds that of the aluminium and magnesium alloy sheets.

Table 1.1

Strength to specific gravity ratios for various sheet metals.

Sheet	Tensile strength	Specific gravity	Strength to specific gravity ratio
Ultra-high strength steel	980-1470 MPa	7.8	126-188 MPa
High strength steel	490-790 MPa	7.8	63-101 MPa
Mild steel SPCC	340 MPa	7.8	44 MPa
Aluminum alloy A6061(T6)	310 MPa	2.7	115 MPa
Magnesium alloy	210 MPa	1.8	116 MPa

The application of the high strength steel sheets to the structural body parts which need higher strength is thought of a measure for reducing the weight of automobiles. The areas of the body structure which is considered for applying high strength steel sheets is shown in Fig. 1.3. By applying high strength steel sheets with strength replacing the mild steel sheets, the reinforcements parts is eliminated and the material thickness is decreased, thus the body mass is reduced. However, in stamping operations of high strength steel sheets, large springback, small formability, short tool life, etc. are problematic, particularly for ultra-high strength steel sheets having a tensile strength above 1 GPa [16-18].

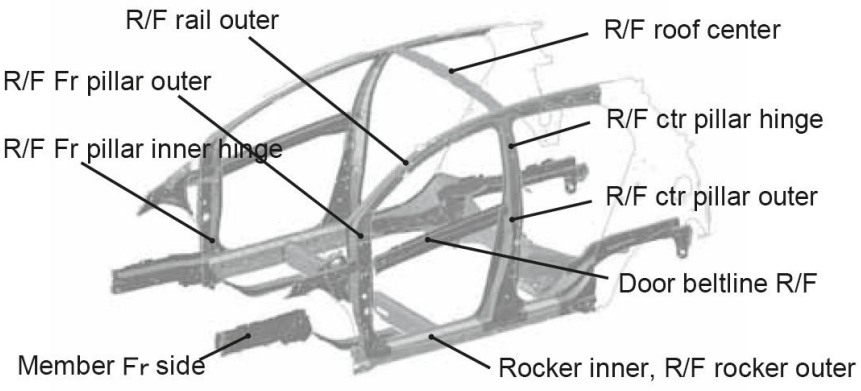

Fig. 1.3. Application of high strength steel sheets to automobile parts [6].

1.1.2. Punching of high strength steel sheets

Body-in-white parts are generally punched to make many holes for joining, paint removing, attachment, reduction in weight, etc. Since the high strength steel sheets have large strength and small ductility, not only forming but also punching becomes difficult. In the punching of the high strength steel sheets, large tool wear and rough sheared edges becomes problems [19-22] (see Fig. 1.4). Tools tend to wear and chip due to large punching load, and thus the tool life is short. The quality of the sheared edge deteriorates since the onset of cracks in the shearing is early due to the small ductility, thus the rough fracture surface increases. In addition, worn and chipped tools bring about the deterioration in dimensional accuracy of the punched hole and in the quality of the sheared edge.

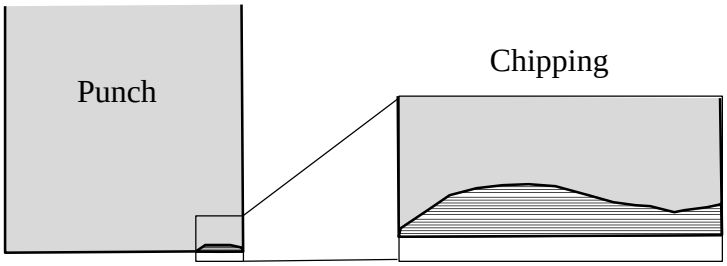

(a) Large tools wear

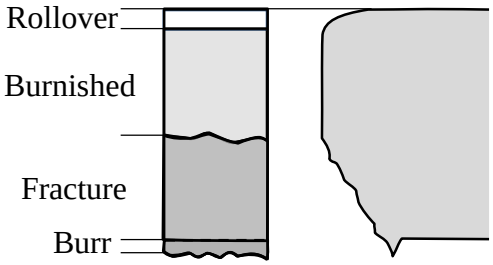

(b) Rough sheared edge

Fig. 1.4. Problems in punching of high strength steel sheets.

In high strength steel sheets, the static strength of formed products is almost proportional with the strength of the sheet, whereas the increase in fatigue strength becomes gradually small [23]. In addition, onset and progress of fatigue cracks of the punched high strength steel sheets are accelerated around holes due to concentration of stress, particularly for rough fracture surface and sharp burr of the sheared edge [24,25].

Therefore, the improvement of the quality of the sheared edge of punched sheets is useful for increasing the fatigue life.

Although the hot punching process indicated the effectiveness for reducing the punching load and improving the quality of the sheared edge of the ultra-high strength steel sheets [26,27], additional apparatus preheating and cooling systems, and oxidation for the heating [28] become problems, and thus cold punching process is preferable. Although shaving is generally used to improve the quality of sheared edge [29], it is not easy to shave high strength steel sheets. The shape of the punch head and the punching clearance ratio are among the major factors that affecting the quality of the sheared edge in cold punching of high strength steel sheets [30,31].

1.2. Research objectives

1.2.1. Improvement of quality of sheared edge of high strength steel sheets

The aim of this dissertation is to develop high quality punching process of high strength steel sheets for improving the quality of the sheared edge. The special shape of the punch is developed and the clearance ratio is adjusted for improving the quality of the sheared edge. In addition the effect of punch shape and clearance ratio on the quality of the sheared edge to the punching of inclined ultra-high strength steel is investigated.

1.2.2. Improvement of fatigue strength of punched of high strength steel sheets

The concentration of stress around the punched hole is relaxed by thickening of the hole edge by means of flanging. This leads to the improvement of the fatigue strength. In this study, the effect of thickening of hole edge on the fatigue strength of the punched high strength steel sheets is examined. Furthermore, a punching process including thickening of a hole edge of high strength steel sheets is developed. In this process, the pair of punch and die is designed so as to have both functions of punching and thickening in one stroke process and easily install in conventional die sets.

1.3. Outline of dissertation

This dissertation discusses about the thickening of hole edge in punching of high strength steel sheets for improvement of fatigue strength of the punched sheets, followed by the improvement of quality of sheared edge in punching of ultra-high strength steel sheets by punches having small corner radius. Finally, a punching of inclined ultra-high strength steel sheet is presented.

This dissertation consists of seven chapters:

Chapter 2 presents the one side and both sides thickening of hole edge of punched high strength steel sheets by hole flanging for improvement of fatigue strength of the punched sheets. The hole edge of the punched sheets is thickened by flanged the edge of the hole. The influence of the punch and die shape to the thickened edge is examined. The improvement of the strength of the punched sheets with the thickening of hole edge is then investigated and compared with that without the thickening.

Chapter 3 presents the development of punching including thickening of hole edge of high strength steel sheet. Conventionally, a hole flanging operation is performed as a next stage after the punching operation, and thus the number of stages increases. In this process, the pair of punch and die was designed so as to have both functions of punching and thickening in one stroke process and easily installed in conventional die sets.

Chapter 4 presents the optimization of tools shape in punching including thickening of the hole edge of the ultra-high strength steel sheet. In this study the shape of the punch and die is optimised to increase the amount of thickening of ultra-high strength steel sheet. The effect of thickening on the fatigue strength, delayed fracture and static strength is examined. Finally, a repeated punching including thickening of the hole edge with realistic punching conditions is performed to investigate the performance of coating of the punch and the applicability of the present punching process to actual stamping operations.

Chapter 5 presents the improvement of quality of the sheared edge in punching of the ultra-high strength steel sheets by punch having a small round corner under a slight clearance. The small round edge has the functions of avoiding the contact between the punch and die in the slight clearance punching and of delaying the onset of cracks. The effect of round edge radius in improving the quality of the sheared edge is investigated. The galling resistance of coating of the punch is examined in a repeated punching with realistic punching speed.

Chapter 6 presents the improvement of quality of the sheared edge in punching of an inclined ultra-high strength steel sheet. The effect of the punching clearance and punch head shape on the quality of the sheared edge is investigated.

Finally concluding remarks and future prospective are given in Chapter 7.

1.4. References

[1] E. Uherek, T. Halenka, J. Borken-Kleefeld, Y. Balkanski, T. Berntsen, C. Borrego, M. Gauss, P. Hoor, K. Juda-Rezler, J. Lelieveld, D. Melas, K. Rypdal, S. Schmid, Transport impacts on atmosphere and climate: Land transport, Atmospheric Environment 44 (37) (2010) 4772-4816.

[2] Georgios Fontaras, Zissis Samaras, On the way to 130 g CO_2/km – Estimating the future characteristics of the average European passenger car, Energy Policy 38 (4) (2010) 1826-1833.

[3] J. Romm, The car and fuel of the future, Energy Policy 34 (17) (2006) 2609-2614.

[4] K. Jorgensen, Technologies for electric, hybrid and hydrogen vehicles: Electricity from renewable energy sources in transport, Utilities Policy 16 (2008) 72-79.

[5] J.M. Ogden, M.M. Steinbugler, T.G. Kreutz, A comparison of hydrogen, methanol and gasoline as fuels for fuel cell vehicles: Implications for vehicle design and infrastructure development, Journal of Power Sources 79 (1999) 143-168.

[6] M. Miyanishi, Manufacturing of light weight cars, Steel Research International 81 (9) (2010), Supplement Metal Forming 2010, 1-8.

[7] K. Yamane, S. Furuhama, M. Miyanishi, A study on the effect of the total weight of fuel and fuel tank on the driving performances of cars, International Journal of Hydrogen Energy 23 (9) (1998) 825-831.

[8] M. Kleiner, M. Geiger, A. Klaus, Manufacturing of lightweight components by metal forming, CIRP Annals - Manufacturing Technology 52 (2) (2003) 521-542.

[9] M. Kleiner, S. Chatti, A. Klaus, Metal forming techniques for lightweight construction, Journal of Materials Processing Technology 177 (1-3) (2006) 2-7.

[10] R. Neugebauer, T. Altan, M. Geiger, M. Kleiner, A. Sterzing, Sheet metal forming at elevated temperatures, Annals of the CIRP 55(2) (2006),793–816.

[11] D. Carle, G. Blount, The suitability of aluminium as an alternative material for car bodies, Materials & Design 20 (5) (1999) 267-272.

[12] A. Tharumarajah, P. Koltun, Is there an environmental advantage of using magnesium components for light-weighting cars? Journal of Cleaner Production 15 (11-12) (2007) 1007-1013.

[13] B.L. Mordike, T. Elbert, Magnesium: Properties – applications – potential, Materials Science and Engineering A302 (1) (2001) 37-45.

[14] P. Groche, R. Huber, J. Dorr, D. Schmoeckel, Hydromechanical deep-drawing of aluminium-alloys at elevated temperatures, Annals of the CIRP 51 (1) (2002), 215-218.

[15] K. Siegert, S. Jager, M. Vulcan, Pneumatic bulging of magnesium AZ31 sheet metals at elevated temperatures, Annals of the CIRP 52 (1) (2003), 241-244.

[16] K. Mori, S. Maki and Y. Tanaka, Warm and hot stamping of ultra-high tensile strength steel sheets using resistance heating, Annals of the CIRP 54 (1) (2005), 209-212.

[17] K. Mori, K. Akita, Y. Abe, Springback behaviour in bending of ultra-high-strength steel sheets using CNC servo press, International Journal of Machine Tools & Manufacture 47 (2) (2007) 321–325.

[18] K. Mori, T. Kato, Y. Abe, Y. Ravshanbek, Plastic joining of ultra-high strength steel and aluminium alloy sheets by self-piercing rivet, Annals of the CIRP 55(1) (2006), 283-286.

[19] K. Mori, Y. Abe, Y. Suzui, Improvement of stretch flangeability of ultra-high strength steel sheet by smoothing of sheared edge, Journal of Material Processing Technology 210 (4) (2010) 653-659.

[20] K. Mori, T. Maeno, S. Fuzisaka, Punching of ultra-high strength steel sheets using local resistance heating of shearing zone, Journal of Materials Processing Technology, 212-2 (2012), 534- 540.

[21] J. Eriksson, M. Olssson, Tribological testing of commercial CrN, (Ti,Al)N and CrC/C PVD coatings – Evaluation of galling and wear characteristics against different high strength steels, Surface & Coating Technology 205 (16) (2011) 4045-4051.

[22] K. Inoue, M. Suzuki, S. Nishino, K. Ohya, Y. Tomota, Effect of coating microstructure of press-working dies on sliding damage, Steel Research International 81 (9) (2010), Supplement Metal Forming 2010, 849–852.

[23] Y. Murakami, S. Kodama, S. Konuma, Quantitative evaluation of effects of non-metallic inclusions on fatigue strength of high strength steels. I: Basic fatigue mechanism and evaluation of correlation between the fatigue fracture stress and the size and location of non-metallic inclusions, International Journal of Fatigue 11 (5) (1989) 291-298.

[24] D.J. Thomas, M.T. Whittaker, G. Bright, Y. Gao, The influence of mechanical and CO_2 laser cut-edge characteristics on the fatigue life performance of high strength automotive steels, Journal of Material Processing Technology 211 (2) (2011) 263-274.

[25] L. Sanchez , F. Gutierrez-Solana, D. Pesquera, Fatigue behavior of punched structural plates, Engineering Failure Analysis 11 (5) (2004) 751-764.

[26] K. Mori, S. Saito, S. Maki, Warm and hot punching of ultra-high strength steel sheet, CIRP Annals - Manufacturing Technology 57 (1) (2008) 321-324.

[27] K. Mori, T. Maeno, Y. Maruo, Punching of small hole of die-quenched steel sheets using local resistance heating of shearing zone, Annals of CIRP, 61 (1) (2012), 255-258.

[28] K. Mori and D. Ito, Prevention of oxidation in hot stamping of quenchable steel sheet by oxidation preventive oil, CIRP Annals 58 (1) (2009), 267-270.

[29] S. Thipprakmas, S. Rojananan, P. Paramaputi, An investigation of step taper-shaped punch in piercing process using finite element method, Journal of Material Processing Technology 197 (1/3) (2008) 132-139.

[30] H. Murakami, N. Kasahara, Y. Mochiduki, H. Kanamaru, T. Imura: Evaluation of adhesion resistance of PW punch in fine piercing of steel plate, Journal of JSTP, 50-577 (2009), 119-123 [In Japanese].

[31] T. Matsuno, Y. Kuriyama, H. Murakami, S. Yonezawa, H. Kanamaru, Effects of punch shape and clearance on hole expansion ratio and fatigue properties in punching of high strength steel sheets, Steel Research International 81 (9) (2010), Supplement Metal Forming 2010, 853-856.

Chapter 2

Thickening of hole edge of punched high strength steel sheets by hole flanging

2.1. Introduction

The reduction in the weight of cars is intensively required in the automobile industry to improve the fuel consumption, and forming processes of lightweight materials have been actively developed [1]. The application of high strength steel sheets to the automobile parts is effective in reducing the weight of cars due to the high specific strength [2].

Body-in-white parts are generally punched to make many holes for joining, paint removing, attachment, reduction in weight, etc. When the punched high strength steel sheet is loaded, stress concentrates in the vicinity of the hole, and thus cracks are generated by the stress concentration, particularly for the rough fracture surface of the sheared edge [3]. Therefore, the fatigue strength of the sheet deteriorates [4]. It was also reported that the fatigue strength for the high strength steel sheets does not increases proportionally with increasing the tensile strength [5].

The improvement of the quality of the sheared edge of punched sheets is useful to increase the fatigue life. Mori et al. [6] smoothed the fracture surface of the sheared edge using the conical punch to improve the hole expansion ratio of the punched high strength steel sheet. Thipprakmas et al. [7] improved the quality of the punched edge of aluminium sheets by shaving with a taper punch. In addition the stiffness of the sheet deteriorates due to the punching. Murakami et al. [8] developed the PW (Press Working) punch to shear thicker steel plates accurately. Matsuno et al. [9] employed the PW punch to improve the fatigue strength and the hole expansion ratio of the punched high strength steel sheets. Although the fatigue strength is improved by the quality of the sheared edge, the improvement is not enough to extend the applicable range of ultra-high strength steel sheets.

In the present study, a hole edge of a punched high strength steel sheets was thicken to improve the strengths of the punched sheets. The shapes of the punches were designed for

the thickening of the hole edge by finite element simulation. The quality of the sheared edge for the thickening was compared with those without the thickening. In addition, the static and the fatigue strength of the punched sheets were measured.

2.2. Thickening of hole edge by hole flanging

To improve fatigue strength of a punched high strength steel sheet, the edge of the hole is thickened by a hole flanging process as shown in Fig. 2.1. In this process, a punch forces the edge of the punched hole into a die, thus the thickness around the hole edge increases. In the conventional hole flanging process using a straight die, a sharp edge is formed in the thickened edge, thus the stress is concentrated and the strength of the punched sheets deteriorates. To eliminate the sharp edge in the thickened edge, a step die is employed. By using the step die, the sharp edge is removed by the step of the die and the hole edge is compressed, thus the strength of the punched sheet is improved.

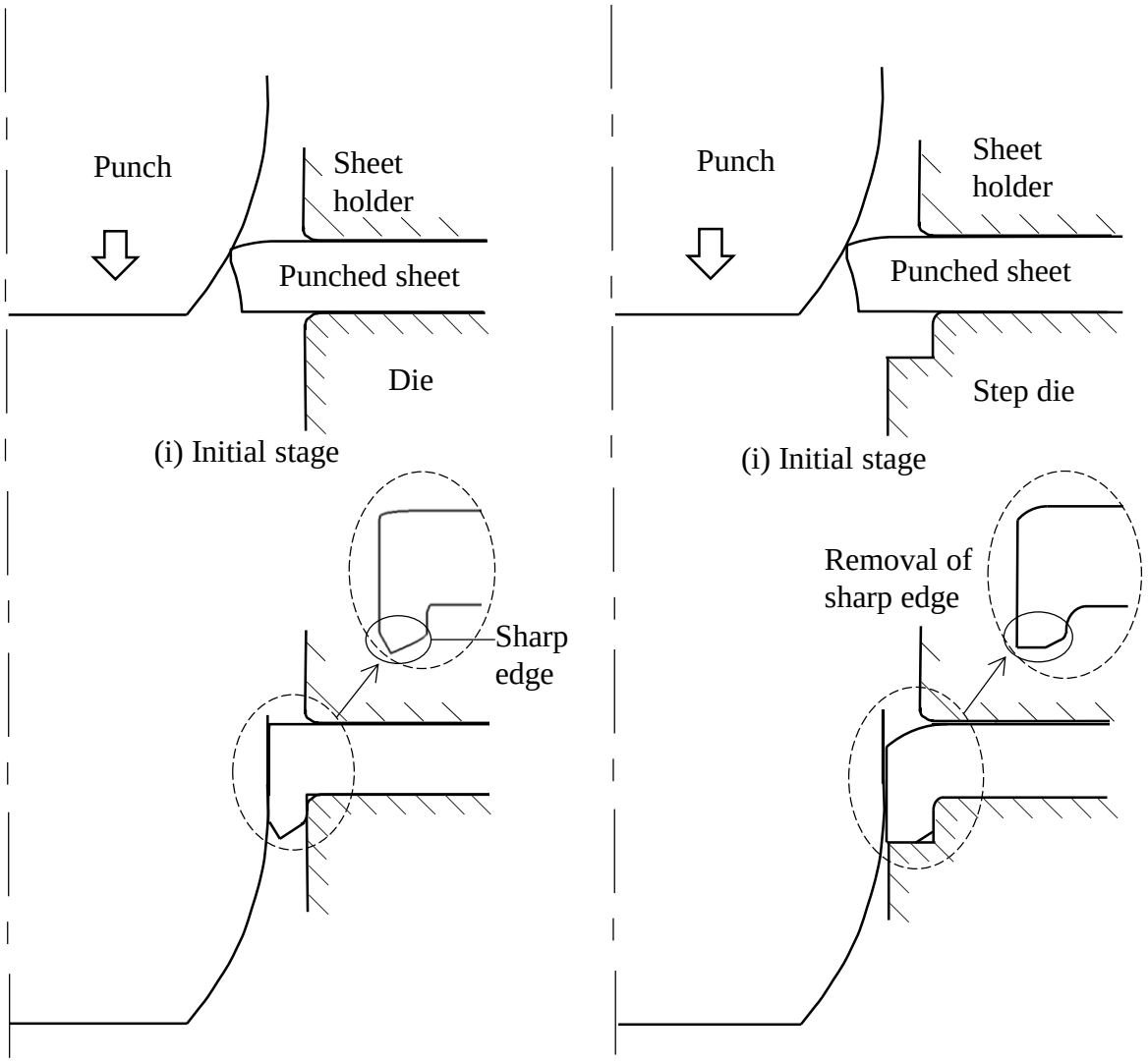

Fig. 2.1. One side thickening of hole edge of high strength steel sheet by hole flanging process for (a) straight and (b) step dies.

The above process was developed for one side thickening of hole edge. To thicken both sides of the hole edge of the punched high strength steel sheets, a two-stage plate forging process shown in Fig. 2.2 was developed. In the 1st stage, the edge of the punched hole is flanged with the upper punch. In the 2nd stage, both sides of the flanged edge are thickened with the lower punch. The thickness increase is changed by the punch stroke for the 1st stage, s_1.

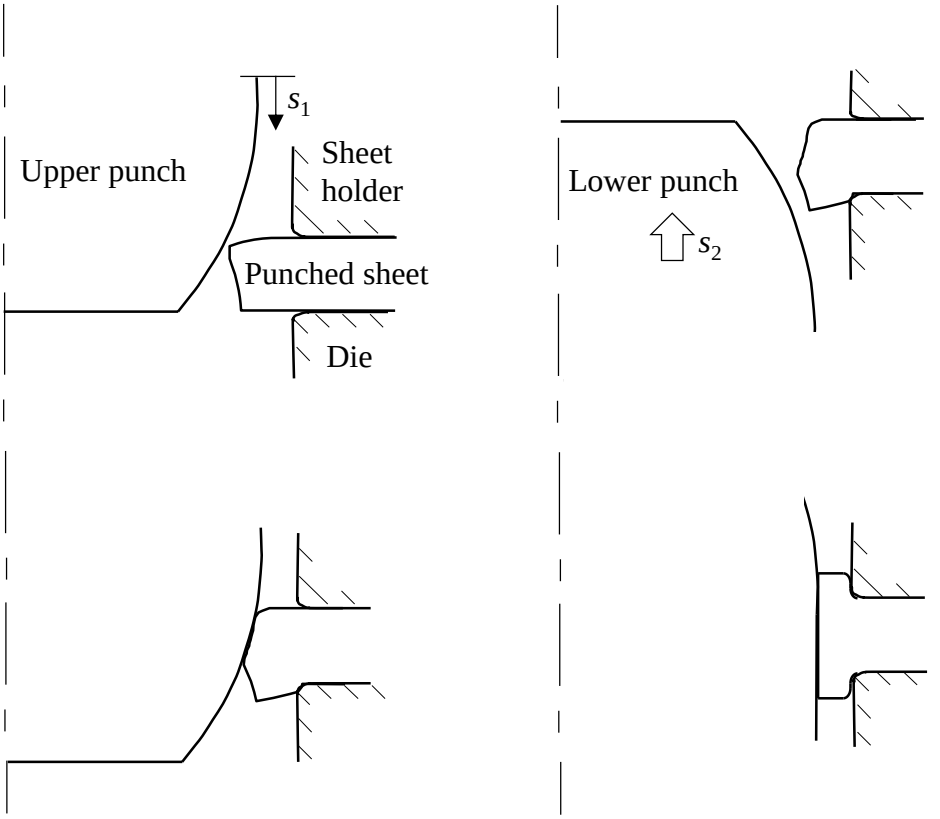

(a) 1st stage (b) 2nd stage

Fig. 2.2. Two-stage plate forging for both sides thickening hole edge of punched high strength steel sheets.

The dimensions of the tools used in the one side and both sides thickening of the hole edge of the punched high strength steel sheets are shown in Fig. 2.3, where *h* is the step height of the die. The high strength steel sheets JSC590 and ultra-high strength steel sheet JSC980 having 1.4 mm in thickness were used in the experiment. The sheet was punched with a flat punch having 9 mm in diameter before the thickening.

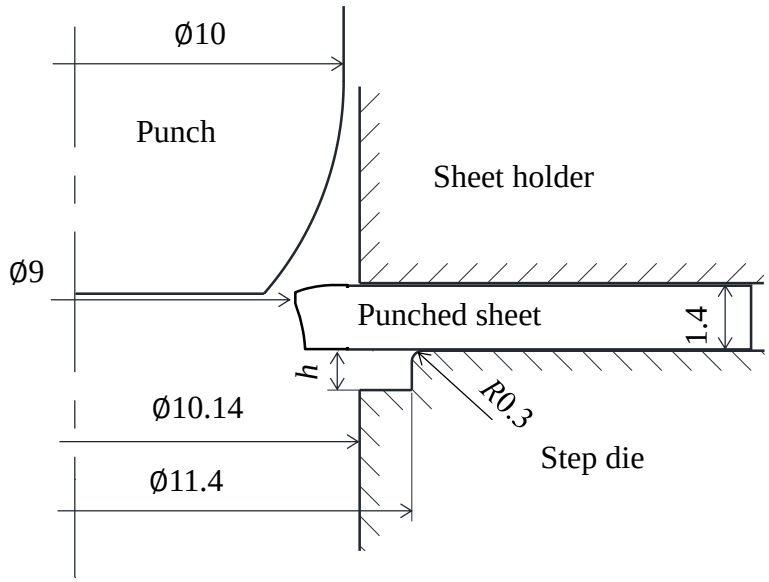

(a) One side thickening

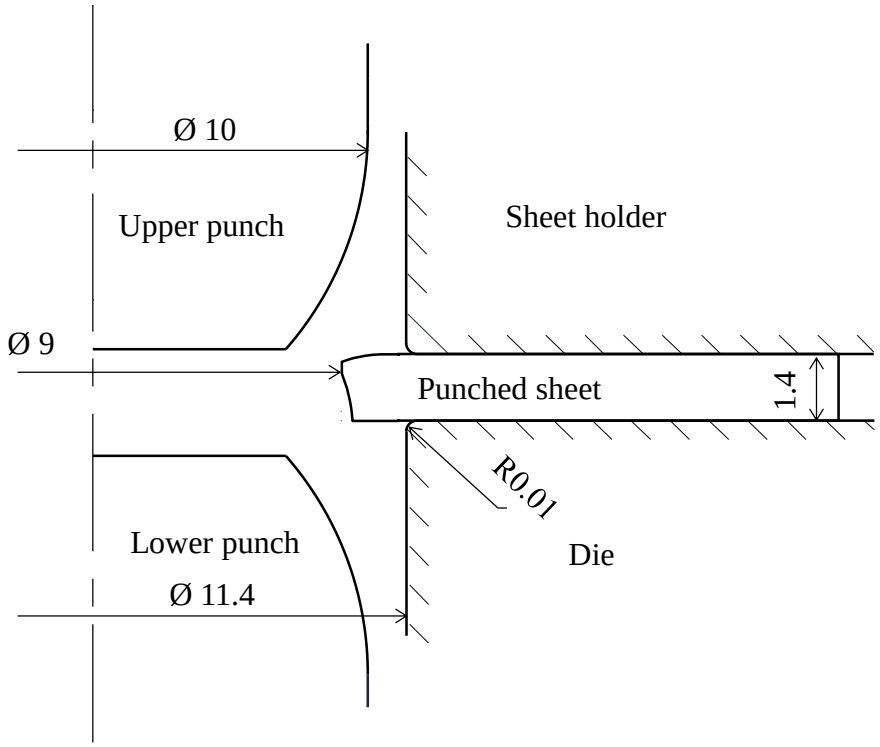

(b) Both sides thickening

Fig. 2.3. Dimensions of tools used in thickening of hole edge of high strength steel sheets.

The mechanical properties of the high strength steel sheets are given in Table 2.1. The sheets are cold-rolled ones generally used for automobile parts, and are made of dual-phase steel. The mechanical properties of the sheets were measured from the tensile test. The

specimens were cut in the 0, 45 and 90º directions with respect to the rolling direction of the sheet, and the averages of the measured values are shown. The dimension of the specimen is illustrated in Fig. 2.4. The length and width of the punched sheet were 30 and 30 mm, respectively.

Table 2.1.

Mechanical properties of high strength steel sheets.

	JSC590	JSC980
Thickness (mm)	1.4	
Flow stress curve (MPa)	$\sigma = 979\varepsilon^{0.16}$	$\sigma = 1574\varepsilon^{0.14}$
Tensile strength (MPa)	632	1071
Elongation (%)	24	16
Reduction of area (%)	55	41

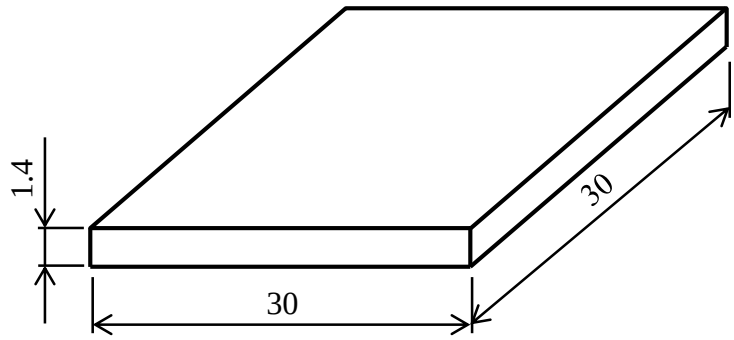

Fig. 2.4. Dimension of specimen for thickening of hole edge.

The conditions of the thickening of the hole edge of high strength steel sheets are given in Table 2.2. The sheets were punched by a 50 kN screw driven type universal testing instrument. Each punching test was performed at least two times. The tool used for the punching and the thickening of hole edge of the high strength steel sheets is shown in Fig. 2.5.

Table 2.2.

Conditions of thickening of hole edge of high strength steel sheets.

Die material	SKD11
Punch material	SKD11
Punch diameter (mm)	10
Die diameter (mm)	10.14
Punching speed (mm/s)	0.08
Lubricant	Rust prevention oil

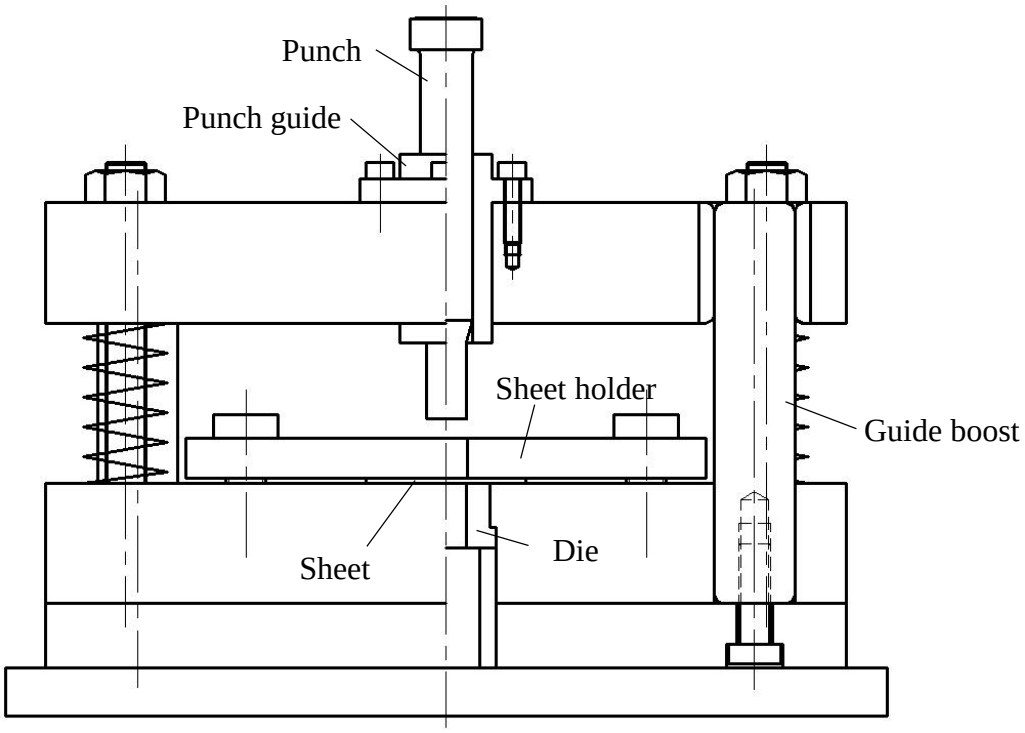

Fig. 2.5. Tools used for punching and thickening of hole edge of high strength steel sheets.

The four punches used to thicken the hole edge of the punched sheet are shown in Fig. 2.6, i.e. the taper punches having angles α of 30 and 45^{o} and the round punches having corner radii R of 4 and 6 mm.

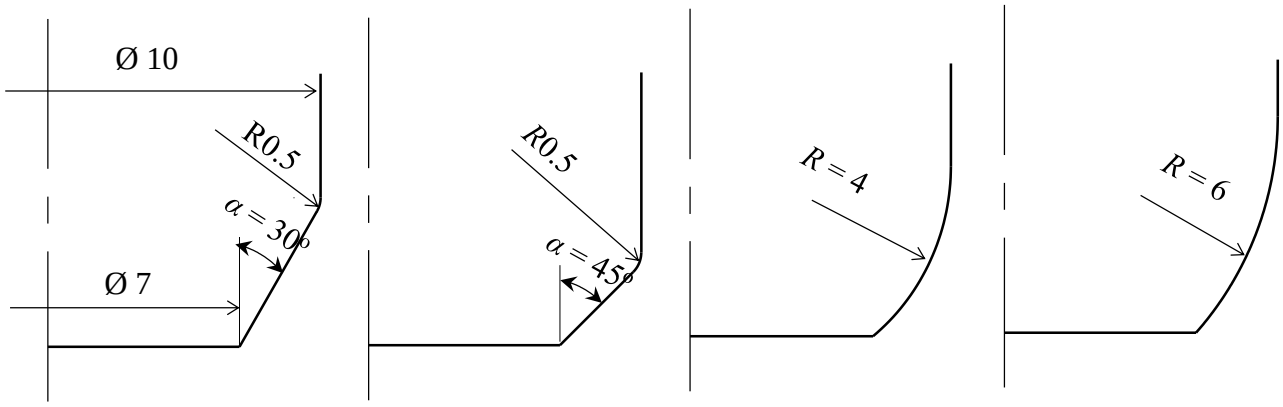

(a) Taper, α = 30° (b) Taper, α = 45° (c) Round, R = 4 mm (d) Round, R = 6 mm

Fig. 2.6. Punches used to thicken hole edge of punched high strength steel sheets.

Finite element simulation of the thickening of hole edge using the commercial software ABAQUS was performed under axi-symmetric deformation. The conditions used for the finite element simulation of the thickening of hole of high strength steel sheets are shown in Table 2.3. The die, sheet holder and upper and lower punches were assumed to be rigid in the simulation. The simulation was performed for JSC590.

Table 2.3.
Conditions used for finite element simulation of thickening of hole of high strength steel sheets.

Flow stress curve (MPa)	$\sigma = 937\varepsilon^{0.14}$ MPa
Young`s modulus (MPa)	210000
Poisson`s ratio	0.3
Coefficient of friction	0.1

2.3 Results of thickening of hole edge

2.3.1. One side thickening of hole edge

The cross-sectional shape of the punched sheet before the thickening for JSC590 is shown in Fig. 2.7, where the ratio of the clearance to the sheet thickness for punching process was 20%. This shape was input for the finite element simulation of the thickening process. The work-hardening by the punching was neglected in the simulation.

The cross-sectional shape of the punched sheet before the thickening for JSC590 is shown in Fig. 2.7, where the ratio of the clearance to the sheet thickness for punching process was 20%. This shape was input for the finite element simulation of the thickening process. The work-hardening by the punching was neglected in the simulation.

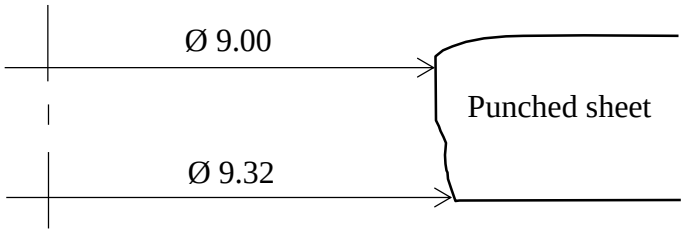

Fig. 2.7. Cross-sectional shape of punched sheet before thickening for JSC590.

The shapes of the hole edge in the one side thickening process obtained from the calculation for different punches, the straight die and JSC590 are shown in Fig. 2.8. The thickened edges for the taper punches have sharp edges. Although the folding occurs in the upper side of the thickened edge for the round punch of R = 4 mm, no defects are caused for the round punch of R = 6 mm.

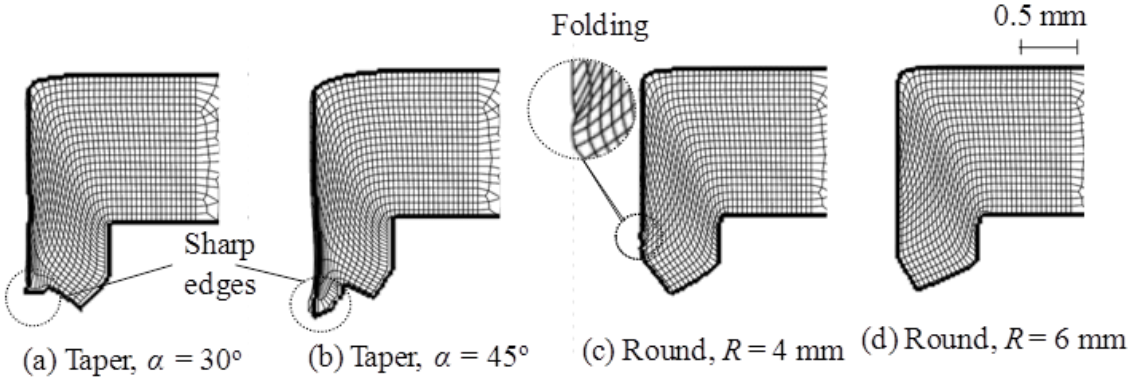

Fig. 2.8. Shapes of hole edge after one side thickening process obtained from calculation for different punches, straight die and JSC590.

To determine the step height of the die, the calculation was performed for the different step height of the die. The shapes of the hole edge in the one side thickening process obtained from the calculation for different step height of the die, R = 6 mm and JSC590 are shown in Fig. 2.9. The burr is formed for h = 0.5 mm due to the excessive filling of the die,

whereas the sharp edge in the thickened edge is not removed for h = 0.7 mm due to the under filling of the die. The die height is optimized for h = 0.6 mm, thus this die was fixed for the following experiments.

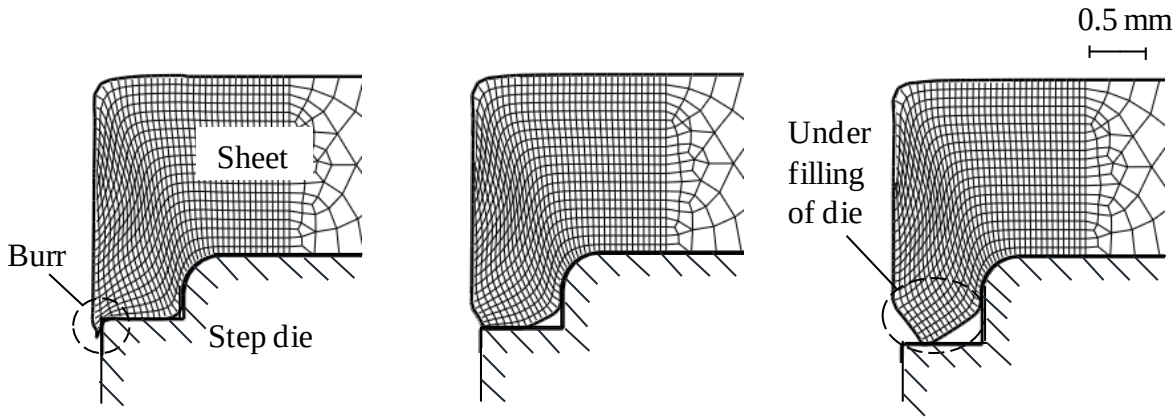

(a) h = 0.5 mm (b) h = 0.6 mm (c) h = 0.7 mm

Fig. 2.9. Shapes of hole edge after one side thickening process obtained from calculation for different step height of die, R = 6 mm and JSC590.

The deformation behaviours of the sheet during the one side thickening of hole edge process obtained from the experiment for the straight and step die, R = 6 mm and JSC590 are shown in Fig. 2.10. Although the fracture surface is appeared on the thickened edge for the straight die, the fracture portion is eliminated by the step of the die for the thickening using step die.

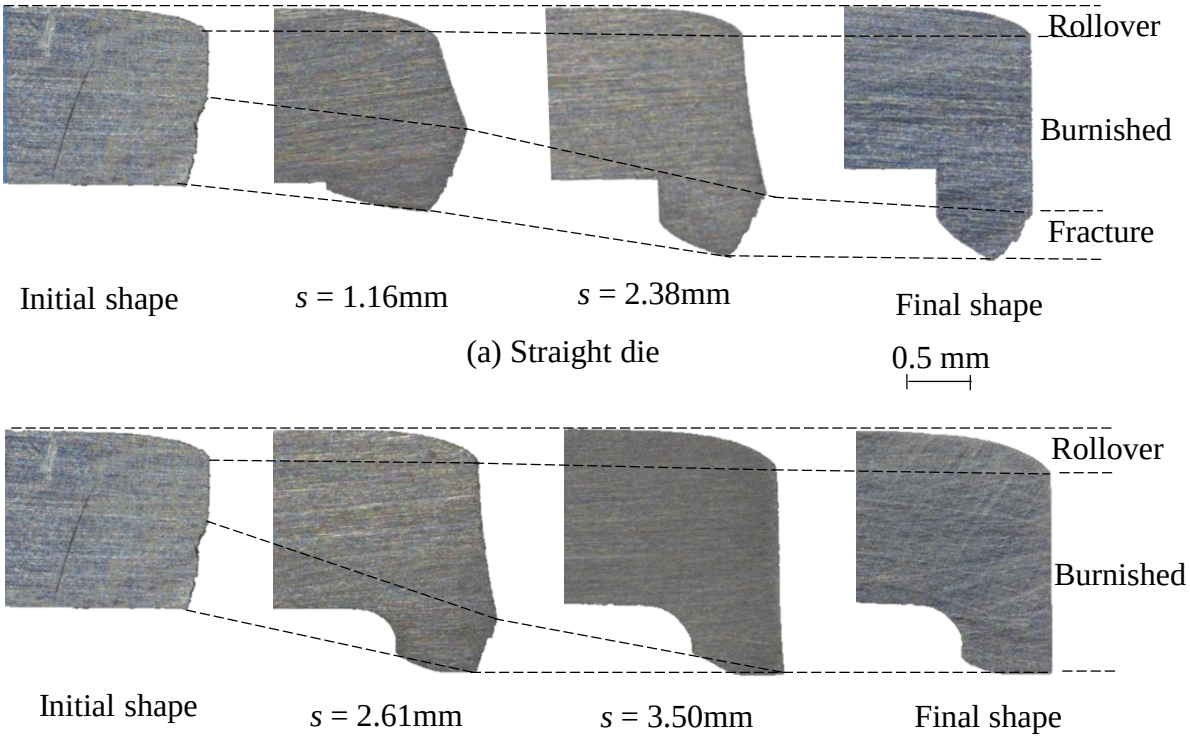

Fig. 2.10. Deformation behaviours of sheet during thickening of hole edge process obtained from experiment for straight and step die, R = 6 mm and JSC590.

The forming load for thickening using straight and step die is compared with that without thickening using a flat punch in Fig. 2.11, where the ratio of clearance between the punch and die to the sheet thickness for the flat punch was 20%. The forming load for the step die is larger than that for the straight die, and has a sharp peak due to the compression of the hole edge with the step of the die. The punching stroke for the thickening is larger than that without thickening, whereas the forming load is smaller.

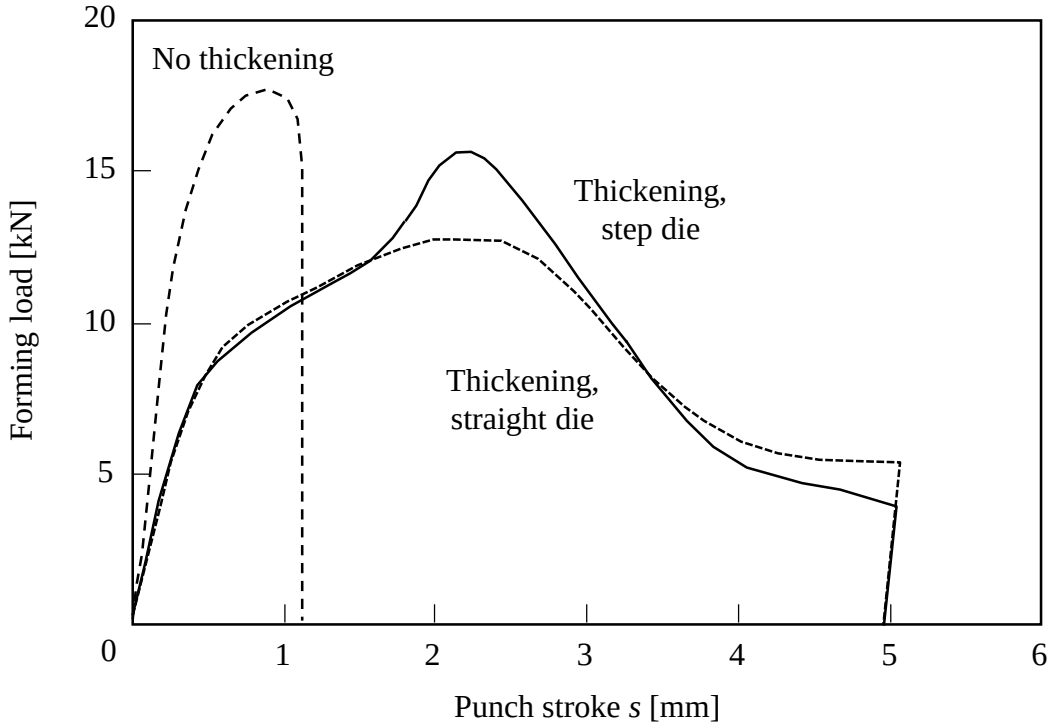

Fig. 2.11. Forming load-punch stroke curves obtained from experiment with thickening for straight and step die and R = 6 mm and without thickening.

2.3.2. Both sides thickening of hole edge

The shapes of the hole edge in the both sides thickening process obtained from the calculation for different punches and s_1 = 1.3 mm are shown in Fig. 2.12, where s_1 is the punch stroke in the 1st stage. The thickened edges for the taper punches have a sharp edge in the upper side. Although the folding occurs in the upper side of the thickened edge for the round punch of R = 4 mm, no defects are caused for the round punch of R = 6 mm.

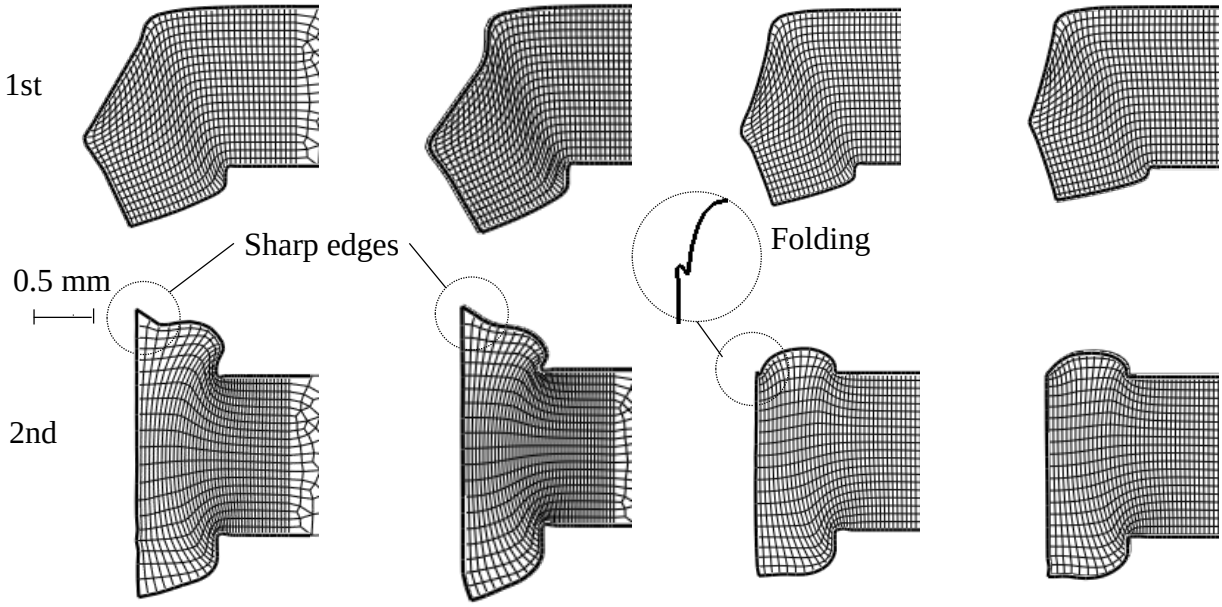

(a) Taper, α = 30^{o} (b) Taper, α = 45^{o} (c) Round, R = 4 mm (d) Round, R = 6 mm

Fig. 2.12. Shapes of hole edge in thickening process obtained from calculation for different punches and s_1 = 1.3 mm.

It is desirable that the thickness increases h_u, h_l for the upper and lower sides of the hole edge are equal. The relationship between the ratio of the thickness increase to the sheet thickness and the punch stroke in the 1st stage obtained from the experiment and calculation for R = 6 mm is shown in Fig. 2.13. The punch stroke in the 1st stage s_1 was set between 0.9 and 1.5 mm. As the punch stroke in the 1st stage increases, the thickness increase for the upper side h_u decreases and that h_l for the lower side increases. The punch stroke in the 1st stage was determined to be s_1 = 1.3 mm from the experimental results.

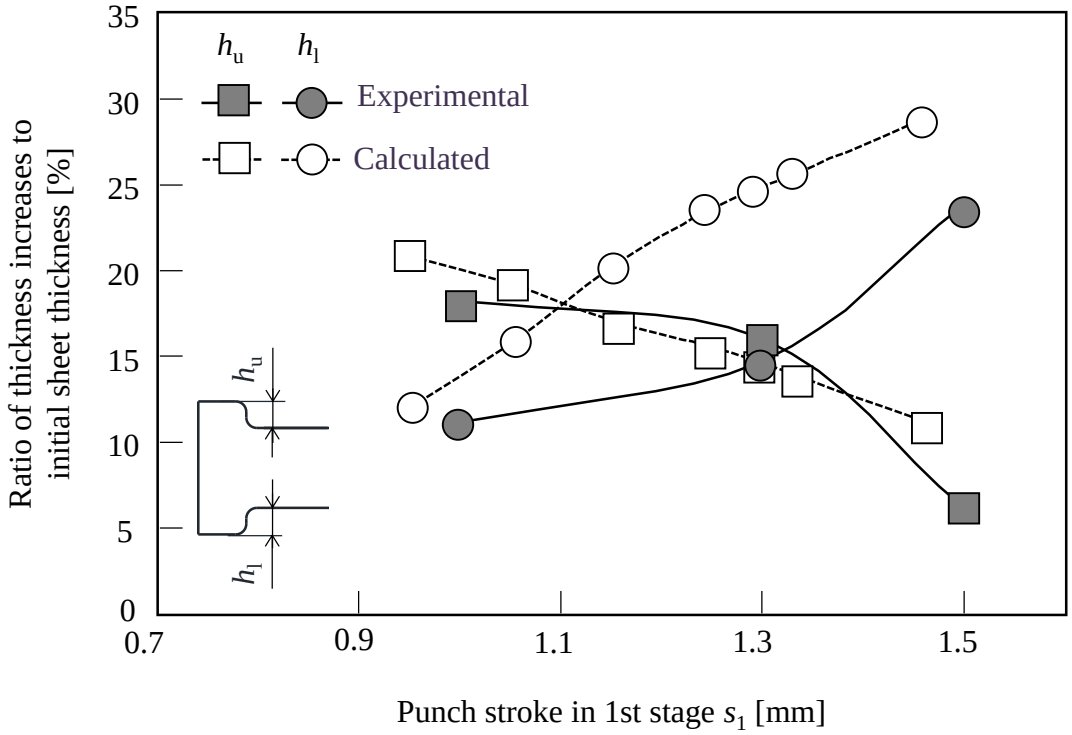

Fig. 2.13. Relationship between ratio of thickness increases to sheet thickness and punch stroke in 1st stage s_1 for R = 6 mm.

A comparison between the deformed shapes obtained from the calculation and experiment for R = 6 mm and s_1 = 1.3 mm is shown in Fig. 2.14. The height of the thickened hole edge in the 1st stage and the total thickness increase for both sides in the 2nd stages obtained by the calculation are 4% and 7% larger than those for the experiment, respectively. The increase in thickness of the thickened hole edge obtained from the experiment is 31% of the initial sheet thickness.

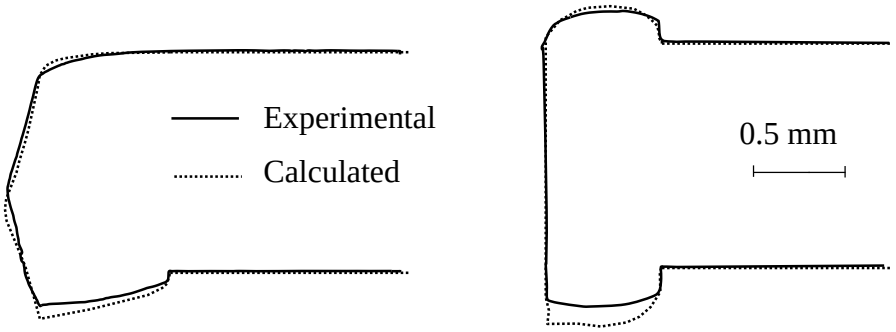

(a) 1st stage (b) 2nd stage

Fig. 2.14. Comparison between deformed shapes obtained from calculation and experiment for R = 6 mm and s_1 = 1.3 mm.

The forming load for thickening using straight and step die is compared with that without thickening using a flat punch in Fig. 2.15, where the ratio of clearance between the punch and die to the sheet thickness for the flat punch was 20%. The forming load with thickening for 1st stage is almost similar with that for 2nd stage, and smaller than that for without thickening.

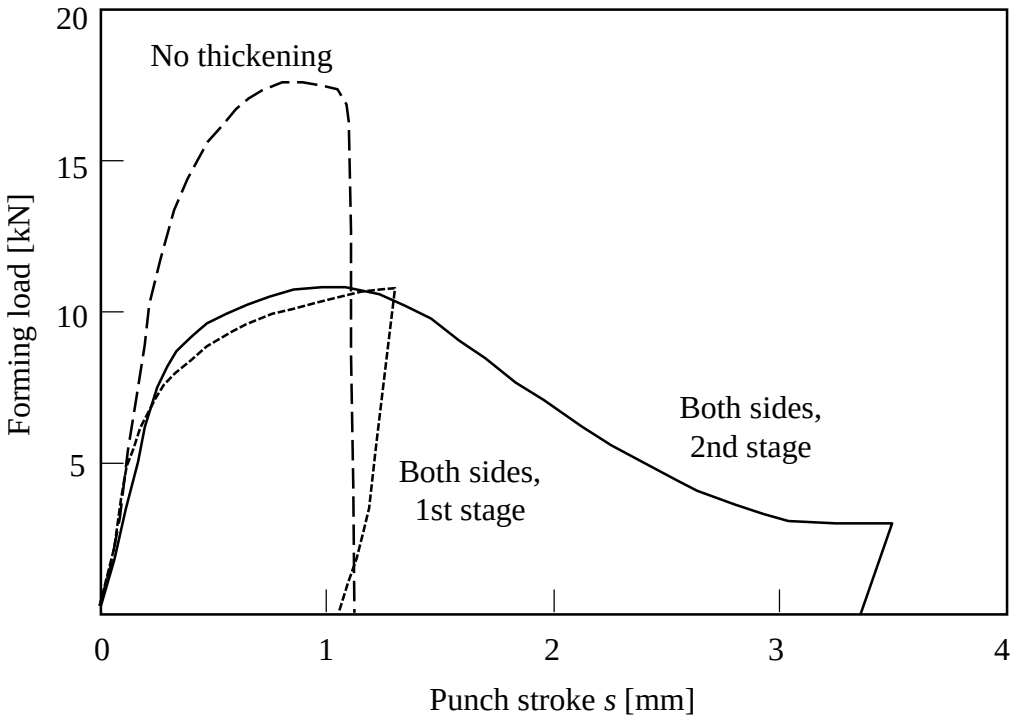

Fig. 2.15. Forming load-punch stroke curves obtained from experiment with thickening for straight and step die and R = 6 mm and without thickening.

2.3.3. Quality of sheared edge

The surface and cross-section of the sheared edge for one side and both sides thickening, R = 6 mm and JSC590 are compared with those without thickening in Fig. 2.16. Although the area of the rough fracture surface for the punched sheet without the thickening is large, the rough fracture surface is considerably reduced for the thickening and almost disappears for the step die and the both sides thickening.

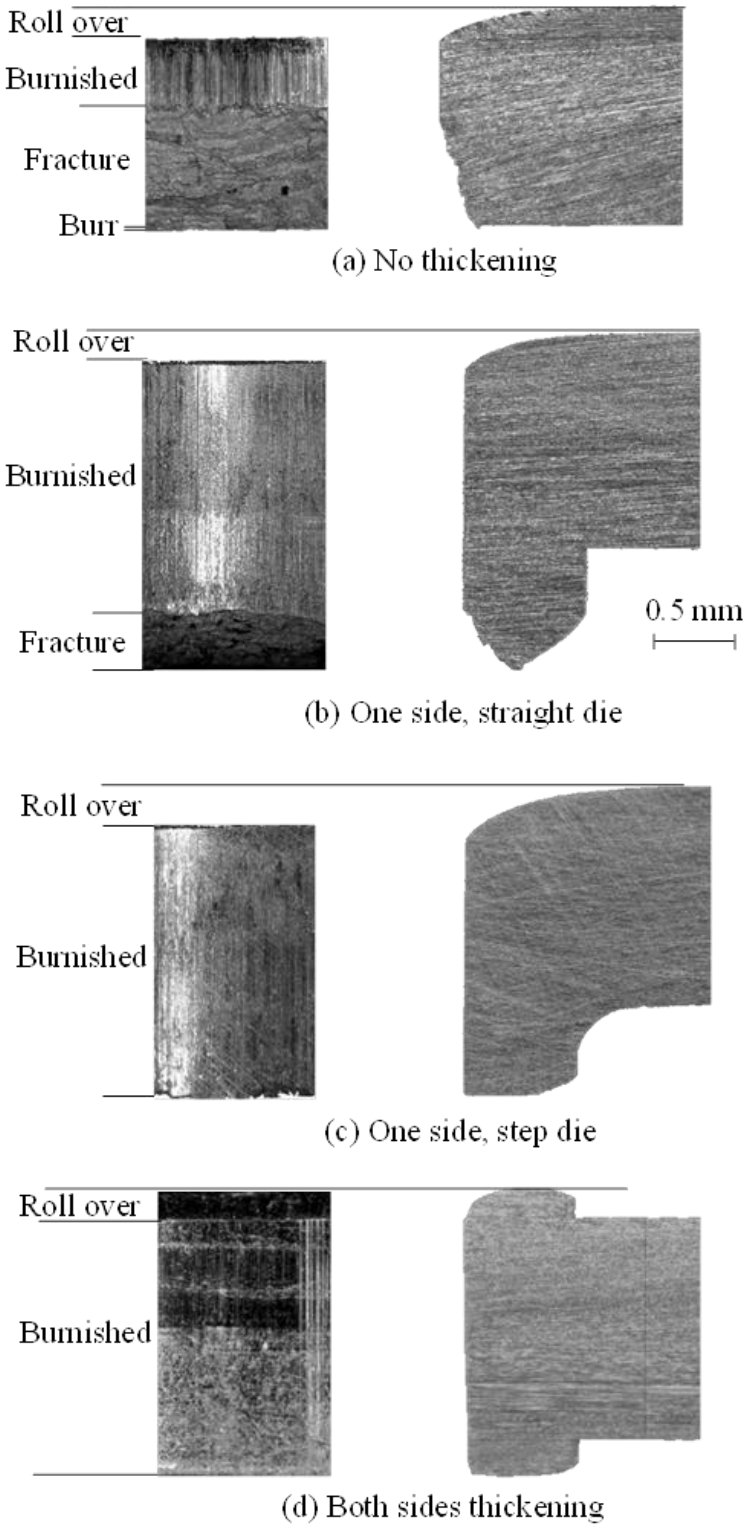

Fig. 2.16. Surface and cross-section of sheared edge with and without thickening for R = 6 mm and JSC590.

Ratio of rollover, burnished and fracture depths and burr height on the sheared edge with and without thickening for R = 6 mm and JSC590 are shown in Fig. 2.17. For the thickening, the burnished surface becomes considerably large and the burr is eliminated. The fracture surface almost disappears for the step die and both sides thickening.

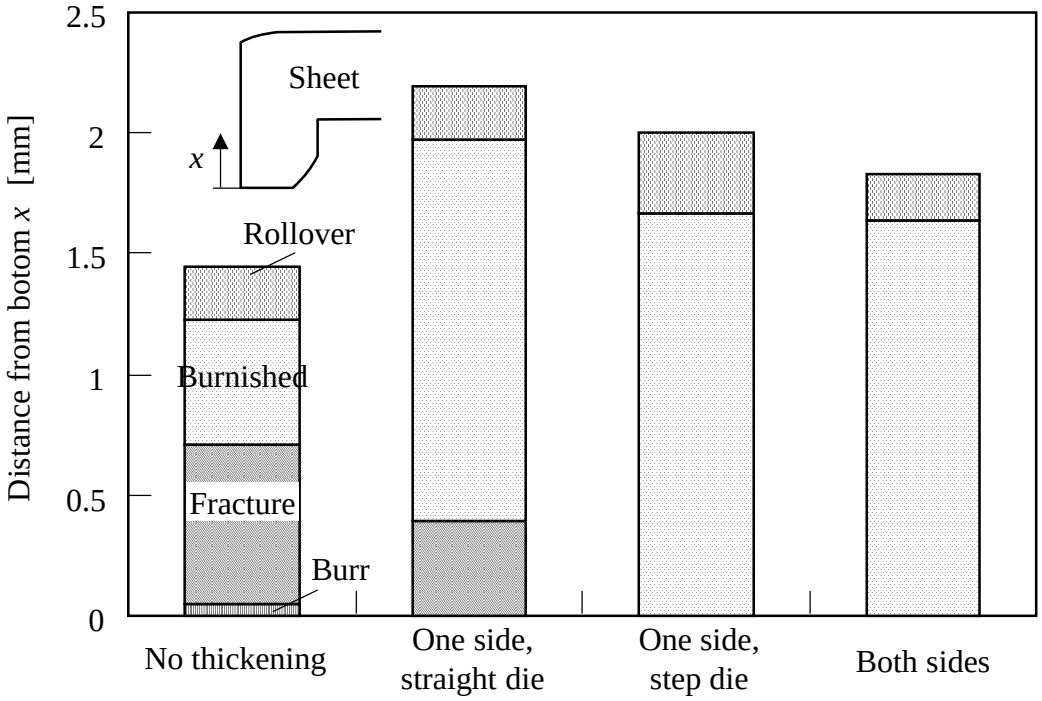

Fig. 2.17. Ratio of rollover, burnished and fracture depths and burr height on sheared edge with and without thickening for R = 6 mm and JSC590.

The distributions of the surface roughness of the sheared edge in the thickness direction with and without the thickening for R = 6 mm and JSC590 are shown in Fig. 2.18. The surface roughness was measured at intervals of 0.1 mm in the thickness direction. The surface roughness for the thickening is smaller than that for no thickening.

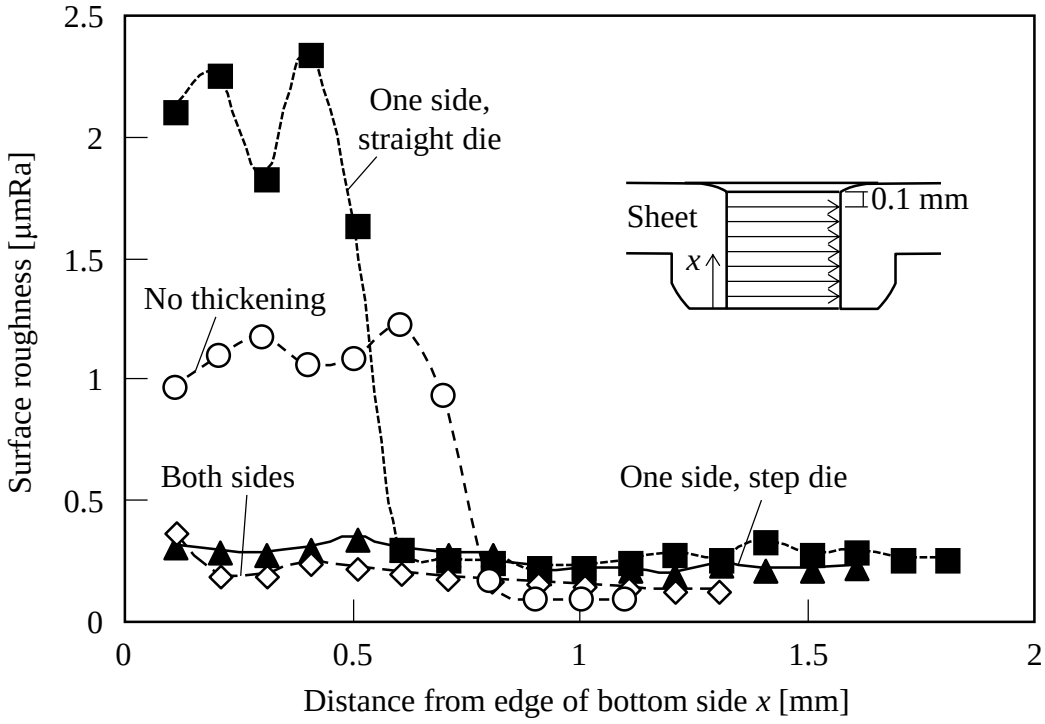

Fig. 2.18. Distributions of surface roughness of sheared edge in thickness direction with and without thickening for R = 6 mm and JSC590.

The distributions of Vickers hardness in the thickness direction around the sheared edge with and without thickening for R = 6 mm and JSC590 are shown in Fig. 2.19. The hardness was measured in the cross-section at 0.2 mm from the sheared edge. The hardness with thickening is higher than that without thickening due to ironing during the thickening stage. The hardness for both sides thickening along thickness direction is more uniform than that for one side thickening.

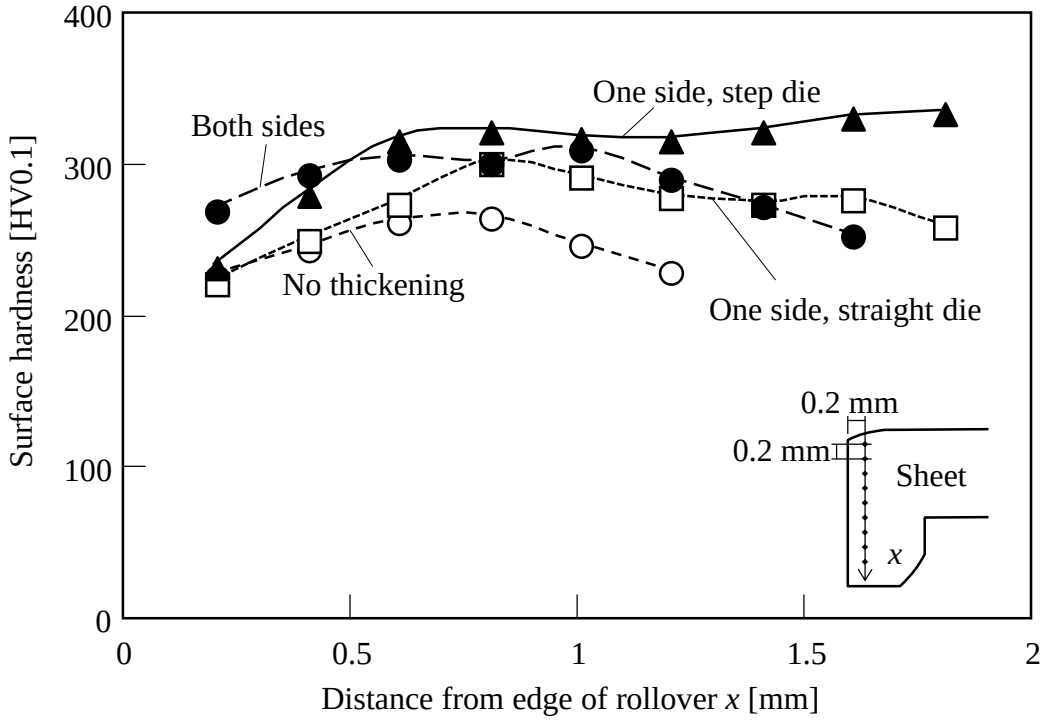

Fig. 2.19. Distributions of surface hardness of sheared edge in thickness direction with and without thickening for R = 6 mm and JSC590.

2.4. Strengths of punched sheet

2.4.1. Static strength

A static tensile strength were measured to evaluate the static strength of the punched sheet with the thickening of the hole edge. The procedure and dimension of specimen for the static tensile test are shown in Fig. 2.20. The static strength of the punched sheets was measured as the maximum loads in the static tensile test.

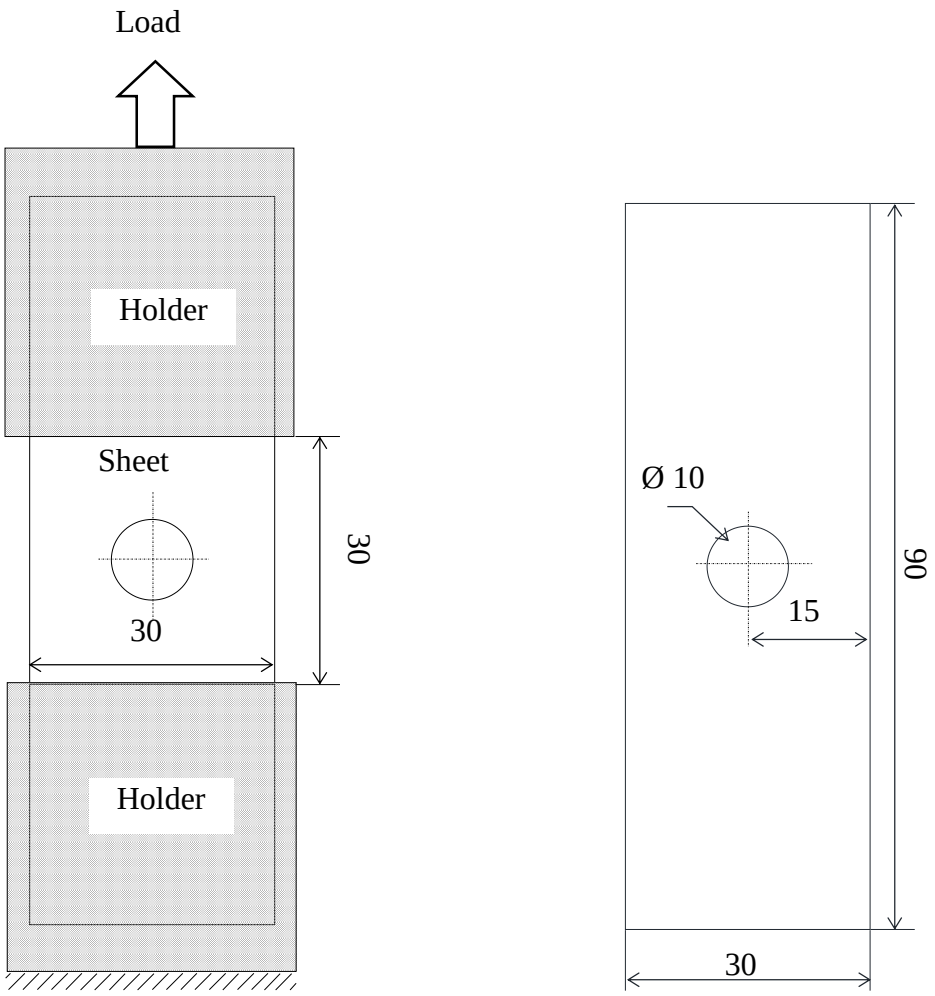

(a) Static tensile test (b) Dimensions of specimen

Fig. 2.20. Procedure and dimension of specimen for static tensile test.

The comparison of maximum load in the static tensile test between the punched sheets with and without thickening for R = 6 mm and JSC590 is shown in Fig. 2.21. The small increase in the static strength for the thickening was due to the relatively small thickening area around the hole edge.

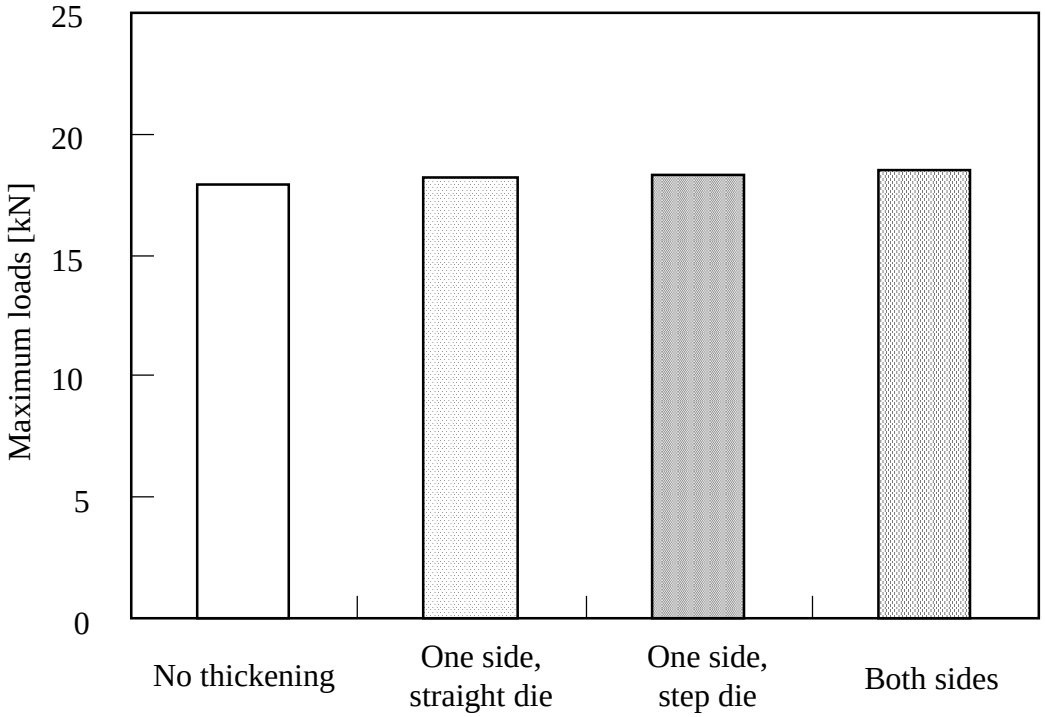

Fig. 2.21. Comparison of maximum load in static tensile test between punched sheets with and without thickening of hole edge for R = 6 mm and JSC590.

2.4.2. Fatigue strengths

The plane bending and tensile fatigue tests of the punched sheets with the thickened hole edge were performed. The procedure and dimensions of specimens for the plane bending fatigue tests are shown in Fig. 2.22. The frequency was set at 25 Hz and the ratio of the minimum stress to maximum stress was -1.0. The fatigue tests were ended when the sheet was ruptured.

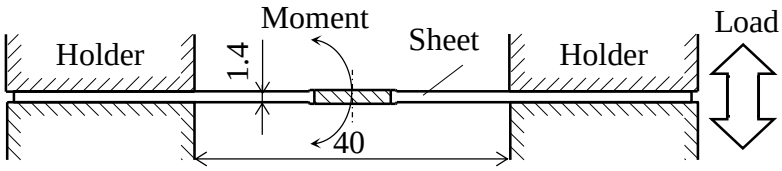

(a) Plane bending fatigue test

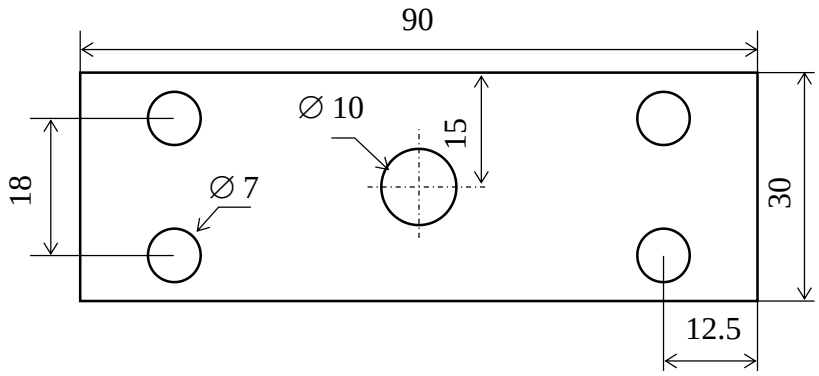

(b) Dimensions of specimen

Fig. 2.22. Procedure and dimensions of specimen for plane bending fatigue test.

A comparison of the number of cycles to failure between the punched sheets with and without the thickening of the hole edge is shown in Fig. 2.23. The bending moment for the fatigue test was set for 2.74 N·m. The number of cycles to failure for the one side thickening using straight and step dies were two and six times of that for no thickening, while the increasing of fatigue life for botgh sides thickening was not as high as one side thickening. The fatigue life of the punched sheet for the step die was higher than that for the straight die due to the elimination of the rough fracture surface in the thickened edge.

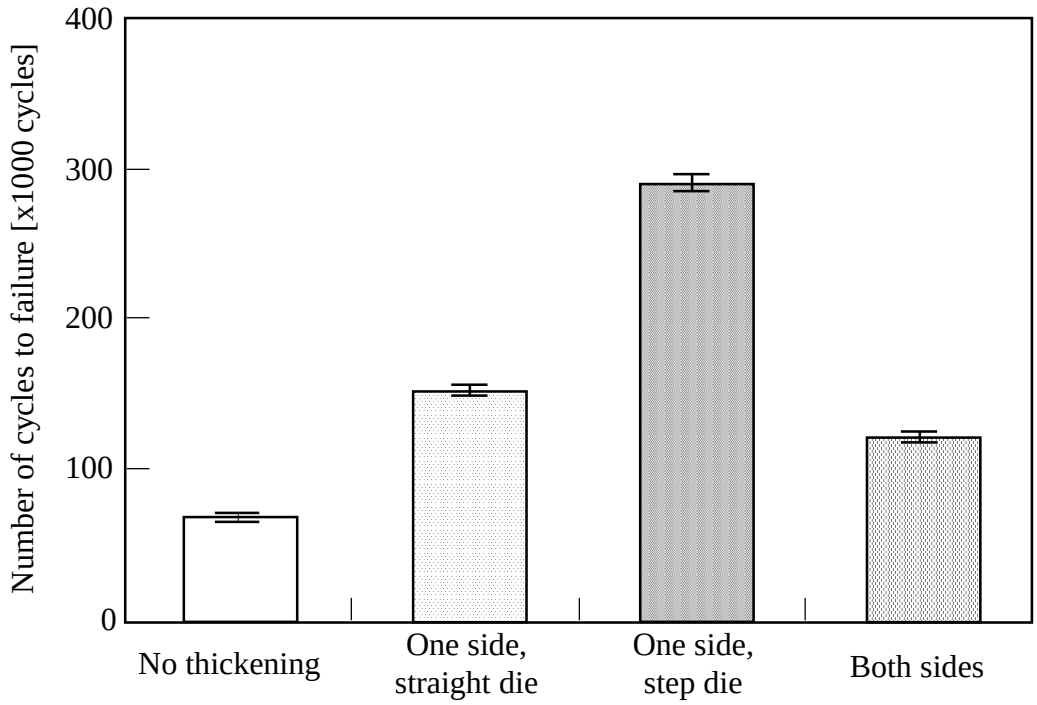

Fig. 2.23. Comparison of number of cycles to failure for bending fatigue test between punched sheets with and without thickening of hole edge, R = 6mm and JSC590.

The procedure for the tensile fatigue tests are shown in Fig. 2.24, whereas the dimensions of specimen was was similar to that for the static tensile test shown in Fig. 2.20(b). The frequency was set at 50 Hz and the ratio of the minimum stress to maximum stress was 0.

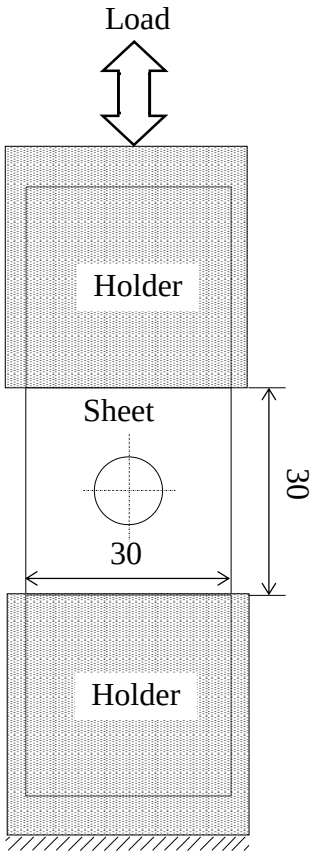

Fig. 2.24. Procedure for tensile fatigue test.

A comparison of the number of cycles to failure between the punched sheets with and without the thickening of the hole edge is shown in Fig. 2.25. The maximum load for the fatigue test was set for 9.92 kN. The number of cycles to failure for the one side thickening was almost three times of that for no thickening, whereas for both sides thickening was five times higher than that for no thickening. The fatigue life for the punched sheet for the thickened hole edge is improved by the thickness increase, the smooth sheared surface and the harder the surface around the hole edge.

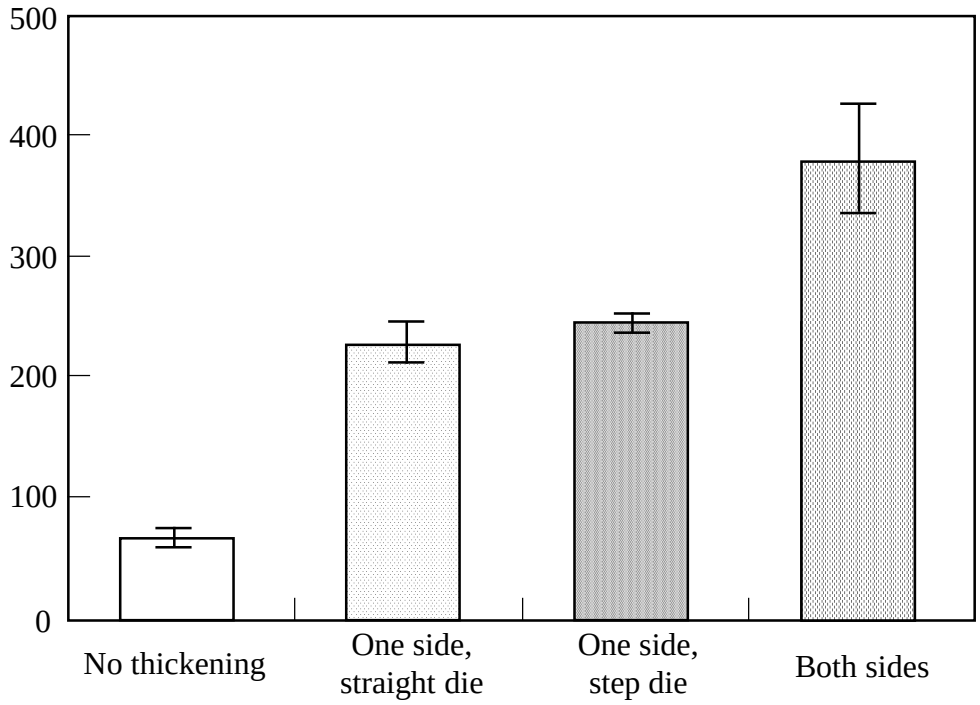

Fig. 2.25. Comparison of number of cycles to failure for bending fatigue test between punched sheets with and without thickening of hole edge, R = 6 mm and JSC590.

To investigate the effect of one side and both sides thickening on the fatigue strength, elastic deformation in the bending and tensile tests of the punched sheet was simulated by the commercial finite element software ABAQUS. The shapes of the punched sheets with and without thickening obtained from the experiment for R = 6 mm and JSC590 shown in Fig. 2.16 were employed for the finite element simulation without calculation of the punching process, and the sheets were divided into three-dimensional hexahedral elements. The given loads at the edge of the sheet for the bending and tensile tests were 2.74 N·m and 9.92 kN, respectively. The increase in flow stress of the sheet for work-hardening by punching was neglected.

The distributions of stress in the hoop direction in the cross section of the hole edge calculated from the finite element simulation with and without thickening for bending and tensile tests are compared with cracks initiation in the fracture surface in Fig. 2.26 and 2.27, respectively. In the bending, the stress is concentrated on the upper and bottom of the sheet for no thickening and both sides thickening since the distance to the normal line is almost similar, thus the cracks are initiated from these regions, while for the one side thickening only from the thickened edge. In the tensile, the stress for the one side thickening is

concentrated on the rollover region due to the increasing of the stiffness for the thickened edge portion, whereas for no thickening and both sides thickening on the hole edge. Since the stiffness on the hole edge for both side thickening is increasing, the fatigue strength for the tensile is higher than that for one side thickening. Thus, both sides thickening of the hole edge was effective in the improvement of fatigue life of punched sheet for tensile fatigue test, while one side thickening was effective for plane bending fatigue test.

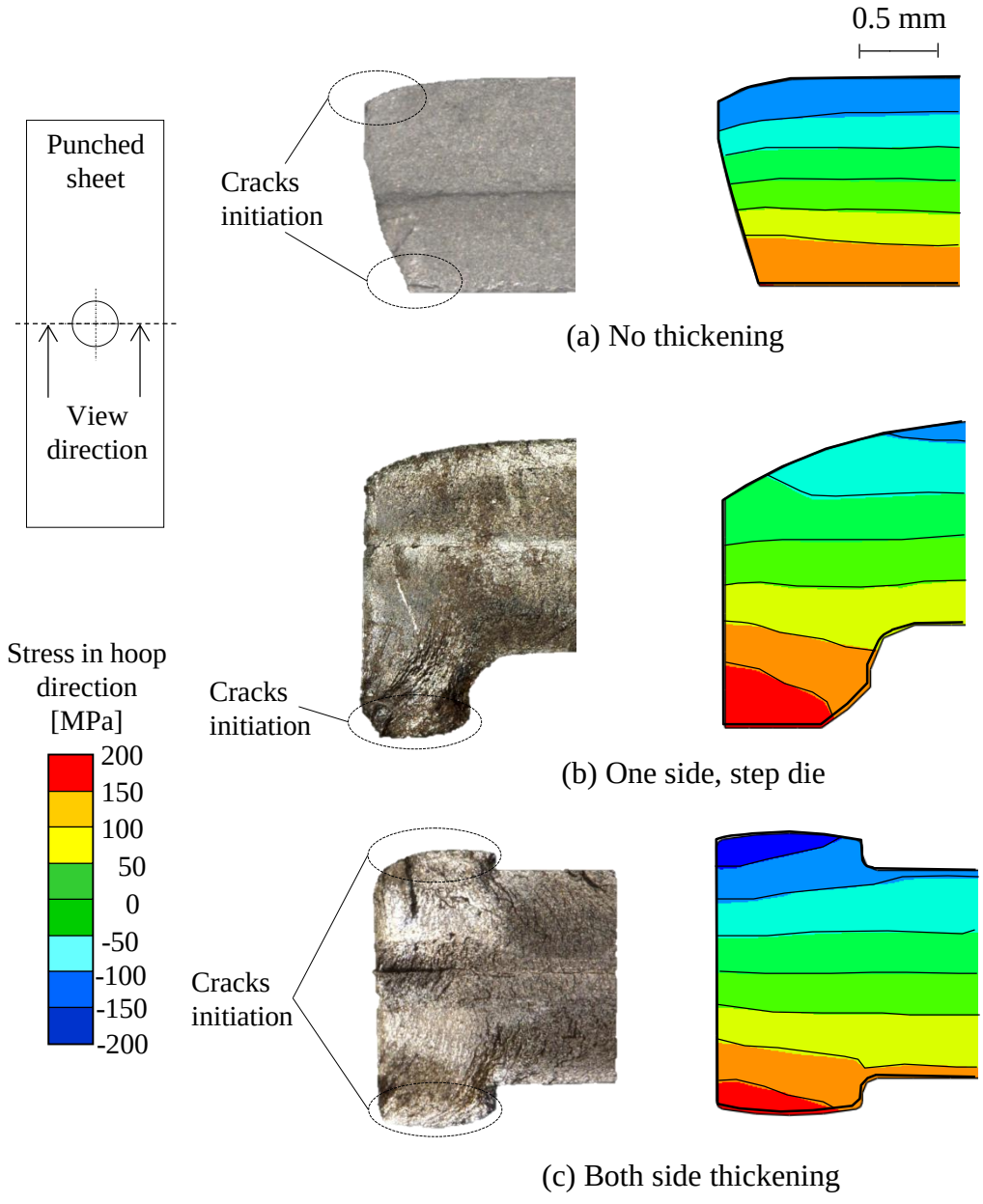

Fig. 2.26. Comparisons between cracks initiation and stress distribution in hoop direction in cross section of hole edge with and without thickening for bending, R = 6 mm and JSC590.

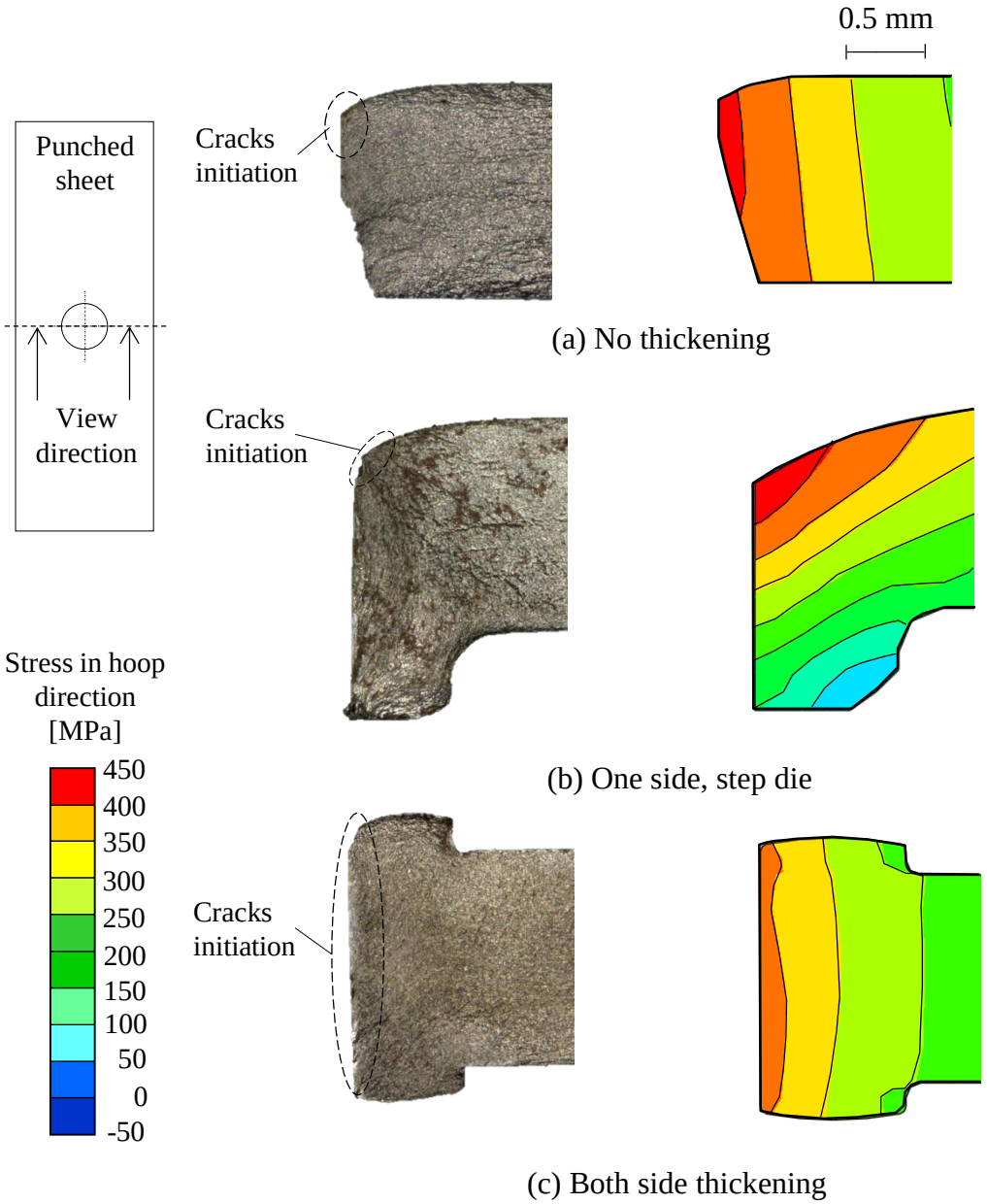

Fig. 2.27. Comparisons between cracks initiation and stress distribution in hoop direction in cross section of hole edge with and without thickening for tensile, R = 6 mm and JSC590.

2.5. Application of thickening of hole edge to punched ultra-high strength steel sheet

The above mentioned results are obtained for the high strength steel sheet JSC590. The pair of R = 6 mm and h = 0.6 mm were employed for thickening of hole edge of the

punched ultra-high strength steel sheet JSC980. The surface and cross-section of the sheared edge with and without thickening for straight and step die, R = 6 mm and JSC980 are shown in Fig. 2.28. Although the area of the rough fracture surface for the punched sheet without the thickening is large, the rough fracture surface is considerably reduced for the thickening and almost disappears for the thickening using step die.

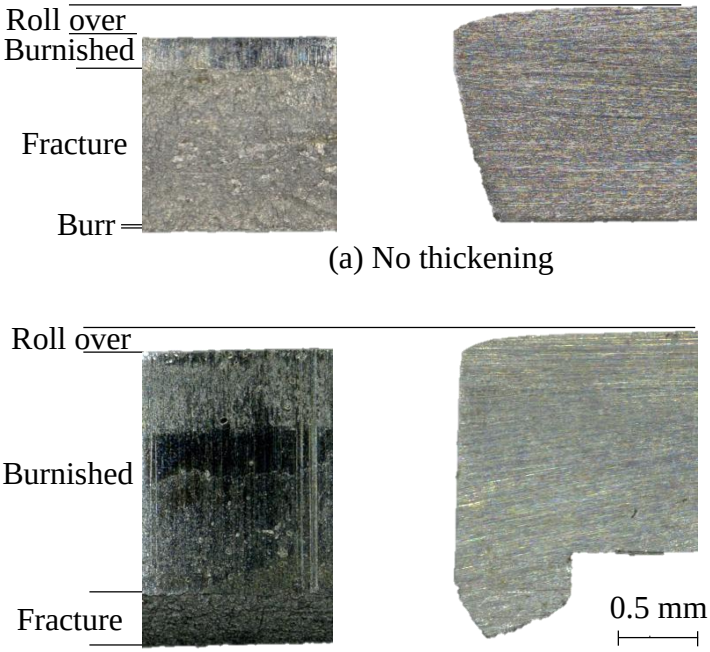

Fig. 2.28. Surface and cross-section of sheared edge with and without thickening for R = 6mm and JSC980.

To investigate the effect of the thickening of hole edge to the fatigue strength of the punched ultra-high strength steel sheets, the plane bending and tensile fatigue tests were performed. The comparison of number of cycles to failure between punched sheets with and without thickening of hole edge for R = 6 mm and JSC980 is shown in Fig. 2.29. The bending moment and maximum load for the fatigue tests were set for 3.2 N·m and 14 kN, respectively. It was found that the thickening of hole edge also effective in improving the fatigue strength of the punched ultra-high strength steel sheets. The effectiveness of the thickening of hole edge in improving the fatigue strength was heightened by utlilization of the step die for the thickening.

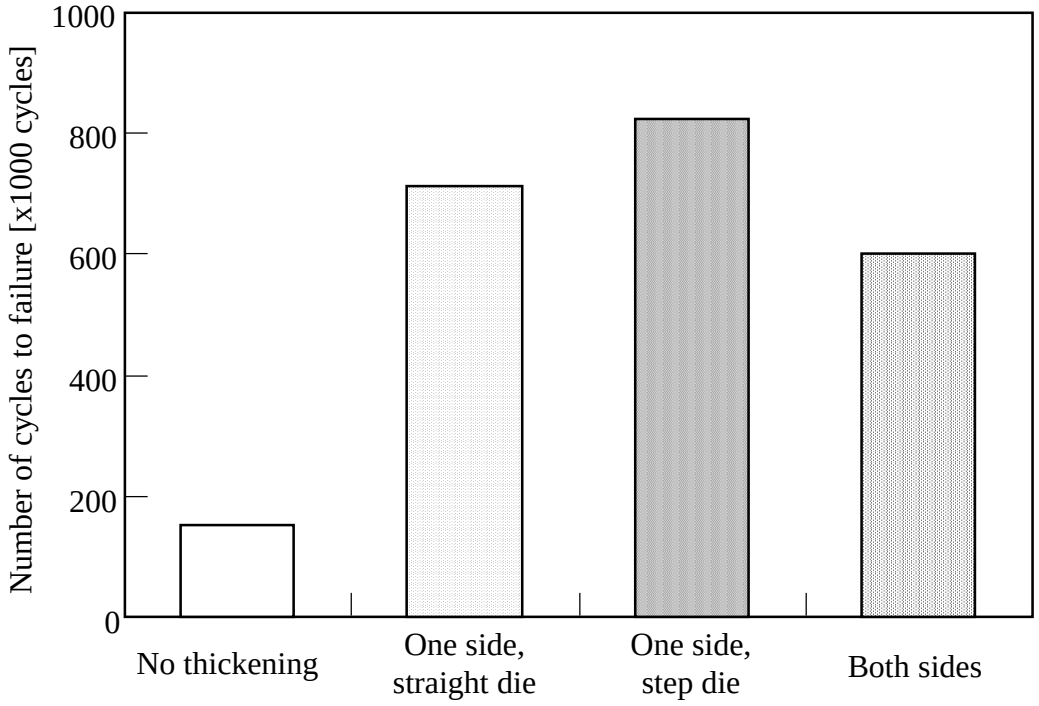

(a) Bending

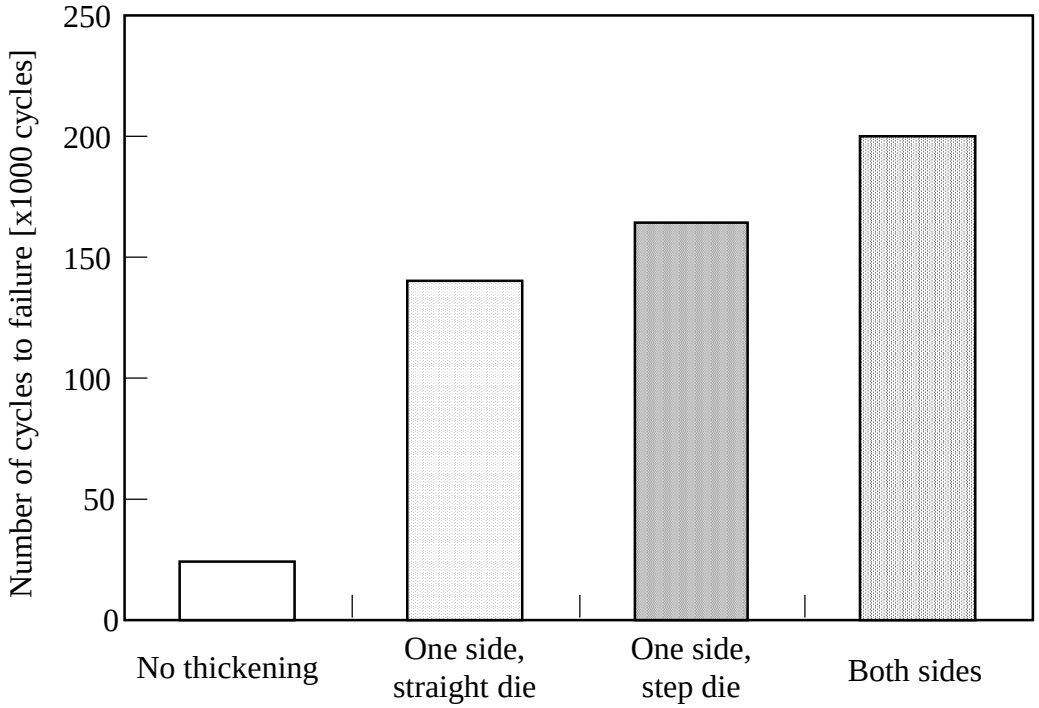

(b) Tensile

Fig. 2.29. Comparison of number of cycles to failure between punched sheets with and without thickening of hole edge for R = 6 mm and JSC980.

2.6. Conclusions

The hole edge of the punched high strength steel sheets was thickened to improve the strengths of the punched sheets. The results are summarized as follows:

1. For the round punch having a corner radius of 6 mm, no defects occurred.
2. The increase in total thickness for both sides and one side thickening of the hole edge was 31% and 54% of the initial sheet thickness, respectively.
3. The fatigue life for the punched sheet for the thickened hole edge was improved by the thickness increase, the smooth sheared surface and the harder the surface around the hole edge.
4. Both sides thickening of the hole edge was effective in the improvement of fatigue life of punched sheet for tensile fatigue test, while one side thickening for plane bending fatigue test.
5. The thickening around the hole edge was effective also in improving fatigue life of the punched ultra-high strength steel sheet.

2.7. References

[1] M. Kleiner, M. Geiger, A. Klaus: Manufacturing of lightweight components by metal forming, CIRP Annals - Manufacturing Technology, 52-2 (2003), 521-542.

[2] K. Mori, S. Maki, Y. Tanaka: Warm and hot Stamping of ultra-high tensile strength steel sheets using resistance heating, CIRP Annals - Manufacturing Technology, 54-1 (2005), 209-212.

[3] D.J. Thomas, M.T. Whittaker, G. Bright, Y. Gao, The influence of mechanical and CO_2 laser cut-edge characteristics on the fatigue life performance of high strength automotive steels, Journal of Material Processing Technology 211 (2) (2011) 263-274.

[4] L. Sánchez, F. Gutiérrez-Solana, D. Pesquera: Fatigue behaviour of punched structural plates, Engineering Failure Analysis, 11-5 (2004), 751-764.

[5] Y. Murakami, S. Kodama, S. Konuma: Quantitative evaluation of effects of non-metallic inclusions on fatigue strength of high strength steels. I: Basic fatigue mechanism and evaluation of correlation between the fatigue fracture stress and the size and location of non-metallic inclusions, International Journal of Fatigue, 11-5 (1989), 291-298.

[6] K. Mori, Y. Abe, Y. Suzui: Improvement of stretch flangeability of ultra-high strength steel sheet by smoothing of sheared edge, Journal of Material Processing Technology, 210-4 (2010), 653-659.

[7] S. Thipprakmas, S. Rojananan, P. Paramaputi: An investigation of step taper-shaped punch in piercing process using finite element method, Journal of Material Processing Technology, 197-1/3 (2008), 132-139.

[8] H. Murakami, N. Kasahara, Y. Mochiduki, H. Kanamaru, T. Imura: Evaluation of adhesion resistance of PW punch in fine piercing of steel plate, Journal of JSTP, 50-577 (2009), 119-123 [In Japanese].

[9] T. Matsuno, Y. Kuriyama, H. Murakami, S. Yonezawa, H. Kanamaru: Effects of punch shape and clearance on hole expansion ratio and fatigue properties in punching of high strength steel sheets, Steel Research International, 81-9 (2010), 853-856.

Chapter 3

Punching process including thickening of hole edge of high strength steel sheet

3.1. Introduction

The reduction in weight of automobiles is effective in improving the fuel efficiency, and forming processes of lightweight materials have been actively developed [1]. Among lightweight materials, high strength steel sheets are the most attractive for body-in-white parts due to the high specific strength and cost competitiveness. In stamping operations of high strength steel sheets, large springback, small formability, short tool life, etc. are problematic [2].

Body-in-white parts are generally punched to make many holes for joining, paint removing, attachment, reduction in weight, etc. In punching of high strength steel sheets, tools tend to wear and chip due to large punching load, and thus the tool life is short [3,4]. In addition, the quality of the sheared edge deteriorates due to early onset of cracks for the small ductility, the increase in rough fracture surface.

In high strength steel sheets, the static strength of formed products is almost proportional with the strength of the sheet, whereas the increase in fatigue strength becomes gradually small [5]. In addition, onset and progress of fatigue cracks of the punched high strength steel sheets are accelerated around holes due to concentration of stress, particularly for rough fracture surface and sharp burr of the sheared edge [6]. Therefore, the improvement of the quality of the sheared edge of punched sheets is useful for increasing the fatigue life. Thipprakmas et al. [7] improved the quality of the punched edge of aluminium sheets by shaving with a taper punch. Kim et al. [8] developed a burr-free punching process consisting of mechanical half piercing and hydro counter punching. Mori et al. [9] smoothed the fracture surface of the sheared edge using the conical punch to improve the hole expansion ratio of the punched ultra-high strength steel sheet. Mori et al. [10] developed a warm and hot punching process using resistance heating to improve the quality of sheared edge of the ultra-high strength steel sheet. Matsuno et al. [11] employed

a punch having a round corner and an inclined bottom for punching of thick high strength steel sheets. Although the fatigue strength is improved by the quality of the sheared edge, the improvement is not enough to extend the applicable range of ultra-high strength steel sheets.

The concentration of stress around the punched hole is relieved by thickening the hole edge by means of hole flanging. This leads to the improvement of the fatigue strength. Since the hole flanging stage is added to the punching process, the number of stages increases by one.

In the present study, a punching process including thickening of a hole edge of high strength steel sheets was developed to improve fatigue strength of the punched sheets. Shapes of a punch and die were design for succession of punching and thickening stages. The effect of the thickening on the strength of the punched sheets was evaluated from the experiment.

3.2. Punching process including thickening of hole edge

To improve the fatigue strength of punched high strength steel sheets, an edge of the punched hole was thickened. A hole flanging operation is conventionally performed subsequently to a punching operation, and thus the number of stages increases by one. In the present study, a pair of punch and step die was designed to include the thickening stage in the punching process as shown in Fig. 3.1. The sheet is punched by the bottom of the punch, and subsequently the hole edge is thickened by the taper of the punch and the step of the die. The punched hole is smaller than the desired hole, and the edge is thickened by deforming the small hole into the desired one. This makes good use of punching loss of material. In addition, it is easy to install the pair of punch and die in conventional die sets.

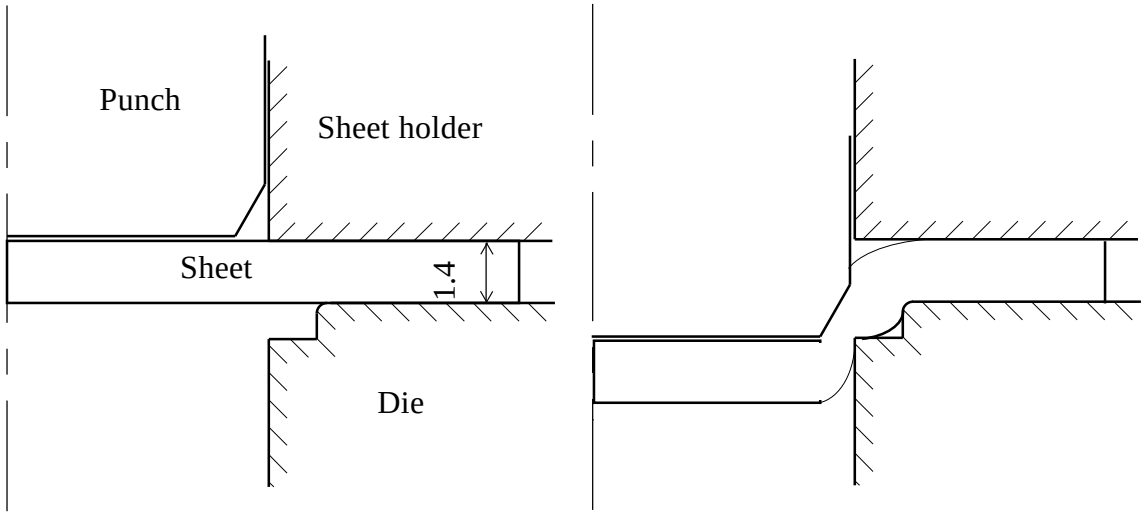

Fig. 3.1. Punching process including thickening of hole edge for increasing fatigue life of high strength steel sheet.

The amount of thickening of hole edge in the punching process including edge thickening is influenced by shapes of the punch and die. The dimensions of the tools used in the punching process of the high strength steel sheets are shown in Fig. 3.2. The shape of the die was fixed in this study.

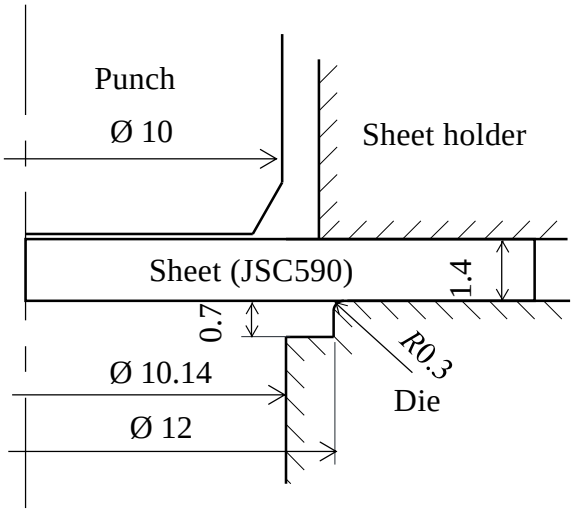

Fig. 3.2. Dimensions of tools used in punching process of high strength steel sheet.

The taper, taper step and round step punches shown in Fig. 3.3 are used for the punching process, where θ and R are the taper angle and the profile radius of the punch,

respectively. In the taper punch, the sheet is punched and thickened simultaneously, whereas in the taper step and round step punches, the sheet is sheared by the bottom of the punch, and then the hole edge is thickened by the taper and round of the punch.

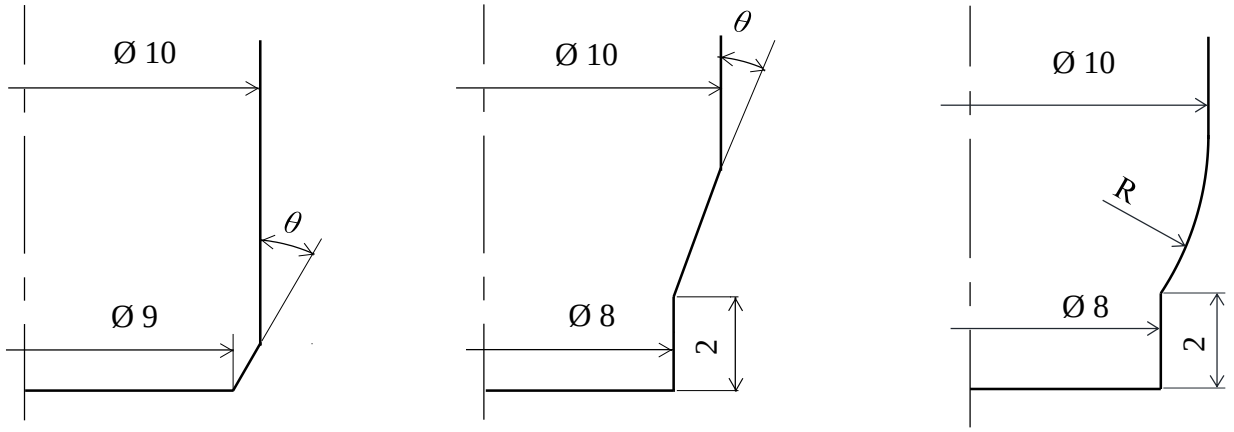

(a) Taper punch (b) Taper step punch (c) Round step punch

Fig. 3.3. Punches used for punching process of high strength steel sheet.

The conditions of the punching process including thickening of hole edge of ultra-high strength steel sheets are given in Table 3.1. The sheets were punched by a 50 kN screw driven type universal testing instrument. The thickness, length and width of the sheet were 1.4, 30 and 30 mm, respectively, and the center of the sheet was punched. Each punching test was performed at least two times to prevent the scatter of results.

Table 3.1.

Conditions of punching process of high strength steel sheet.

Taper angle of punch	θ = 10, 20, 30 and 40^o
Profile radius of punch	R = 2, 4, 6 and 8 mm
Punch	SKD11
Die	SKD11
Punching speed	0.08 mm/s
Lubrication	Rust prevention oil

The high strength steel sheets JSC590 having 1.4 mm in thickness were used in the experiment. The mechanical properties of these sheets measured from the tensile test were shown in Table 2.1.

The finite element simulation using the commercial software ABAQUS was performed under an assumption of axi-symmetric deformation to design the tools. The sheet was modelled to be elastic-plastic and isotropic, whereas the die, sheet holder and punch were assumed to be rigid. The sheet was divided into 4-node quadrilateral ring elements. The coefficient of friction at the interfaces between the tools and sheet was assumed to be 0.1. ALE adaptive remeshing was employed to simulate severe plastic deformation in the punching process, and the Gurson damage model developed by Tvergaard [12] was included to simulate fracture in punching.

Gurson's yield criterion is defined as the following function of a void volume fraction *f*:

$$\Phi = \left(\frac{\bar{\sigma}}{\sigma_y} \right)^2 + 2q_1 f \cosh\left(q_2 \frac{3\sigma_m}{2\sigma_y} \right) - \left(1 - q_3 f^2\right) = 0 , \quad (1)$$

where $\bar{\sigma}$ is the equivalent stress, σ_y is the tensile yield stress and σ_m is the hydrostatic stress. Tvergaard (1991) determined the values of the material parameters, $q_1 = 1.5$, $q_2 = 1$ and $q_3 = q_1^2 = 2.25$.

The total change in the void volume fraction is given as:

$$\dot{f} = \dot{f}_{gr} + \dot{f}_{nucl} , \quad (2)$$

where $\dot{f}_{gr}$ is the change due to growth of existing voids and $\dot{f}_{nucl}$ is the change due to nucleation of new voids given by the strain-controlled relationship:

$$\dot{f}_{nucl} = A\dot{\bar{\varepsilon}}_m^{pl} , \quad (3)$$

where

$$A = \frac{f_N}{s_N \sqrt{2\pi}} \exp\left[-\frac{1}{2} \left(\frac{\dot{\bar{\varepsilon}}_m^{pl} - \varepsilon_N}{s_N} \right)^2 \right], \quad (4)$$

where ε_N is the mean value for void nucleation, s_N is the standard deviation and f_N is the volume fraction of the nucleated voids.

The material constants used in the calculation are shown in Table 3.2. The input parameters for the damage model were determined by equalising the calculated shape of

the sheared surface with that for the experimental result in the simulation of the punching process using a flat punch.

Table 3.2.

Material constant used in calculation.

Young`s modulus (MPa)	210000
Poisson`s ratio	0.3
Initial relative density	0.995 (f_0 = 0.005)
Void nucleation parameters	ε_N = 0.3, s_N = 0.1 and f_N = 0.04
Porous failure criteria	f_F = 0.25 and f_c = 0.15

3.3. Results of punching with thickening of hole edge

3.3.1. Deformed shape

The calculated deformation behaviors of the sheet during the punching for the taper and taper step punches having $\theta = 30^o$ are shown in Fig. 3.4. For the taper punch, the sheet is punched and thickened for the punch stroke s = 2.1 mm. For the taper step punch, the sheet is punched in the former stage, and then the hole edge is thickened.

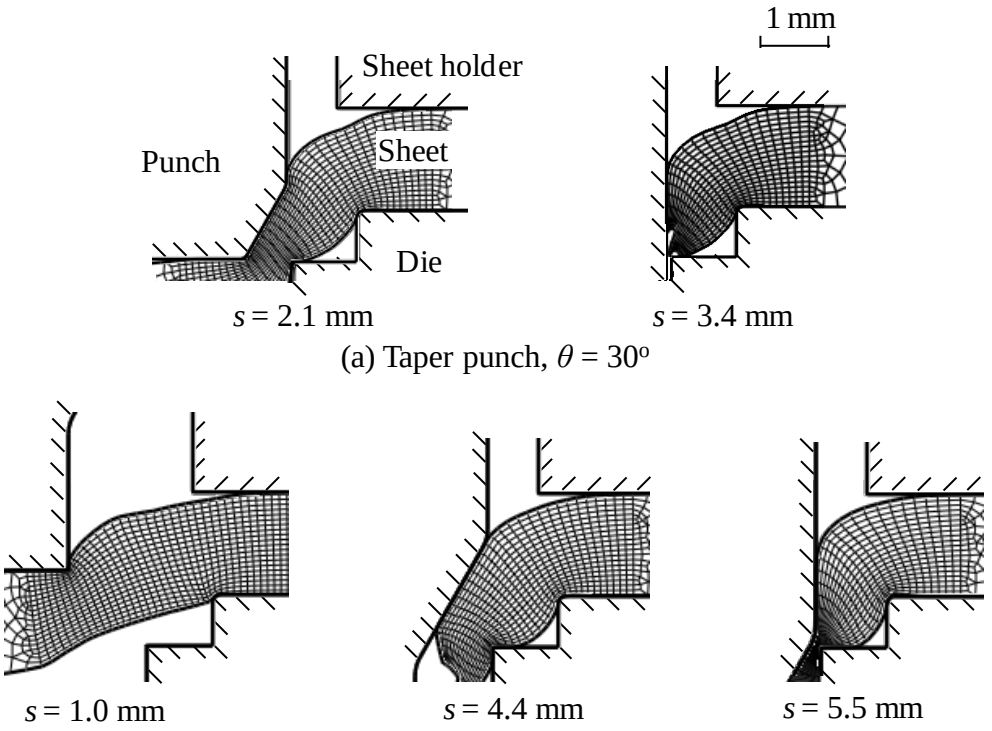

Fig. 3.4. Calculated deformation behaviours of sheet during punching process for taper and taper step punches having $\theta = 30^{o}$.

The variations in the height of the burnished surface h and the width of a thickened edge w with the punch taper angle θ for the taper and taper step punches are shown in Fig. 3.5. As the taper angle of the punch increases, the height of the burnished surface h and the width of the thickened edge w decrease, whereas the taper angle was limited to $\theta = 10^{o}$ due the increase in stroke required for punching. The thickened edge for the taper step punch has larger h and w than that for the taper punch. The width of thickened edge and the height of burnished surface for the taper step of $\theta = 10^{o}$ is the largest.

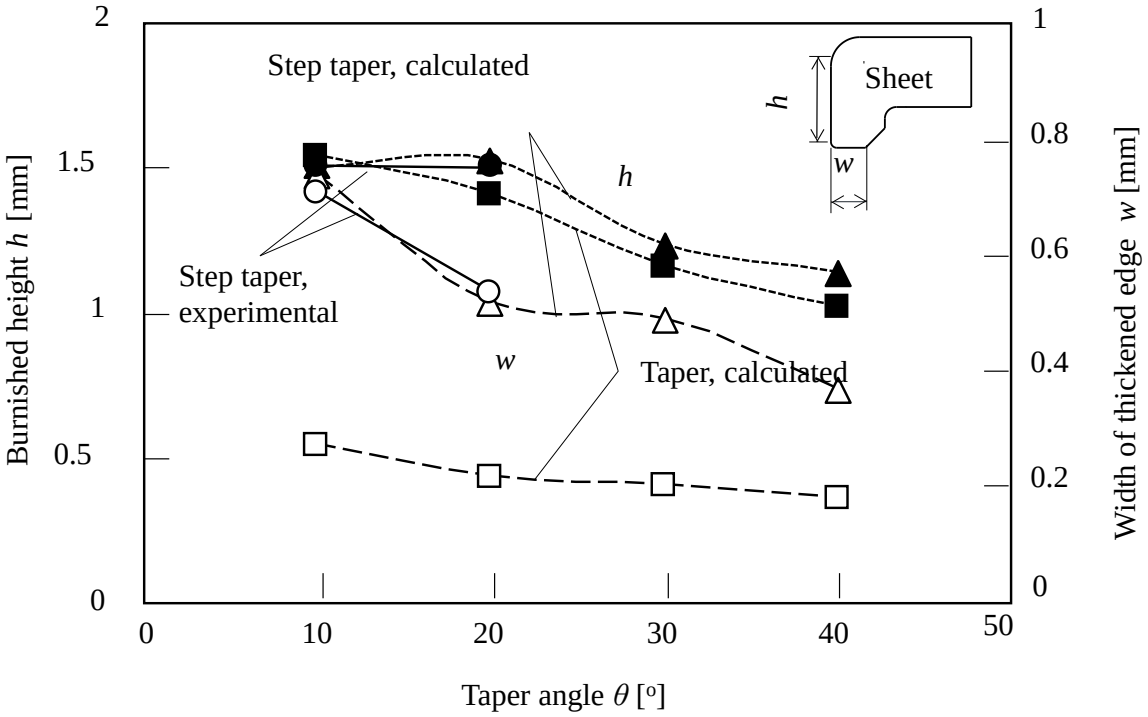

Fig. 3.5. Variations in h and w with punch taper angle θ for taper and step taper punches.

The variations in h and w with the punch profile radius R obtained from the calculation for the round step punch are shown in Fig. 3.6. The height of the burnished surface h and the width of the thickened edge w are optimum for the profile radius R = 6 mm.

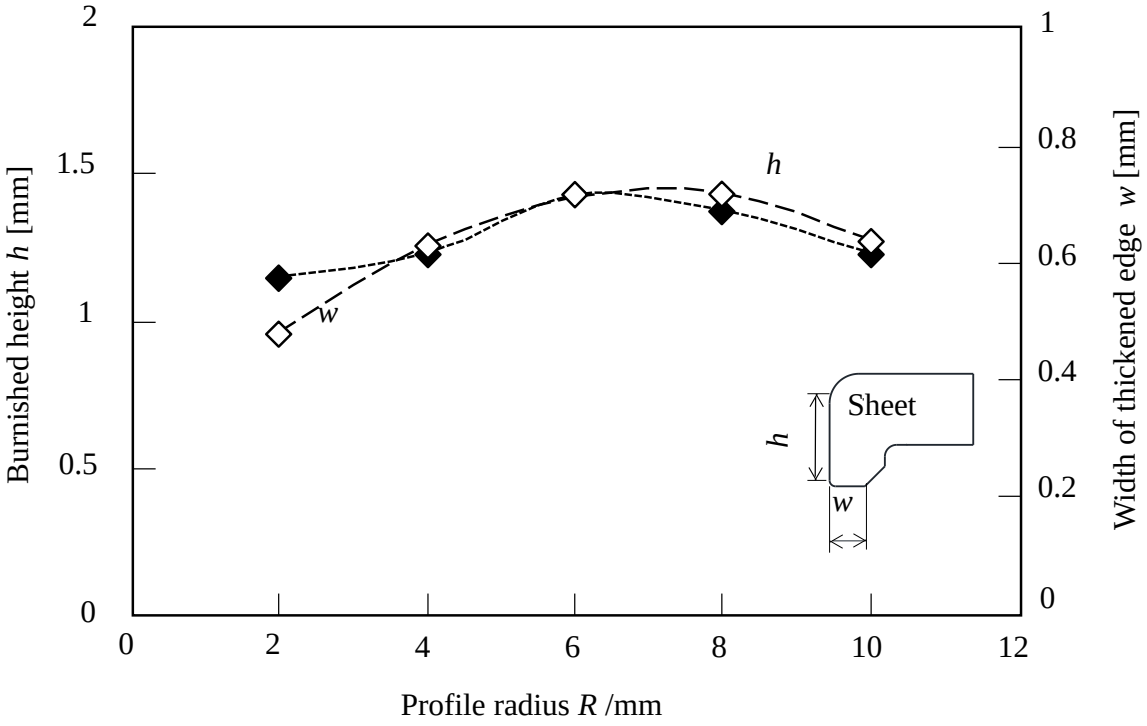

Fig. 3.6. Variations in h and w with punch profile radius R for round step punch.

The forming load-stroke curves obtained from the experiment for thickening using the taper step punch of $\theta = 10^{o}$ and the round step punch of $R = 6$ mm are compared with that without thickening using a flat punch in Fig. 3.7, where the ratio of clearance between the punch and die to the sheet thickness for the flat punch was 20%. The forming loads with thickening have two peaks due the punching and thickening processes. The maximum forming load with the thickening for the taper and round step punches increase by 35% and 28% in comparison with that without thickening, respectively. The stroke for the round step punch is 60% of that for the taper step punch and the forming load is lower.

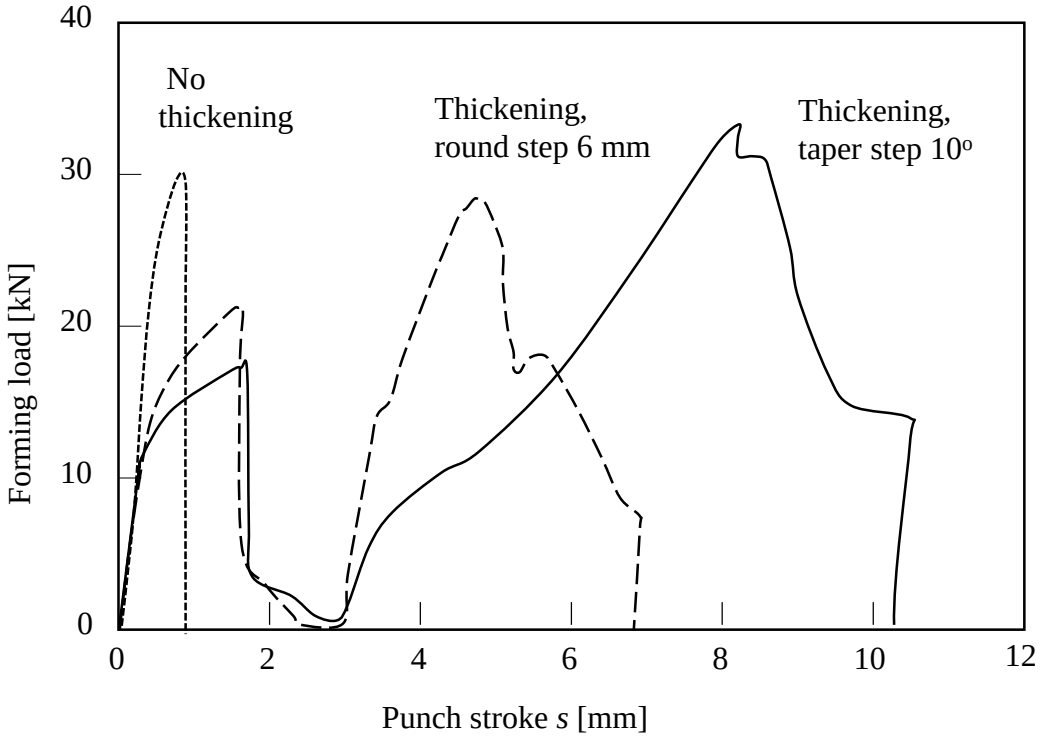

Fig. 3.7. Forming load-stroke curves obtained from experiment for punched sheet with and without thickening for taper step of $\theta = 10^{o}$ and round step punch of $R = 6$ mm.

3.3.2. Quality of sheared edge

A comparison of surface and cross-section of the sheared edge between the punched sheet with and without the thickening of the hole edge are shown in Fig. 3.8. Although the area of the rough fracture surface for the punching is large, the rough fracture surface reduces for the thickening. The cross-section of the sheared edge for taper step

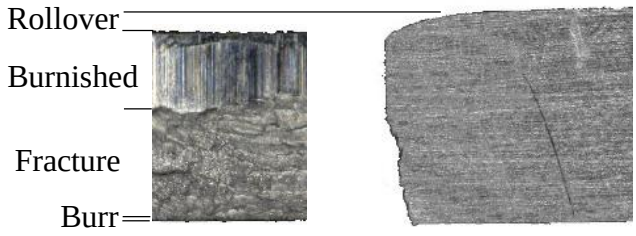

(a) No thickening

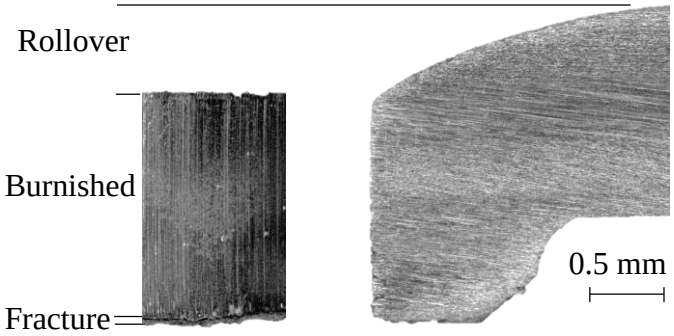

(b) Thickening, taper step 10^{o}

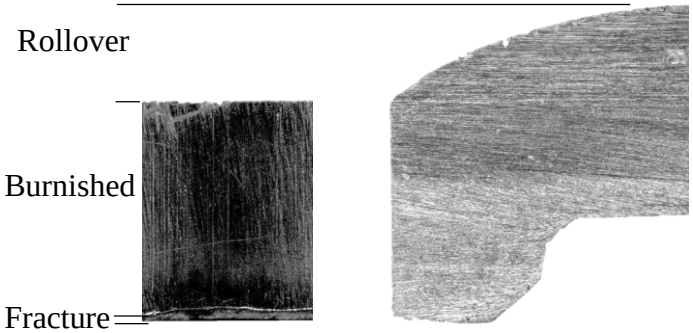

(c) Thickening, round step 6 mm

Fig. 3.8. Comparison of surface and cross-section of sheared edge between punched sheet with and without thickening of hole edge.

The distributions of the surface roughness of the sheared edge in the thickness direction for punched sheets with and without the thickening of the hole edge are shown in Fig. 3.9. The surface roughness was measured at intervals of 0.1 mm in the thickness direction. The surface roughness of the sheared edge for the thickening is smaller than that for no thickening.

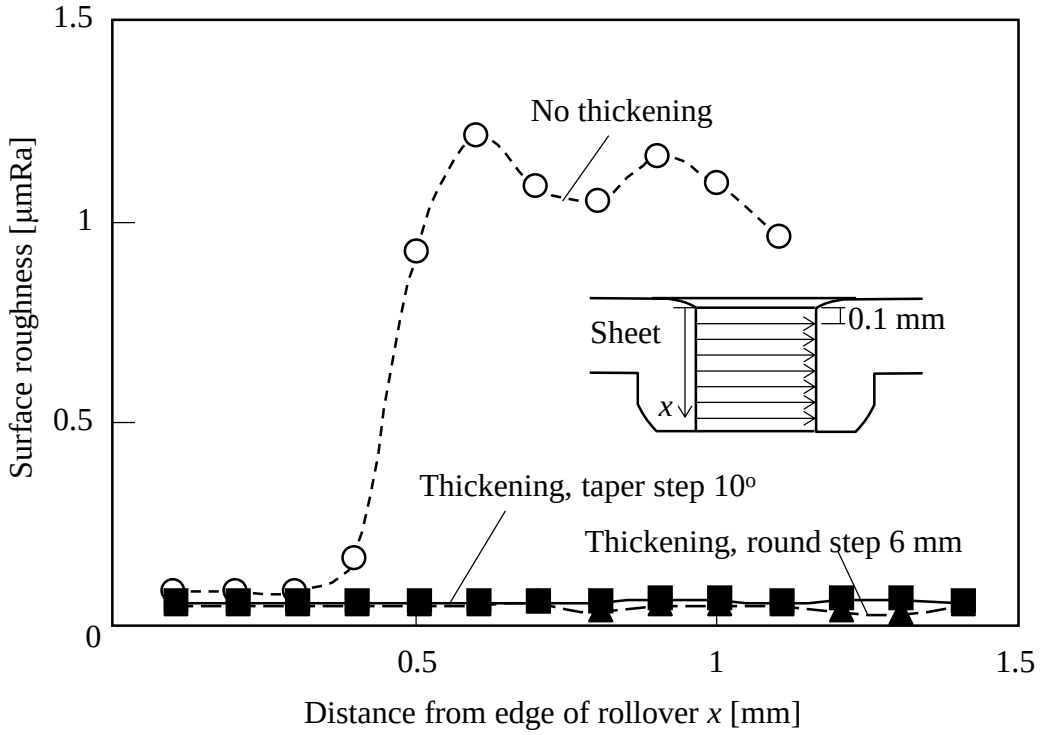

Fig. 3.9. Distributions of surface roughness of sheared edge in thickness direction for punched sheets with and without thickening of hole edge.

The distributions of the surface hardness of the sheared edge in the thickness direction for the punched sheets with and without the thickening of the hole edge are shown in Fig. 3.10. The hardness was measured in the cross-section at 0.2 mm from the sheared edge. The surface hardness for the thickening is higher than that for no thickening, due to the ironing process during the thickening.

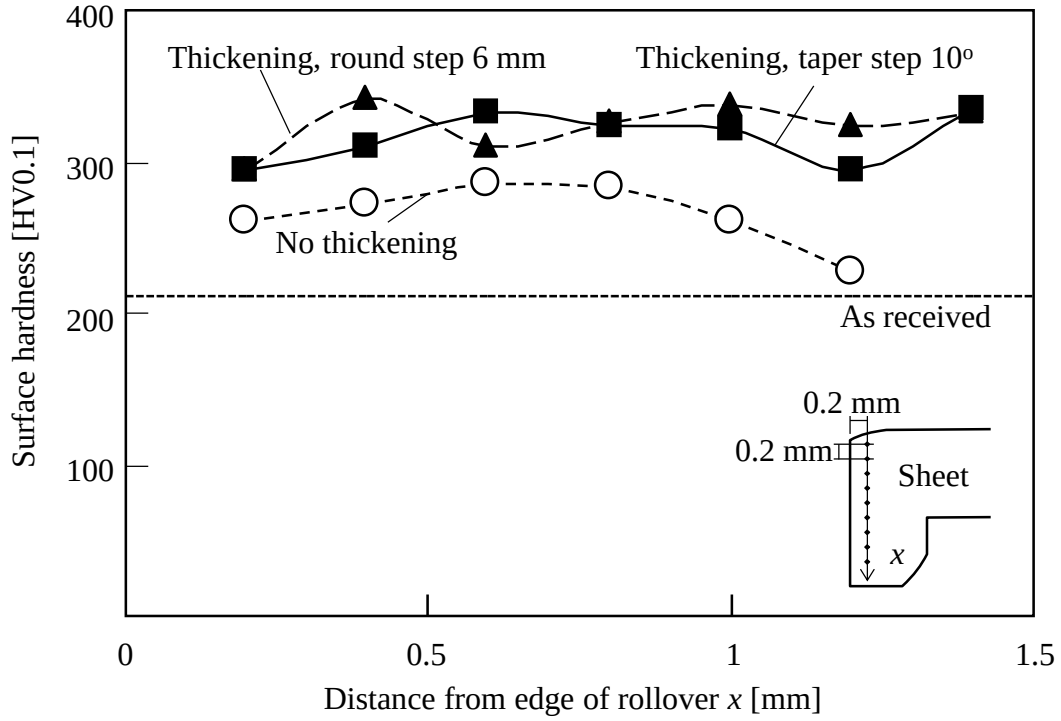

Fig. 3.10. Distributions of surface hardness of sheared edge in thickness direction for punched sheets with and without thickening of hole edge.

3.4. Strength of punched sheet

3.4.1. Static strengths

A static tensile strength were measured to evaluate the static strength of the punched sheet with the thickening of the hole edge. The procedure and dimension of specimen for the static tensile test were shown in Fig. 2.20. The static strength of the punched sheets was measured as the maximum loads in the static tensile test.

The comparison of maximum load in the static tensile test between the punched sheets with and without thickening is shown in Fig. 3.11. The small increase in the static strength for the thickening was due to the relatively small thickening area around the hole edge.

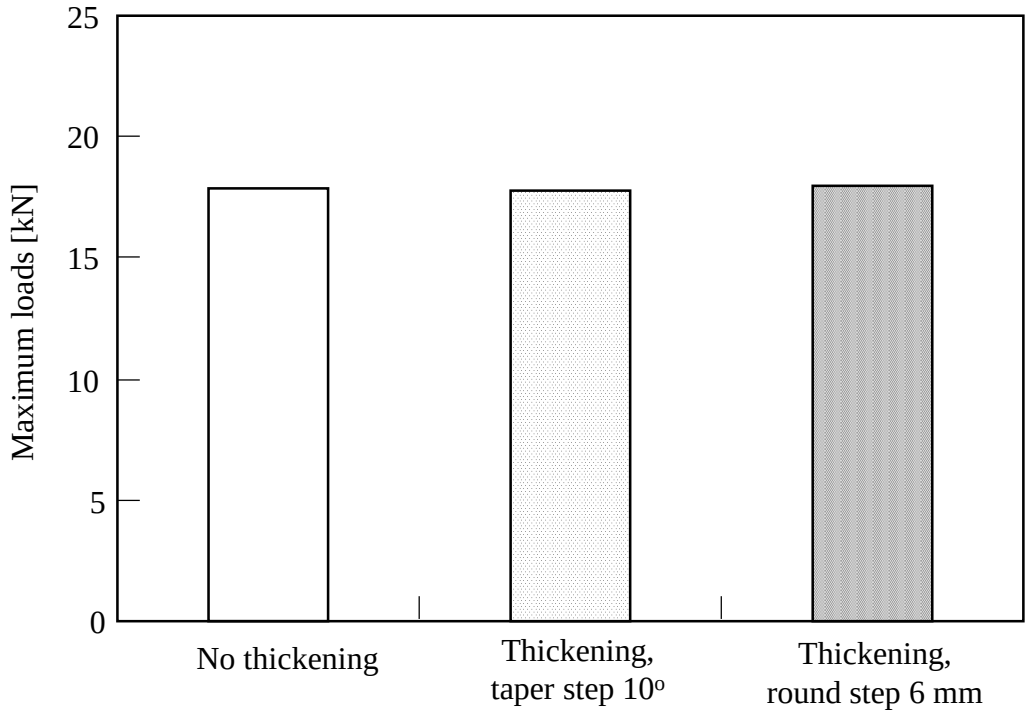

Fig. 3.11. Comparison of tensile static strength between punched sheets with and without thickening of hole edge.

3.4.2. Fatigue strength

The bending and tensile fatigue tests were performed to measure the fatigue strength of the punched sheet with the thickening of the hole edge. The frequency for the alternative bending and repeated tensile fatigue tests were set at 25 Hz and 50 Hz, respectively. The fatigue test was ended up when the sheet was ruptured.

The plots of the bending moments and maximum loads versus the number of cycles to failure for the bending and tensile fatigue tests of the punched sheets with thickening are compared with those without thickening in Fig. 3.12. The fatigue strength of the punched sheets with thickening is higher than that without thickening. The improvement of the fatigue strength for thickening is due to the thickness increases, the small surface roughness and the large hardness around the sheared edge. It was found that thickening of the hole edge is useful for improving the fatigue strength of punched high strength steel sheet.

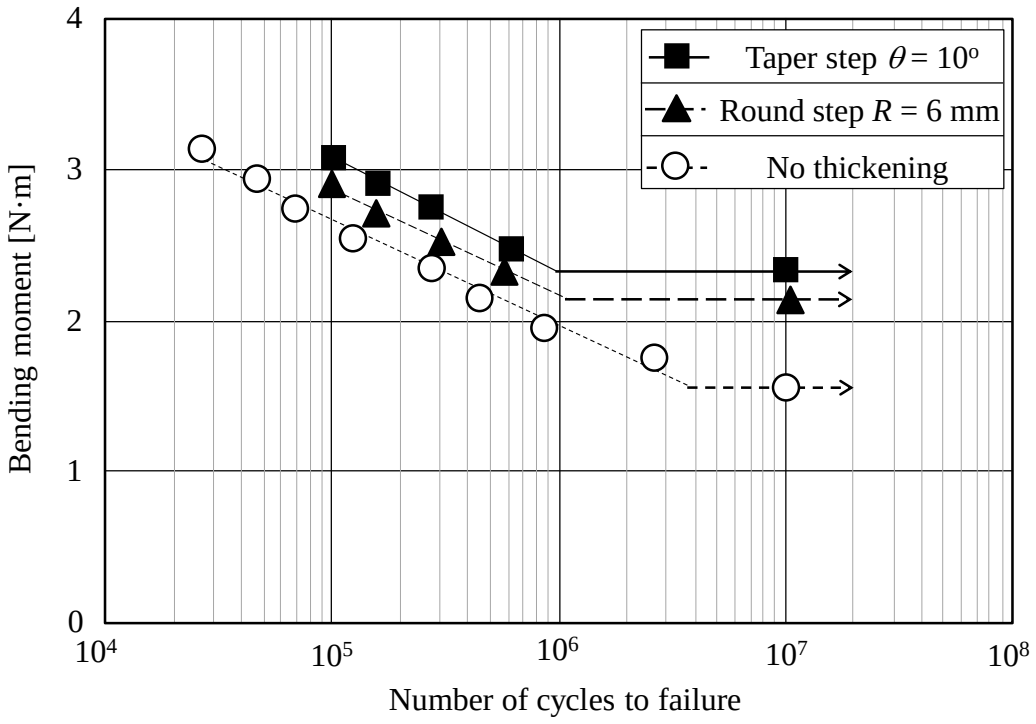

(a) Plane bending fatigue test

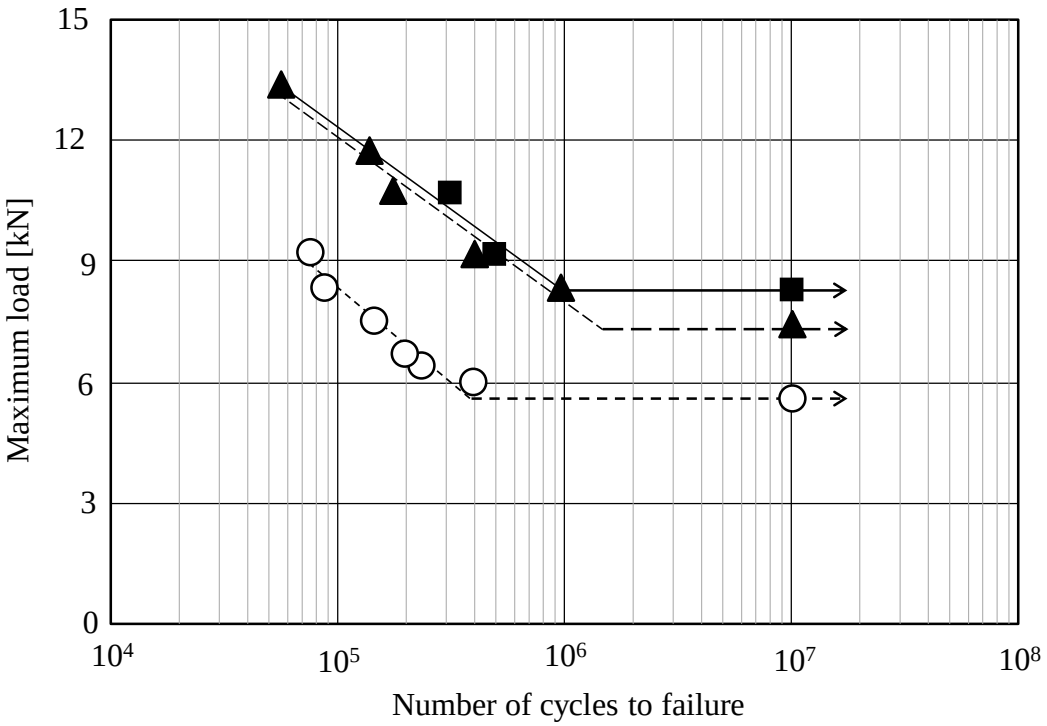

(b) Tensile fatigue test

Fig. 3.12. Plots of bending moments and maximum loads versus number of cycles to failure of punched sheets with and without thickening for (a) bending and (b) tensile fatigue tests.

3.4.3. Measurement of residual stress around hole edge

The effect of the thickening of the hole edge in the residual stress in the thickness direction of the sheared edge was measured by the X-ray diffraction. The procedure of the X-ray diffraction for measurement of the residual stress in the sheared edge is shown in Fig. 3.13. The cconditions for the measurement of residual stress is shown in Table 3.3

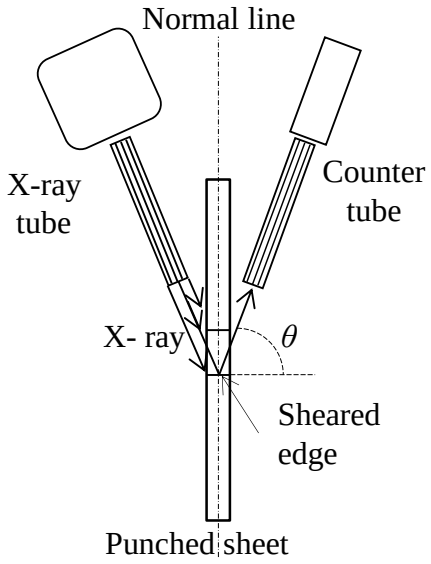

Fig. 3.13. Procedure of X-ray diffraction for measurement of residual stress of sheared edge.

Table 3.3.
Conditions for measurement of residual stress.

Equipment	RINT 1100
ψ angle (deg)	0.00，18.00，27.00，33.00，45.00
Diffraction angle 2θ (deg)	153.0 ~ 157.8

The residual stresses in the thickness direction in the sheared edge of the punched sheets with and without thickening are shown in Fig. 3.14. Although the residual stress without thickening is tensile, the stress with thickening becomes compressive due to the ironing during the thickening stage. The compressive residual stress for the taper step 10^{o} is larger than that for the round step 6 mm, thus the fatigue strength is larger.

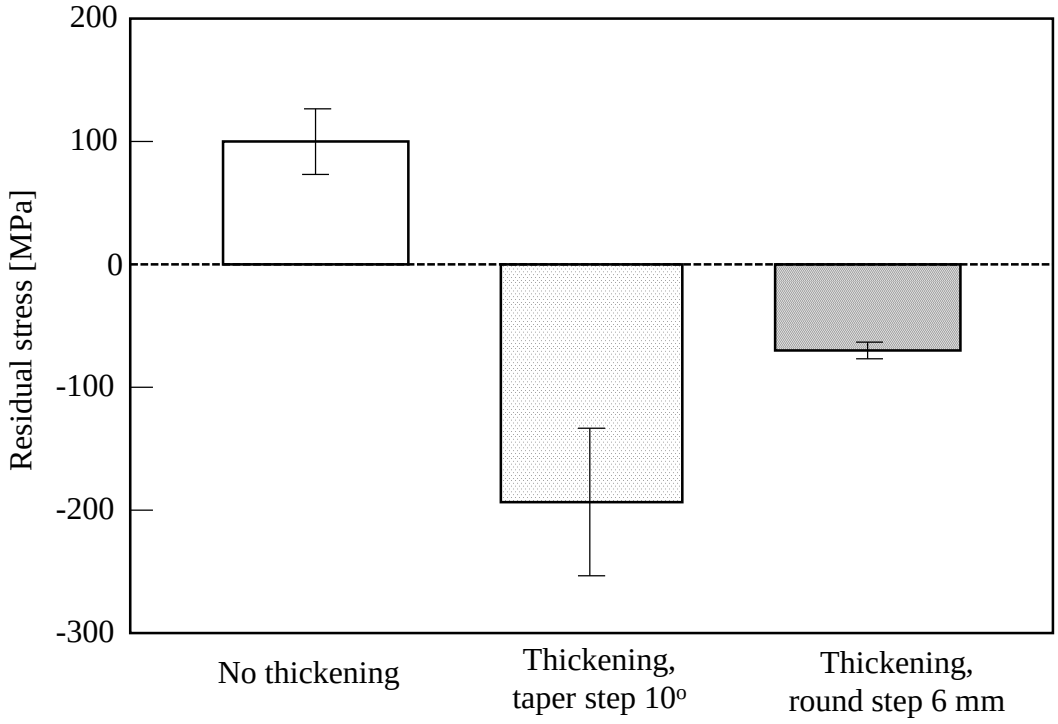

Fig. 3.14. Effect of thickening of hole edge on residual stress in sheared edge.

3.5. Conclusions

The hole edge of the punched high strength steel sheets was thickened by a 1 shot thickening process to improve the strength of the punched sheets. The results are summarized as follows:

1. The height of burnished surface of the hole edge and the width of the thickened edge for the taper step punches were larger than that for the taper punch.
2. The punch stroke for the round step punch is 60% of that for the taper step punch and the forming load is lower.
3. The quality of the sheared edge for the thickening was improved due to ironing process during the thickening stage.
4. The fatigue strength of the punched sheets with thickening was higher than that without thickening due to thicker the edge of the hole, smoother the surface of the sheared edge, and harder the surface around the hole.
5. The fatigue strength for the thickening by taper step punch was higher than that for the round step punch due to larger compressive residual stress in sheared edge.

3.6. References

[1] M. Kleiner, M. Geiger, A. Klaus, Manufacturing of lightweight components by metal forming, CIRP Annals - Manufacturing Technology 52 (2) (2003) 521-542.

[2] K. Mori, K. Akita, Y. Abe, Springback behaviour in bending of ultra-high-strength steel sheets using CNC servo press, International Journal of Machine Tools & Manufacture 47 (2) (2007) 321–325.

[3] K. Inoue, M. Suzuki, S. Nishino, K. Ohya, Y. Tomota, Effect of coating microstructure of press-working dies on sliding damage, Steel Research International 81 (9) (2010) Supplement Metal Forming 2010, 849–852.

[4] J. Eriksson, M. Olssson, Tribological testing of commercial CrN, (Ti,Al)N and CrC/C PVD coatings – Evaluation of galling and wear characteristics against different high strength steels, Surface & Coating Technology 205 (16) (2011) 4045-4051.

[5] Y. Murakami, S. Kodama, S. Konuma, Quantitative evaluation of effects of non-metallic inclusions on fatigue strength of high strength steels. I: Basic fatigue mechanism and evaluation of correlation between the fatigue fracture stress and the size and location of non-metallic inclusions, International Journal of Fatigue 11 (5) (1989) 291-298.

[6] D.J. Thomas, M.T. Whittaker, G. Bright, Y. Gao, The influence of mechanical and CO_2 laser cut-edge characteristics on the fatigue life performance of high strength automotive steels, Journal of Material Processing Technology 211 (2) (2011) 263-274.

[7] S. Thipprakmas, S. Rojananan, P. Paramaputi, An investigation of step taper-shaped punch in piercing process using finite element method, Journal of Material Processing Technology 197 (1/3) (2008) 132-139.

[8] S.S. Kim, C.S., Han, Y.S. Lee, Development of a new burr-free hydro mechanical punching, Journal of Materials Processing Technology 162-163 (2005) 524-529.

[9] K. Mori, Y. Abe, Y. Suzui, Improvement of stretch flangeability of ultra-high strength steel sheet by smoothing of sheared edge, Journal of Material Processing Technology 210 (4) (2010) 653-659.

[10] K. Mori, S. Saito, S. Maki, Warm and hot punching of ultra-high strength steel sheet, CIRP Annals - Manufacturing Technology 57 (1) (2008) 321-324.

[11] T. Matsuno, Y. Kuriyama, H. Murakami, S. Yonezawa, H. Kanamaru, Effects of punch shape and clearance on hole expansion ratio and fatigue properties in punching of high strength steel sheets, Steel Research International 2010 (2010) 853-856 (Supplement Metal Forming).

[12] Tvergaard, V., 1991, Mechanical modelling of ductile fracture. Meccanica 26 (1), 11-16.

Chapter 4

Optimization of tools shape in punching including thickening of hole edge of ultra-high strength steel sheet

4.1. Introduction

The reduction in weight of automobiles is effective in improving the fuel efficiency, and forming processes of lightweight materials have been actively developed [1]. Among lightweight materials, high strength steel sheets are the most attractive for body-in-white parts due to the high specific strength and cost competitiveness. The strength of high tensile strength steel sheets remarkably increases and ultra-high tensile strength steel sheets more than 1 GPa have been developed. In stamping operations of high strength steel sheets, large springback, small formability, short tool life, etc. are problems, particularly ultra-high strength steel sheets having a tensile strength above 1 GPa [2].

Body-in-white parts are generally punched to make many holes for joining, paint removing, attachment, reduction in weight, etc. Since the ultra-high strength steel sheets have large strength and small ductility, not only forming but also punching becomes difficult. In the punching of the high strength steel sheets, large tool wear and rough sheared edges becomes problems [3-5].

In high strength steel sheets, the static strength of formed products is almost proportional with the strength of the sheet, whereas the increase in fatigue strength becomes gradually small [6]. In addition, onset and progress of fatigue cracks of the punched high strength steel sheets are accelerated around holes due to concentration of stress, particularly for rough fracture surface and sharp burr of the sheared edge [7]. Although the fatigue strength is improved by the quality of the sheared edge [8], the improvement is not enough to extend the applicable range of ultra-high strength steel sheets. The concentration of stress around the punched hole is relieved by thickening the hole edge by means of hole flanging. This leads to the improvement of the fatigue strength.

In the previous chapter, the punching process including thickening of a hole edge of high strength steel sheets have been developed to improve fatigue strength of the punched

sheets. In this chapter, the punching process including thickening of a hole edge with a taper step punch and step die was employed to improve the fatigue strength of the punched ultra-high strength steel sheet. The taper angle of the punch and the step height of the die were optimised to increase the amount of thickening. The effect of the thickening on the strength of the punched sheets was evaluated from the experiment.

4.2. Punching process including thickening of hole edge

To improve the fatigue strength of punched ultra-high strength steel sheet, an edge of the punched hole was thickened. A hole flanging operation is conventionally performed subsequently to a punching operation, and thus the number of stages increases by one. In the present study, a pair of taper punch and step die was designed to include thickening of the hole edge in the punching process as shown in Fig. 4.1. The sheet is first punched by the tension between the taper punch and the step die. Subsequently, the hole edge is bent by the taper of the punch into the corner step of the die and the surface of the sheared edge is ironed. After sufficient filling into the corner step of the die, the excessive material is then sheared. The corner step of the die has the function of not only forming the thickened edge but also compressing the edge bottom. The function is effective for ultra-high strength steels sheets having low ductility. Although the firstly punched hole is smaller than the desired hole, the hole is formed into the desired one by the subsequent thickening stage. A part of the punching scrap is effectively utilised as thickening material in the present process. This is an ecological process for improving material efficiency. In addition, it is easy to install the present punching process in the stamping sequence.

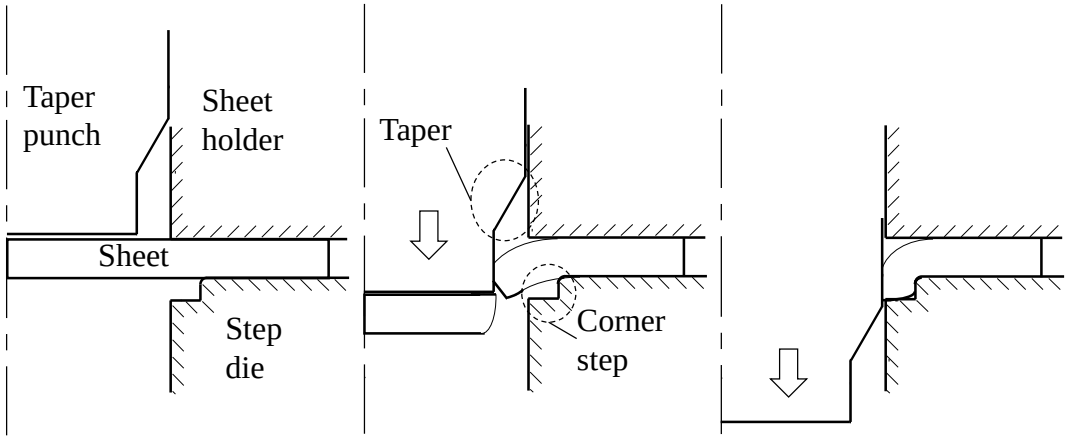

Fig. 4.1. Punching process including thickening of hole edge for improvement of fatigue strength of ultra-high strength steel sheet.

The amount of thickening of the hole edge in the punching process including edge thickening is influenced by shapes of the punch and die. The dimensions of the tools are shown in Fig. 4.2. The sheet was punched into a hole having a diameter of 10 mm after passing of the taper of the punch. The taper angle of the punch θ and the step height of the die h were changed as thickening parameters.

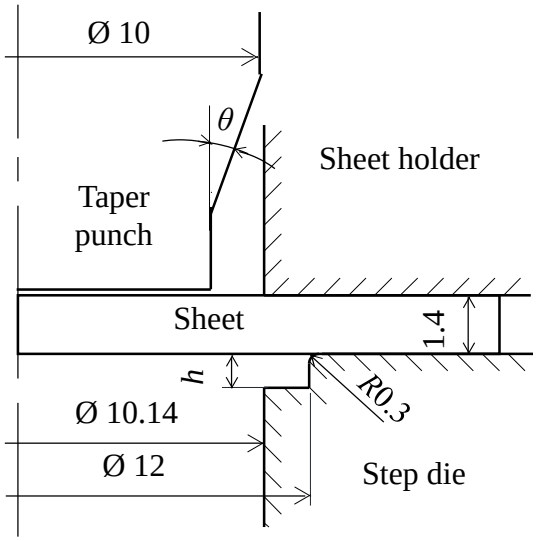

Fig. 4.2. Dimensions of tools used in punching process including thickening of hole edge of ultra-high strength steel sheet.

The conditions of the punching process including thickening of the hole edge of an ultra-high strength steel sheet are given in Table 4.1. The sheets were punched by a 50 kN screw driven type universal testing instrument. A rust prevention oil was applied to the sheets and an additional lubricant was not employed. The punch was VC-coated, whereas the die was not coated. Each punching test was performed at least two times.

Table 4.1.
Conditions of punching process of ultra- high strength steel sheet.

Taper angle of punch θ	10, 13 and 20^o
Step height of die h	0.5, 0.7, 0.9 and 1.1 mm
Punch	SKD11, VC coating
Die	SKD11, no coating
Punching speed	0.08 mm/s
Lubrication	Rust prevention oil

The ultra-high strength steel sheet JSC980 having a nominal tensile strength of 980 MPa and was used in the experiment, where the high strength steel sheet JSC590 was punched as a comparison. The 980 MPa sheets having 1.4 mm in thickness are the commonest ultra-high strength steel sheets and application to automobile body panels is recently increasing. The mechanical properties of these sheets measured from the tensile test were given in Table 2.2.

Finite element simulation using the commercial software ABAQUS was performed under the assumption of axi-symmetric deformation to examine the deformation behaviour during the punching operation. The sheet was modelled to be elastic-plastic, whereas the die, sheet holder and punch were assumed to be rigid. The coefficient of friction at the interfaces between the tools and sheet was assumed to be 0.1. The ALE adaptive remeshing was employed to simulate severe plastic deformation in the punching process, and the Gurson damage model developed by Tvergaard was included to simulate fracture in punching.

The material constants for JSC980 used in the calculation are shown in Table 4.2. The input parameters for the damage model were determined by equalising the calculated shape

of the sheared surface with that for the experimental result in the simulation of the punching process using a flat punch.

Table 4.2.

Material constants for JSC980 used in calculation.

Young's modulus	210 GPa
Poisson's ratio	0.3
Initial relative density	0.995 ($f_0 = 0.005$)
Void nucleation parameters	$\varepsilon_N = 0.3$, $s_N = 0.1$ and $f_N = 0.04$
Porous failure criteria	$f_F = 0.25$ and $f_c = 0.15$

4.3. Results of punching including thickening of hole edge

4.3.1. Deformed shape

The deformation behaviour of the sheet during punching for the taper angle of the punch $\theta = 10^o$, the step height of the die $h = 0.9$ mm and JSC980 is shown in Fig. 4.3, where s is the punch stroke. The sheet is bent and punched in the former stage by the bottom of the punch, and then the hole edge is thickened by the taper of the punch and the corner step of the die. Since the material is sufficiently filled into the corner step, a ring shaped scrap is caused.

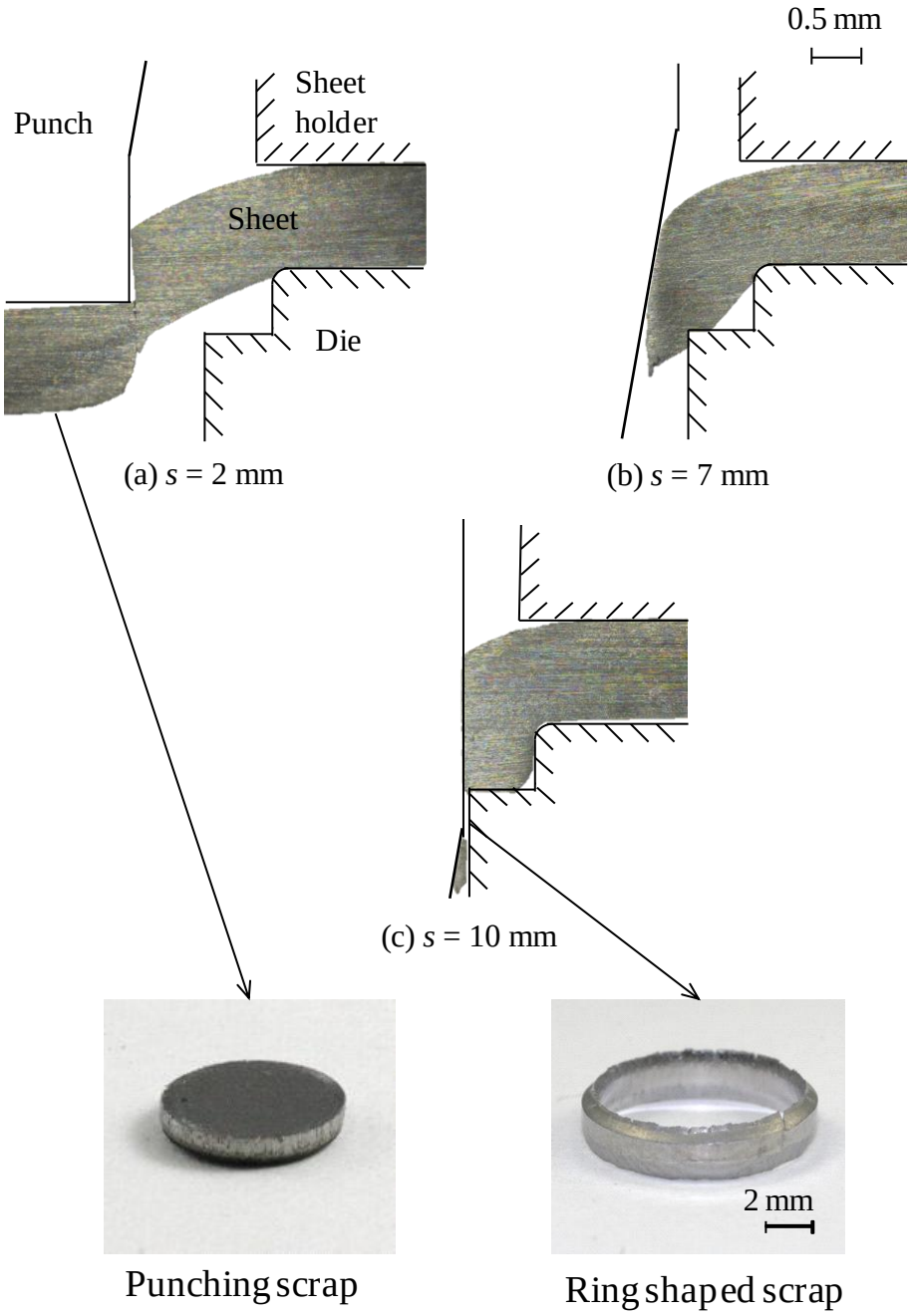

Fig. 4.3. Deformation behaviour of sheet during punching for θ = 10^{o}, h = 0.9 mm and JSC980.

The deformation behaviour during punching was calculated from the finite element simulation in detail. A comparison between the deformation behaviours obtained from the calculation and experiment for θ = 10^{o}, h = 0.9 mm and JSC980 is shown in Fig. 4.4, where the calculation results is shown as a top layer on the cross section of the experiment

results. The deformation behaviour of the sheet during punching obtained by the calculation is in almost good agreement with that by the experiment, whereas the experimental rollover is more remarkable.

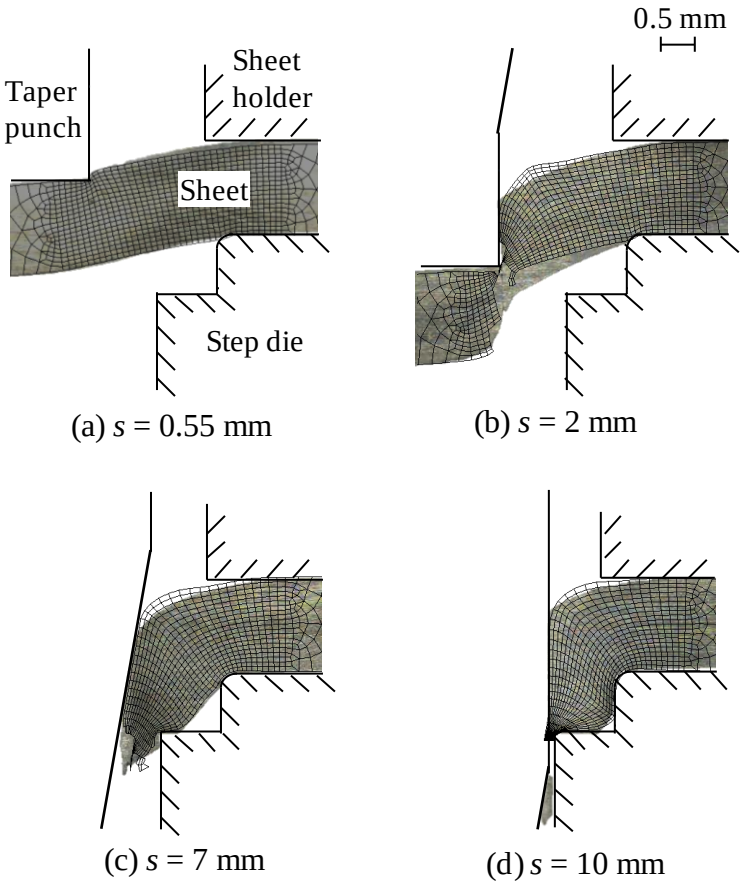

Fig. 4.4. Comparison between deformation behaviours obtained from calculation and experiment for $\theta = 10^{o}$, $h = 0.9$ mm and JSC980.

The distribution of plastic equivalent strain in the sheet calculated by finite element simulation for $\theta = 10^{o}$, $h = 0.9$ mm and JSC980 is shown in Fig. 4.5. As the punch stroke increases, the equivalent strain concentrates around the bottom corner of the punch, and the sheet is punched. The sheared edge undergoes severe deformation with the taper and upper corner of the punch.

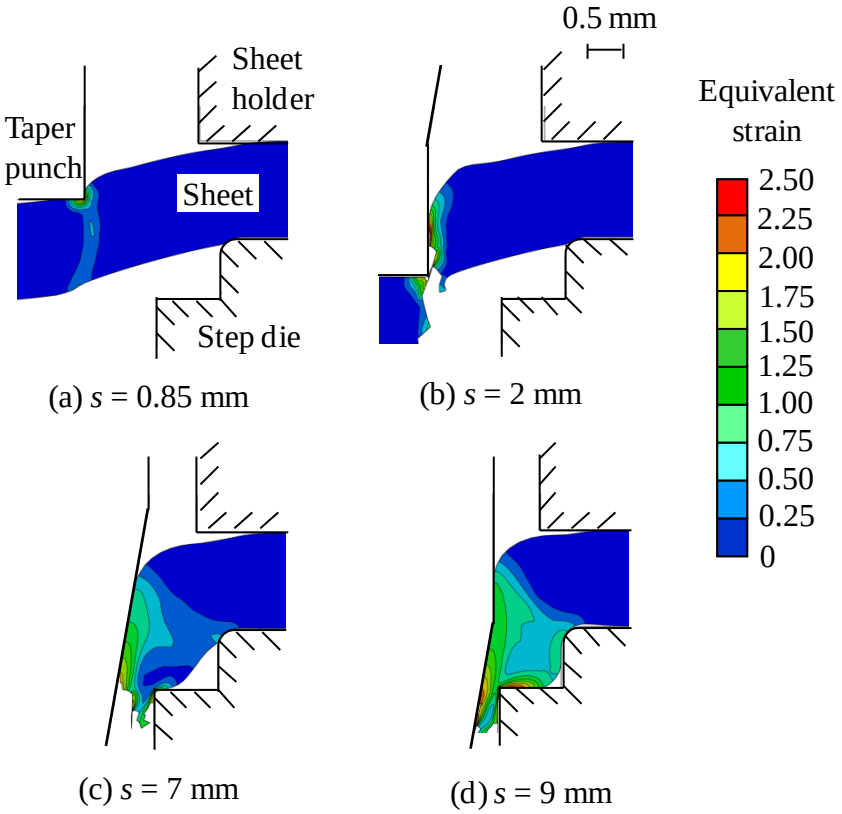

Fig. 4.5. Distribution of plastic equivalent strain in sheet calculated by finite element simulation for $\theta = 10^{o}$, $h = 0.9$ mm and JSC980.

The relationship between the width of the thickened edge and the taper angle of the punch for $h = 0.9$ mm and JSC980 is shown in Fig. 4.6. As the taper angle of the punch decreases, the width of the thickened edge increases, whereas the taper angle was limited to $\theta = 10^{o}$ due the increase in stroke required for punching. For the small taper angle, the material flow in the circumferential direction is accelerated, and thus the material filling into the corner step of the die increases. The width of the thickened edge for $\theta = 10^{o}$ is the largest, and thus $\theta = 10^{o}$ was fixed in the following experiments.

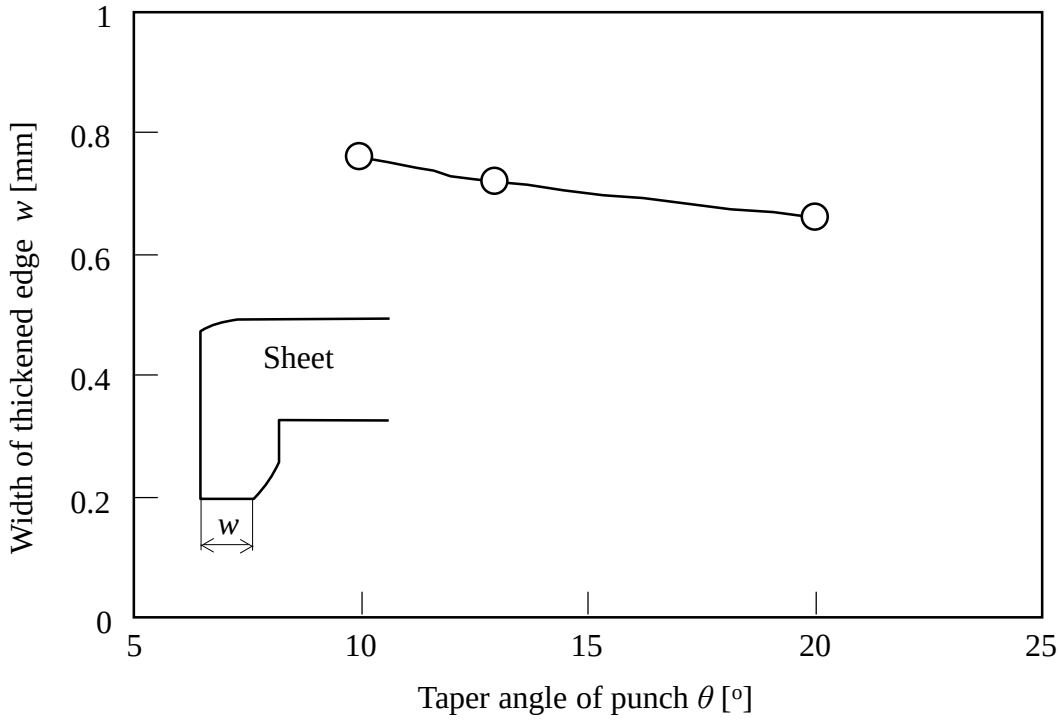

Fig. 4.6. Relationship between width of thickened edge and taper angle of punch for h = 0.9 mm and JSC980.

The relationship between the width of the thickened edge and the step height of the die for JSC980 is shown in Fig. 4.7. As the step height of the die increases, the width of the thickened edge increases. When the step height of the die is small, the sheared edge is not sufficiently flanged because of early contact with the step of the die. For h = 1.1 mm, cracks occurred at the bottom of the thickened edge because of late contact with the die step.

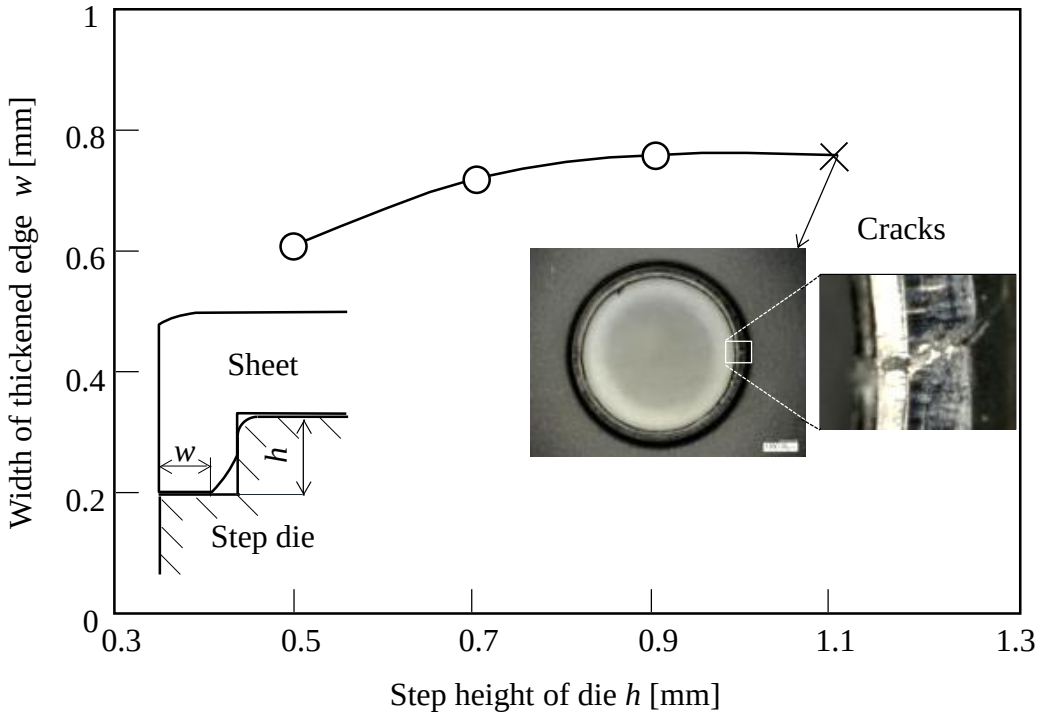

Fig. 4.7. Relationship between width of thickened edge and step height of die for JSC980.

The distributions of void volume fraction in the sheet calculated by the finite element simulation for $\theta = 10^{o}$, s = 9 mm, JSC980 and h = 0.5, 0.9 and 1.1 mm are given in Fig. 4.8. When the void fraction exceeds a certain value, the fracture occurs in the simulation of the punching stage, and thus the void fraction is extremely high around the sheared edge. The void fraction in the bottom of the thicken edge for h = 1.1 mm becomes high, whereas that in the top surface is not very high. This process can be applied to a less ductile material by decreasing the step height of the die, while the amount of thickening decreases.

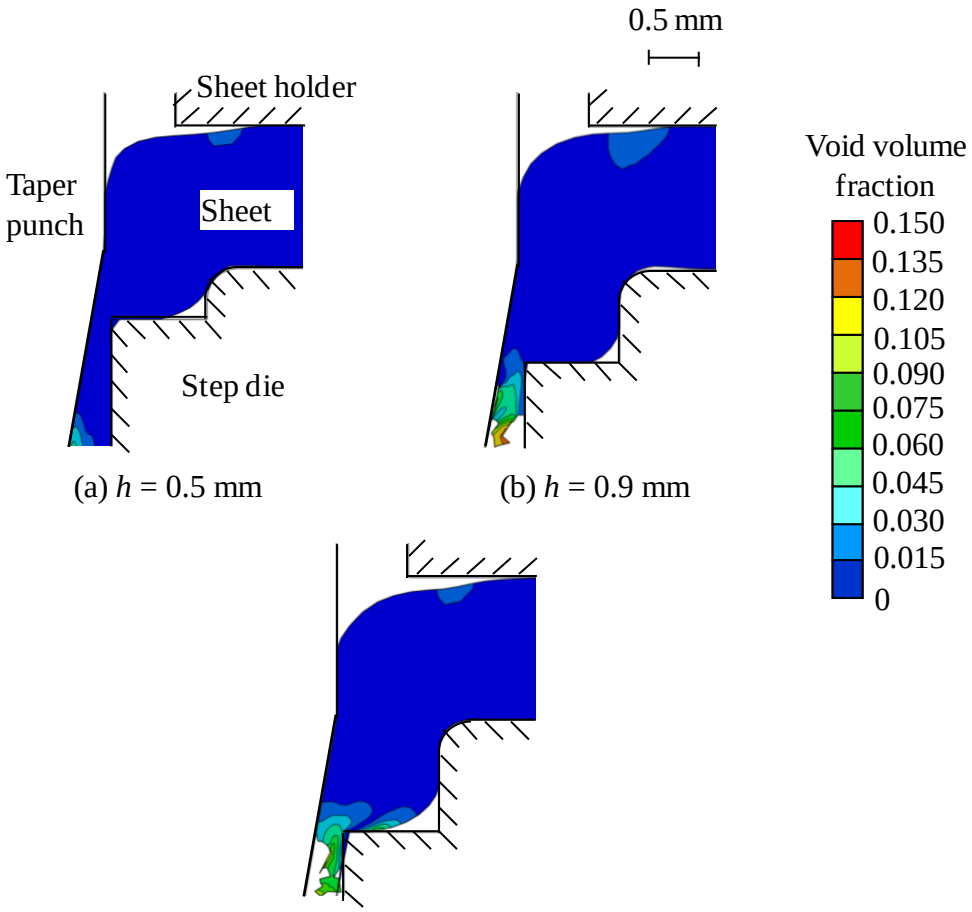

Fig. 4.8. Distributions of void volume fraction in sheet calculated by finite element simulation for θ = 10^{o}, s = 9 mm, JSC980 and (a) h = 0.5 mm (b) h = 0.9 mm and (c) h = 1.1 mm.

The forming load for h = 0.9 mm and JSC980 is compared with that without thickening using a flat punch without a taper in Fig. 4.9, where the ratio of clearance between the punch and die to the sheet thickness for the flat punch was 20%. The forming load with thickening has two peaks. The first peak is caused by punching the sheet and is smaller than that without thickening and the second peak. The second peak is mainly generated by ironing the sheared edge and by shearing excessive material after sufficient filling into the corner step of the die. The punching stroke with thickening is much larger than that without thickening.

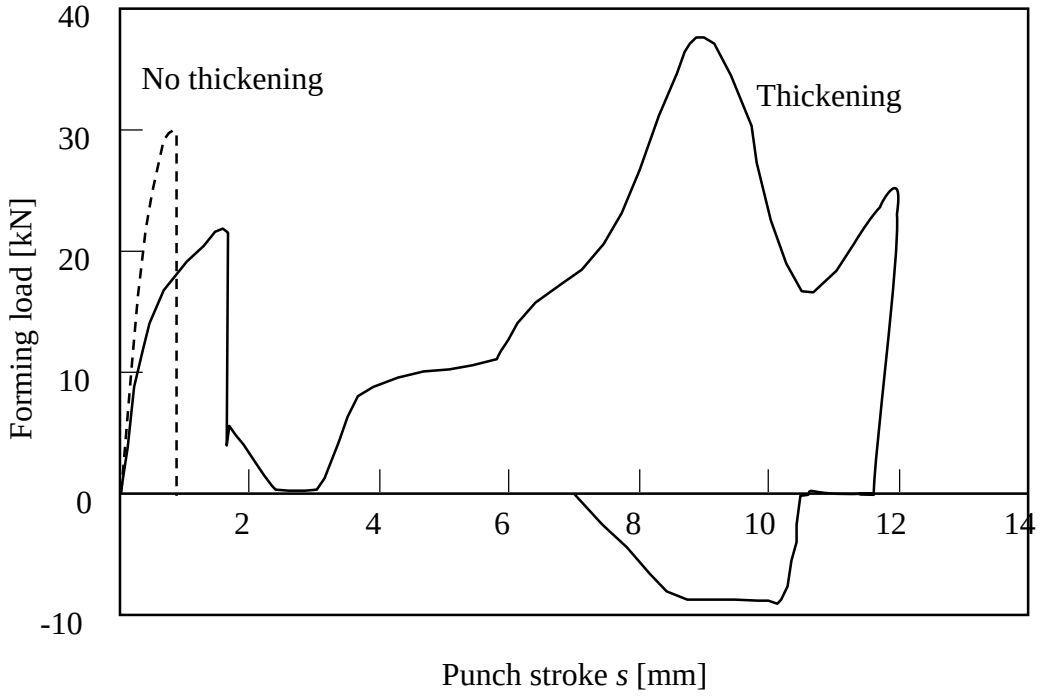

Fig. 4.9. Forming load-punch stroke curves with thickening for h = 0.9 mm and JSC980 and without thickening.

The maximum forming load and forming energy for JSC980 are illustrated in Fig. 4.10. The forming energy was calculated by integrating the forming load-punch stroke curve shown in Fig. 4.9. As the step height of the die increases, the forming load and energy increase. The forming energy with thickening becomes considerably large due to the enlargement of the punch stroke.

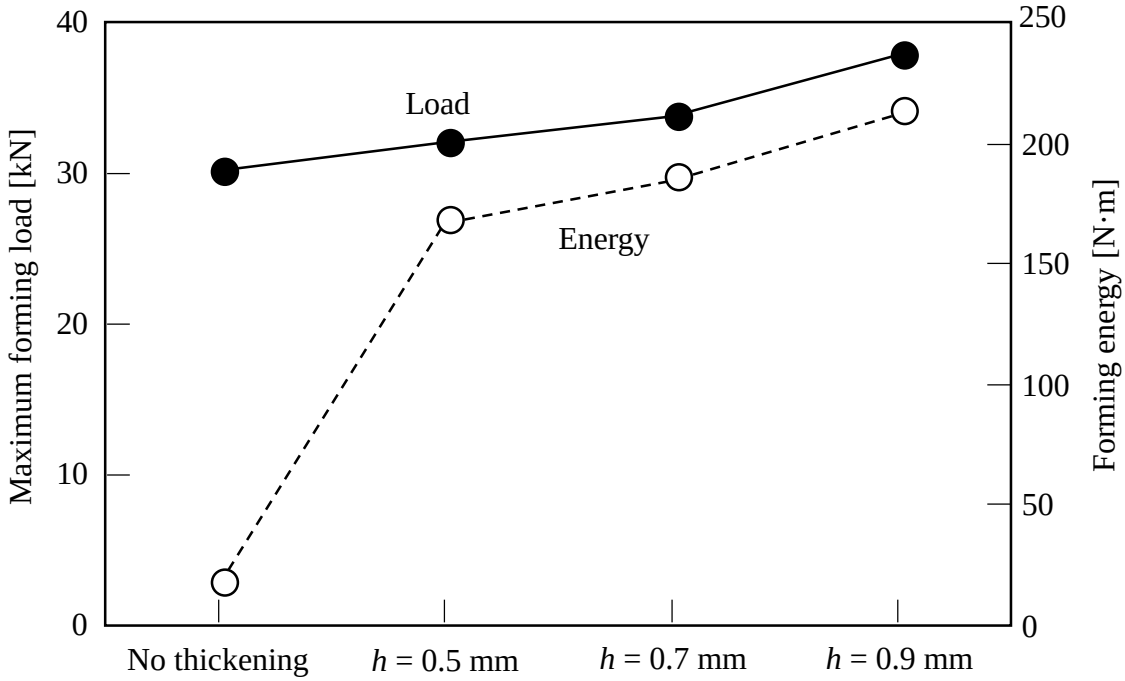

Fig. 4.10. Maximum forming load and forming energy for JSC980.

4.3.2. Quality of sheared edge

The surfaces and cross-sections of the sheared edge with and without thickening for JSC980 are shown in Fig. 4.11. As the step height of the die increases, the amount of thickening increases. The area of the rough fracture surface without thickening is considerably improved by thickening. Although the depth of the rollover for thickening is larger than that without thickening due to bending during punching by the bottom of the punch, the depth is almost constant for the step height of the die. The rollover can be reduced by separating the step portion from the die and by pressing back the sheared edge portion with the separated step portion after thickening. Since this separation complicates structure of tools, the effect of thickening on the fatigue strength was evaluated without improvement of the rollover.

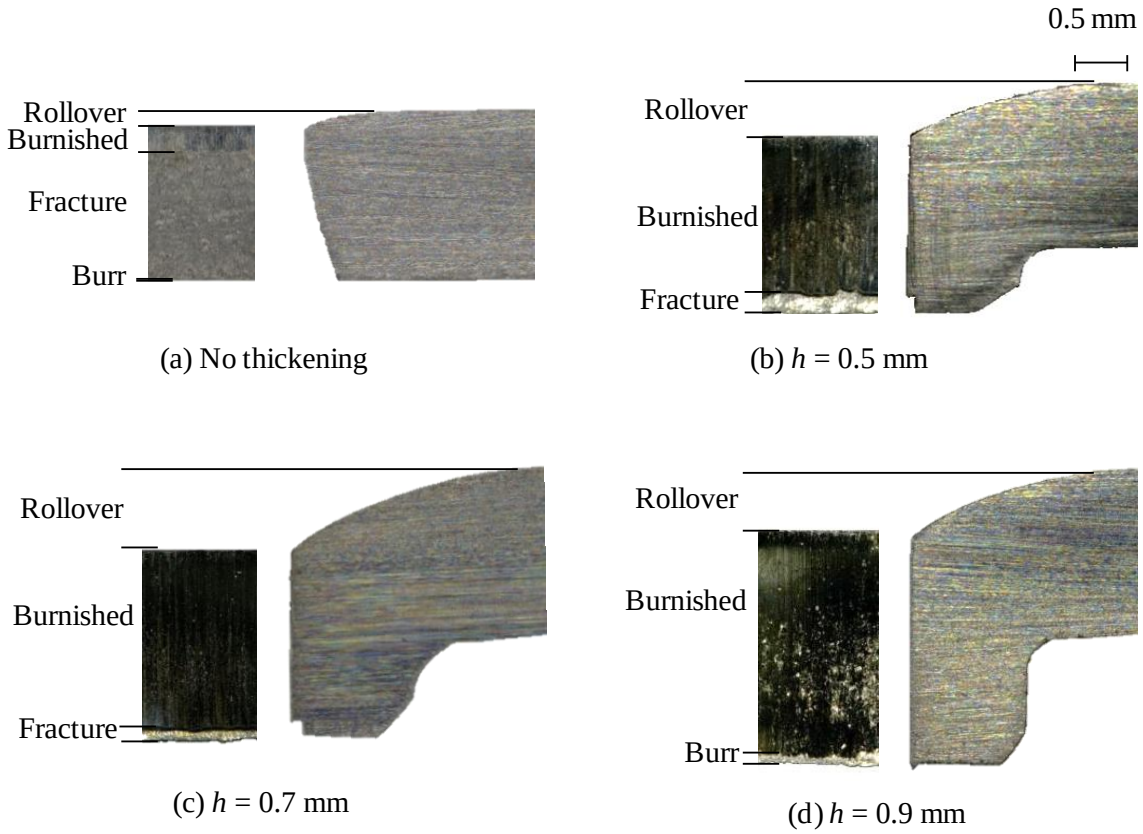

Fig. 4.11. Surface and cross-section of sheared edge for (a) no thickening, (b) h = 0.5 mm, (c) h = 0.7 mm and (d) h = 0.9 mm and JSC980.

The ratio of the rollover, burnished and fracture depths and the burr height on the sheared edge for JSC590 and JSC980 are given in Fig. 4.12. As the step height of the die increases, the height of the burnished surface increases.

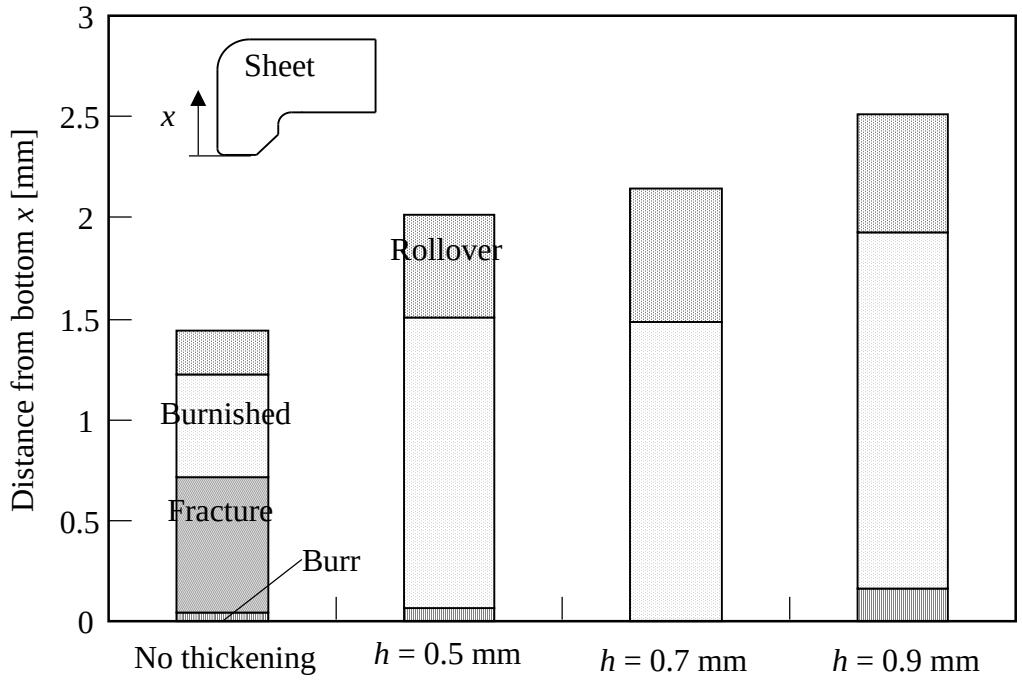

(a) JSC590

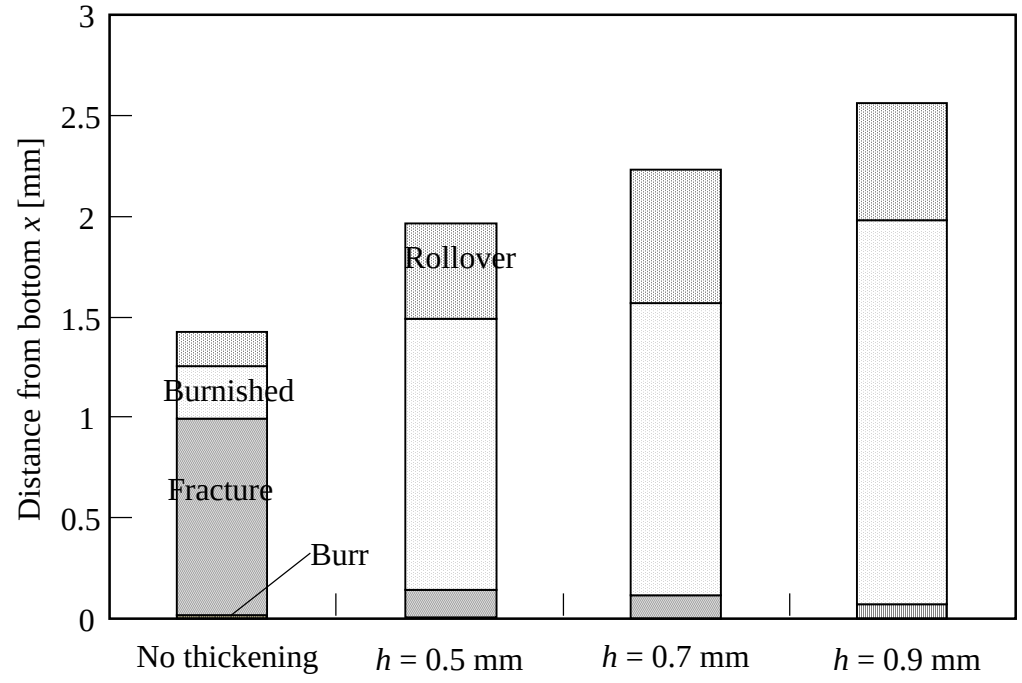

(b) JSC980

Fig. 4.12. Ratio of rollover, burnished and fracture depths and burr height on sheared edge for (a) JSC590 and (b) JSC980.

The distributions of surface roughness of the sheared edge in the thickness direction with and without thickening for h = 0.9 mm and JSC980 are shown in Fig. 4.13. The surface roughness was measured at intervals of 0.1 mm in the thickness direction. The surface roughness of the thickened sheared edge is considerably smaller than that without thickening due to the elimination of fracture surface.

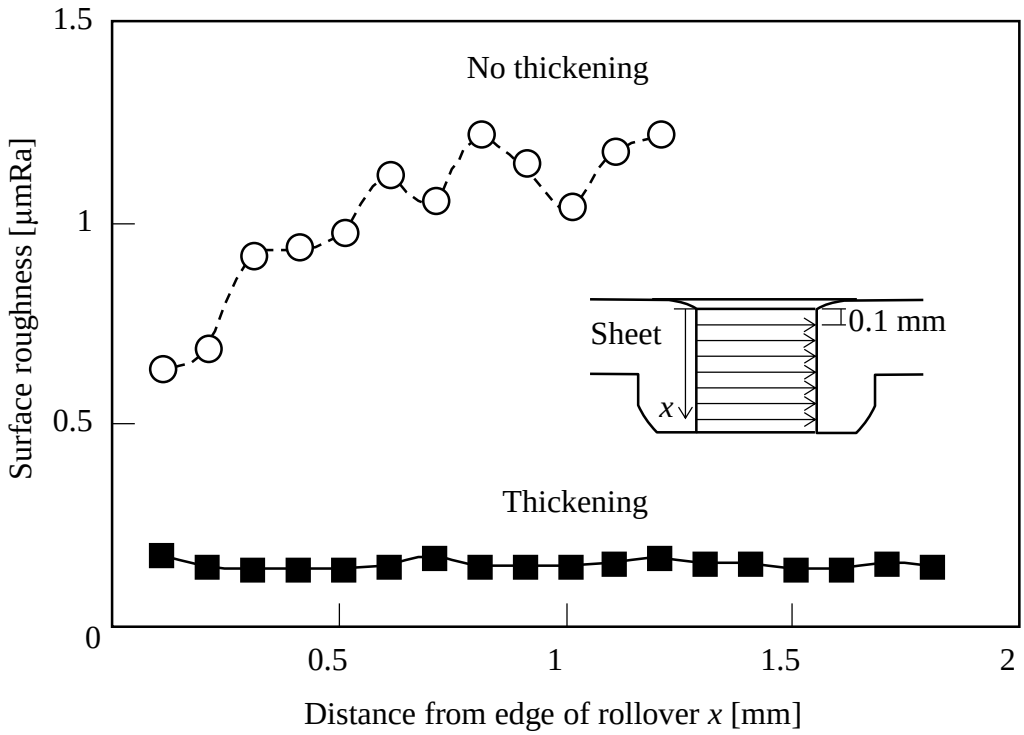

Fig. 4.13. Distributions of surface roughness of sheared edge in thickness direction with and without thickening for h = 0.9 mm and JSC980.

The distributions of Vickers hardness in the thickness direction around the sheared edge with and without thickening for h = 0.9 mm and JSC980 are shown in Fig. 4.14. The hardness was measured in the cross-section at 0.2 mm from the sheared edge. The hardness with thickening is higher than that without thickening due to ironing with the taper of the punch.

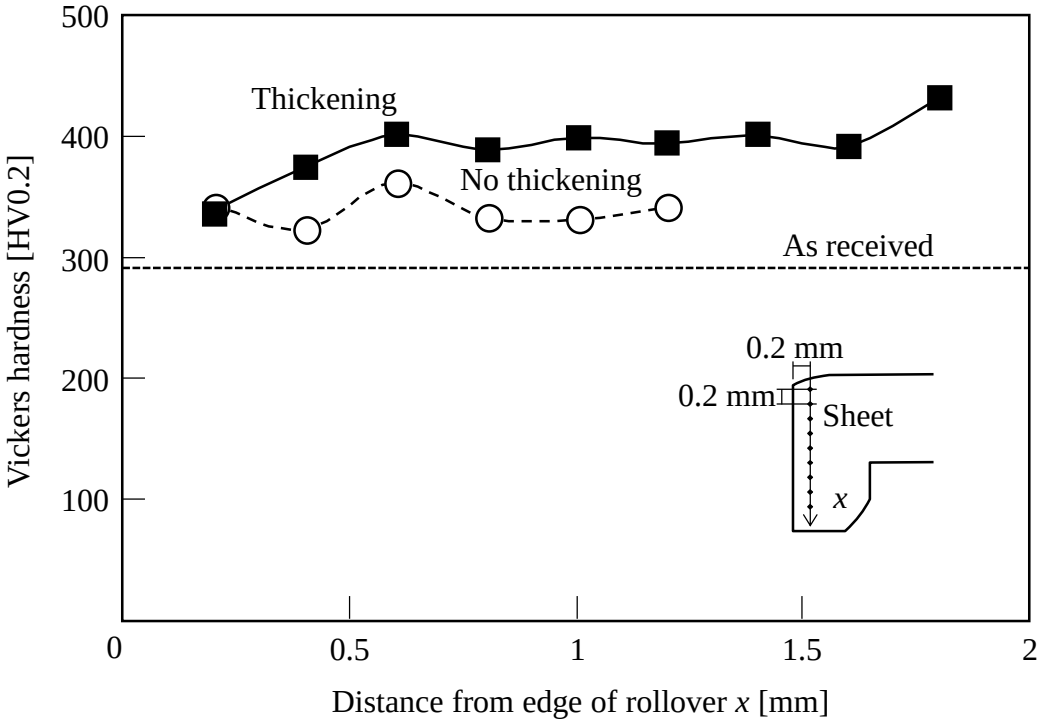

Fig. 4.14. Distributions of Vickers hardness in thickness direction around sheared edge with and without thickening for h = 0.9 mm and JSC980.

To examine the work-hardening behaviour around the sheared edge due to the punching and thickening, the distributions of Vickers hardness was measured for different distances from the sheared edge y, $\theta = 10^{o}$, h = 0.9 mm and JSC980 as shown in Fig. 4.15. The hardness was measured in the cross-section at 0.2, 0.4 and 0.6 mm from the sheared edge at intervals of 0.2 mm in the thickness direction. As the distance from the sheared edge increases, the hardness decreases. The hardness near the sheared edge was the largest due to the influence of ironing with the taper of the punch.

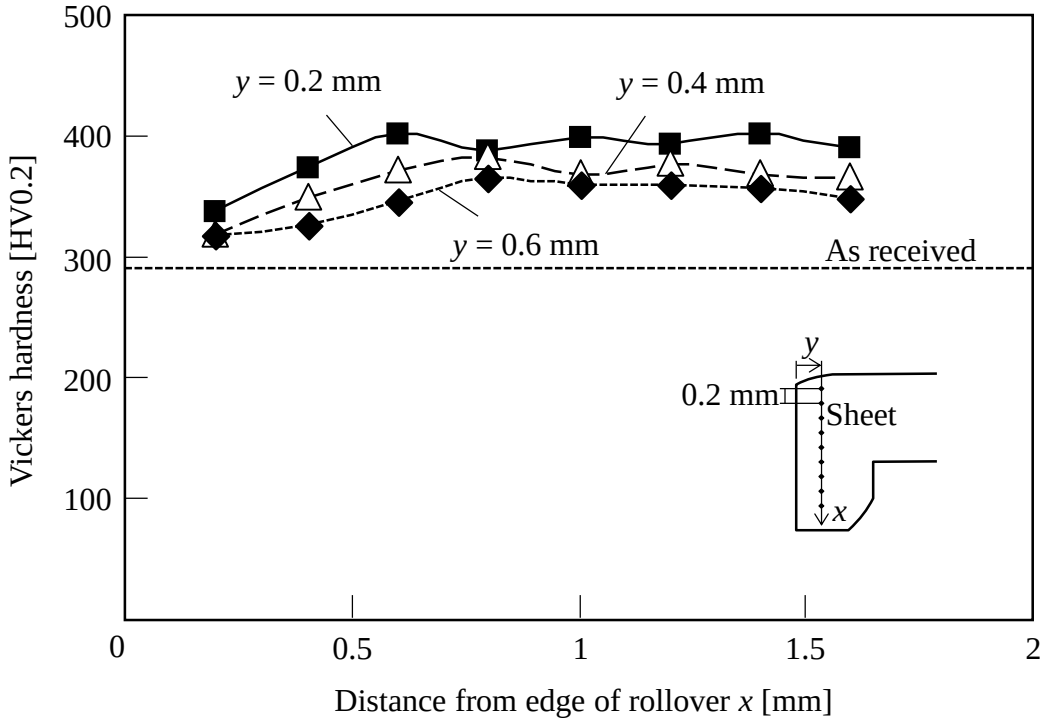

Fig. 4.15. Distributions of Vickers hardness in thickness direction around sheared edge obtained from experiment for different distance from sheared edge y, $\theta = 10^{o}$, $h = 0.9$ mm and JSC980.

4.3.3. Measurement of residual stress around hole edge

The effect of the thickening of the hole edge in the residual stress in the thickness direction of the sheared edge was measured by the X-ray diffraction. The procedure and the conditions of the X-ray diffraction for measurement of the residual stress in the sheared edge were shown in Fig. 3.13 and Table 3.3, respectively

The residual stresses in the thickness direction in the sheared edge of the punched sheets with and without thickening for $h = 0.9$ mm and JSC980 are shown in Fig. 4.16. Although the residual stress without thickening is tensile, the stress with thickening becomes compressive due to the ironing during the thickening stage.

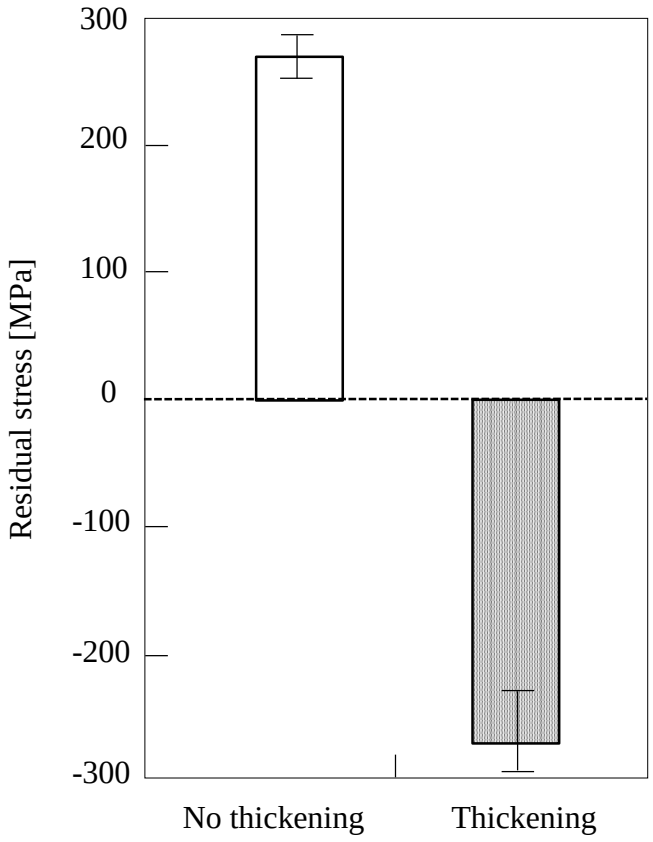

Fig. 4.16. Effect of thickening of hole edge on residual stress in sheared edge for h = 0.9 mm and JSC980.

4.4. Strength of punched sheet

4.4.1. Fatigue strength

The bending and tensile fatigue tests of the punched sheets with the thickened hole edge were performed. The frequencies for the alternative bending and repeated tensile fatigue tests were set at 25 and 50 Hz, respectively. The fatigue test was ended when the sheet was ruptured. The maximum number of cycles for the fatigue tests was 10^7.

The plots of the bending moments and maximum loads versus the number of cycles to failure for the bending and tensile fatigue tests of the punched sheets with thickening are compared with those without thickening in Fig. 4.17 and 4.18, respectively. As the step height of the die increases, the fatigue strength increases. The fatigue strength of the punched sheets with thickening is considerably higher than that without thickening. The improvement of the fatigue strength for thickening is due to the large compressive stress,

the small surface roughness and the large hardness around the sheared edge. It was found that thickening of the hole edge is useful for improving the fatigue strength of punched ultra-high strength steel sheet.

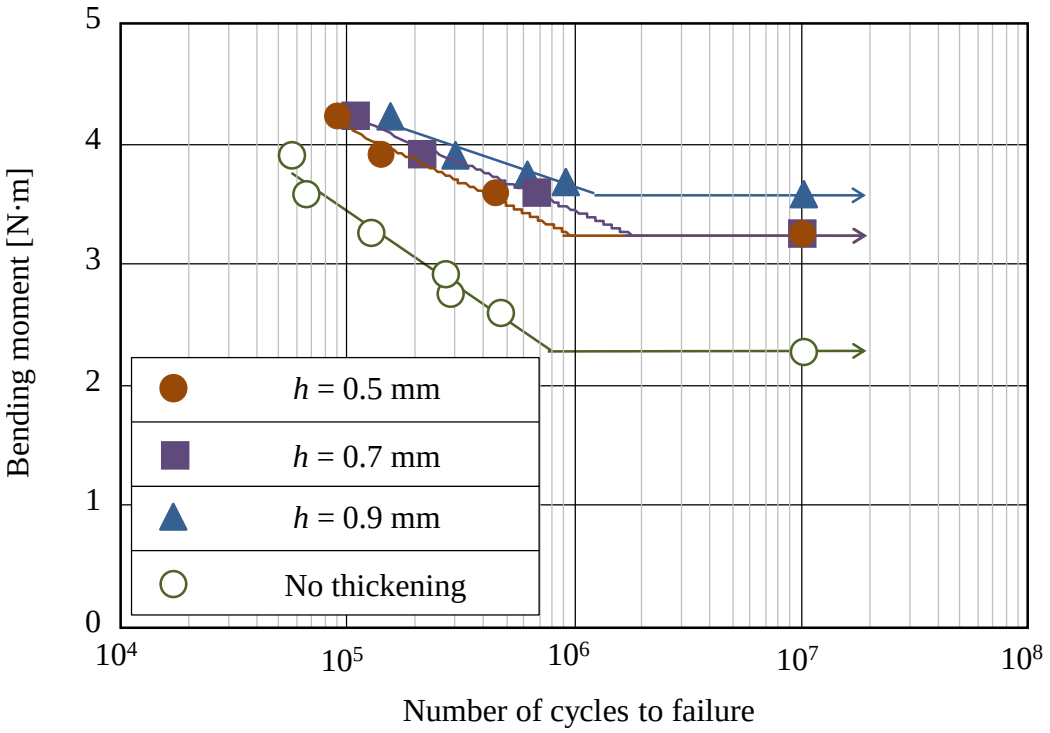

(a) JSC980

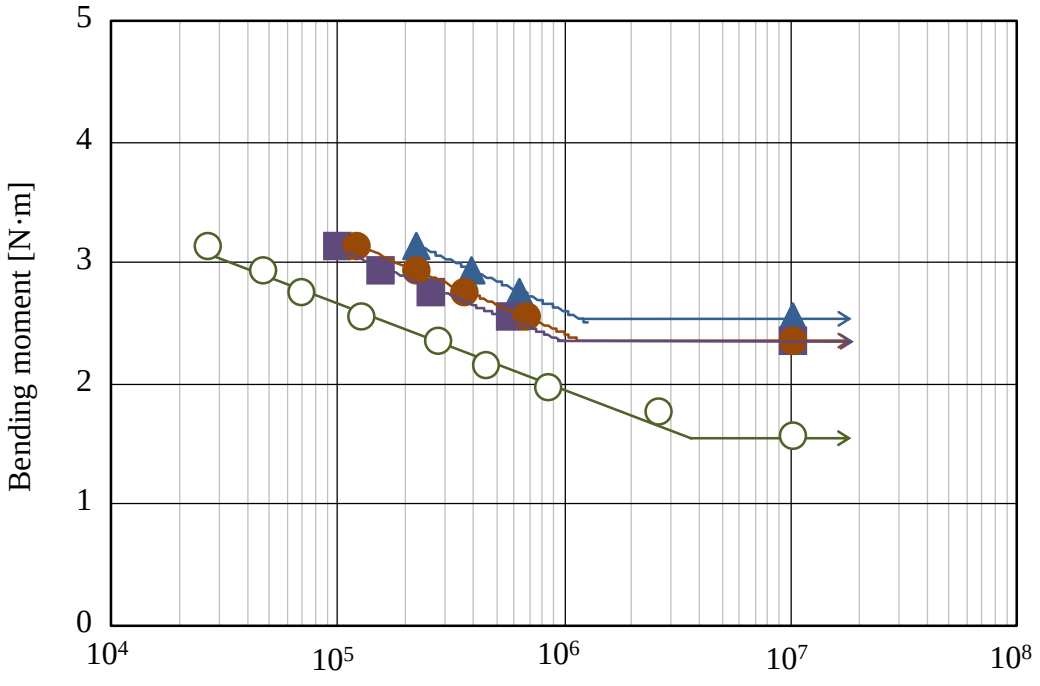

(b) JSC590

Fig. 4.17. Plots of bending moments versus number of cycles to failure of punched sheets with and without thickening for bending fatigue test.

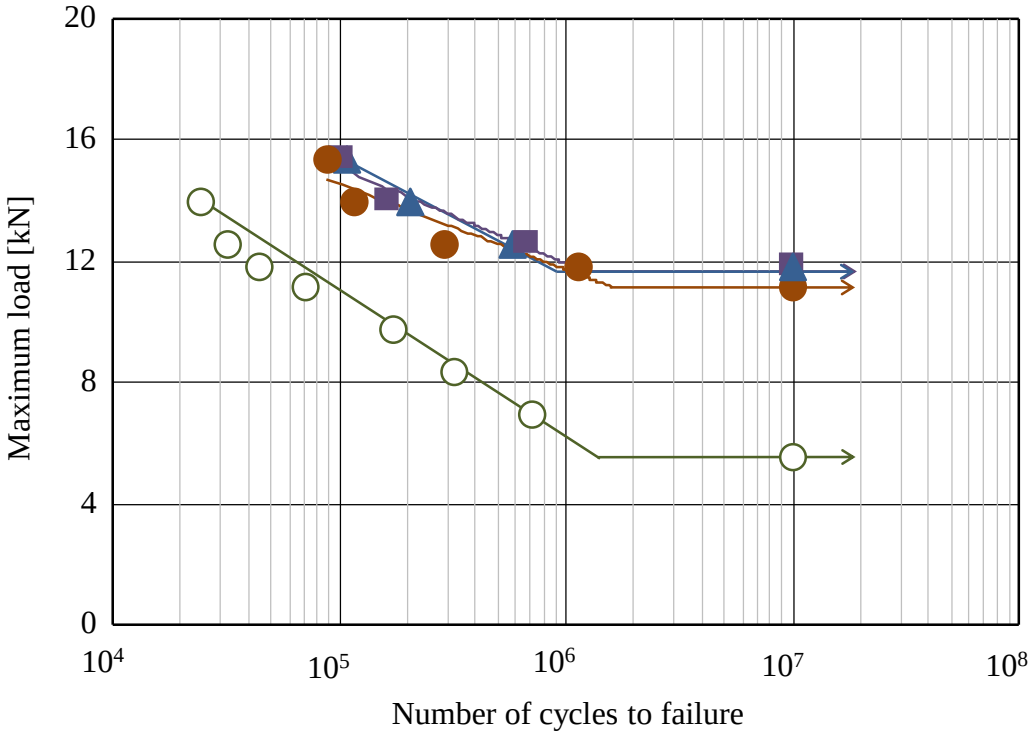

(a) JSC980

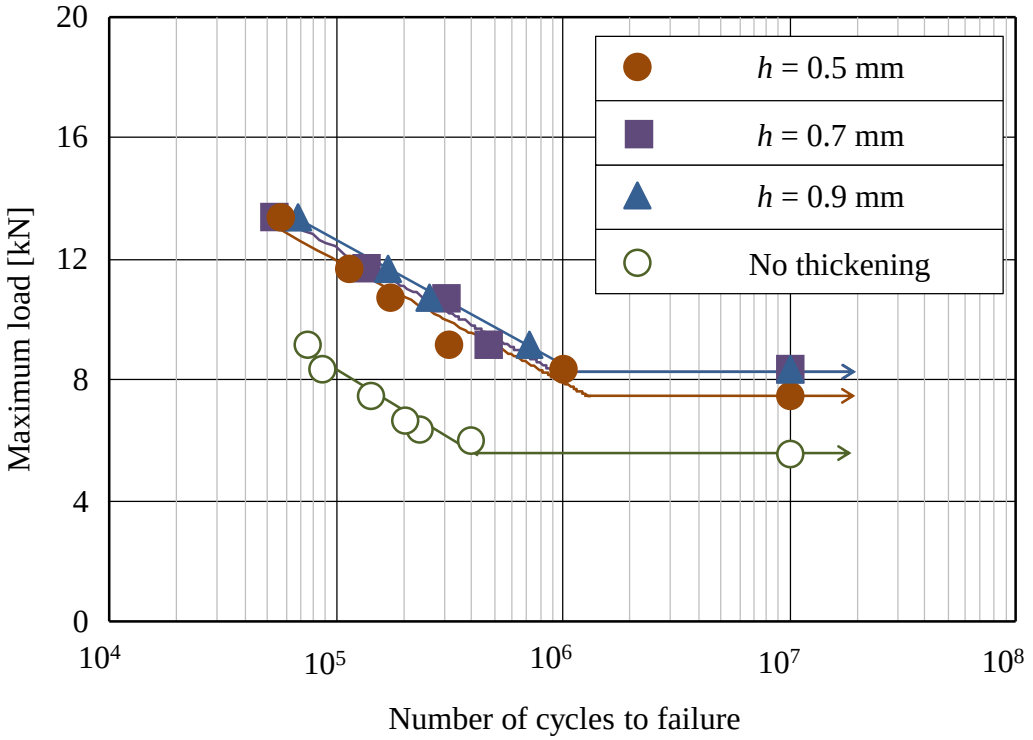

(b) JSC590

Fig. 4.18. Plots of maximum loads versus number of cycles to failure of punched sheets with and without thickening for tensile fatigue test.

To investigate the effect of thickening on the fatigue strength, elastic deformation in the bending and tensile tests of the punched sheet was simulated by the commercial finite element software ABAQUS. The shapes of the punched sheets with and without thickening obtained from the experiment for h = 0.9 mm and JSC980 shown in Fig. 4.11 were employed for the finite element simulation without calculation of the punching process, and the sheets were divided into three-dimensional hexahedral elements. The given loads at the edge of the sheet for the bending and tensile tests were 196 N equivalent to a moment of 3.92 N·m and 14 kN, respectively. The increase in flow stress of the sheet for work-hardening by punching was neglected.

The distributions of stress in the hoop direction in the cross section of the hole edge calculated from the finite element simulation with thickening are compared with those without thickening in Fig. 4.19, where the ruptured sheets obtained from the fatigue tests are also given. The portions for the calculated maximum stress are similar to those for crack initiation observed in the experiments, whereas the calculated maximum stresses of the sheets with and without thickening are similar. The reason for the increase in fatigue stress by thickening is not clarified from the maximum stress.

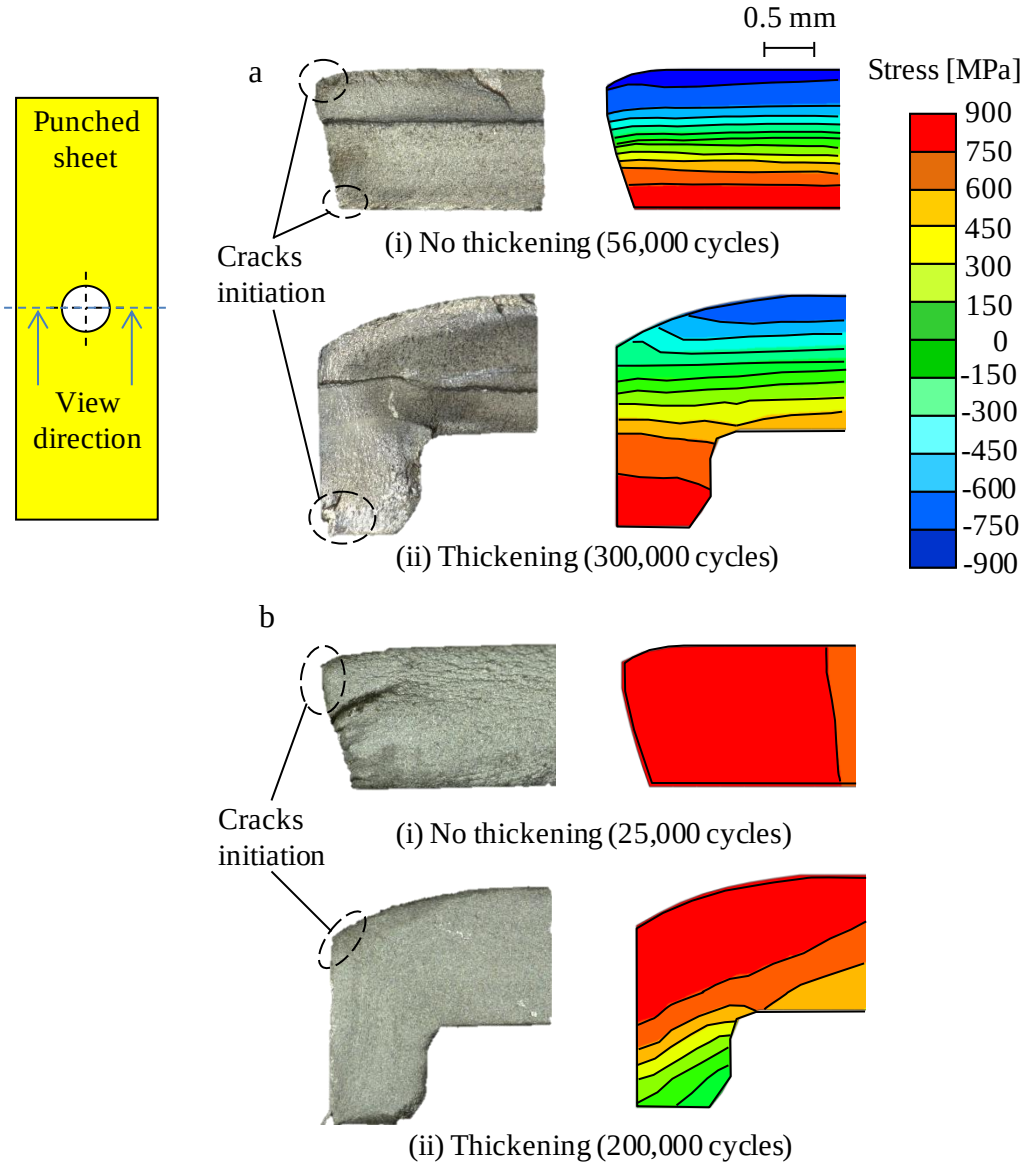

Fig. 4.19. Comparisons between cracks initiation and stress distribution in hoop direction in cross section of hole edge for (a) bending and (b) tensile with and without thickening for h = 0.9 mm and JSC980.

The occurrence of cracks around the hole edge for the fatigue tests of the punched sheets with and without thickening was observed with a digital microscope having 200 times in magnification (see Fig. 4.20). Although the cracks in the fatigue tests have appeared for the thickening and no thickening from the early cycles, the rupture of the sheet for the thickening is delayed. It was found that the thickening of the hole edge is effective for delaying the cracks initiation and propagation in the fatigue test of the punched ultra-high strength steel sheets.

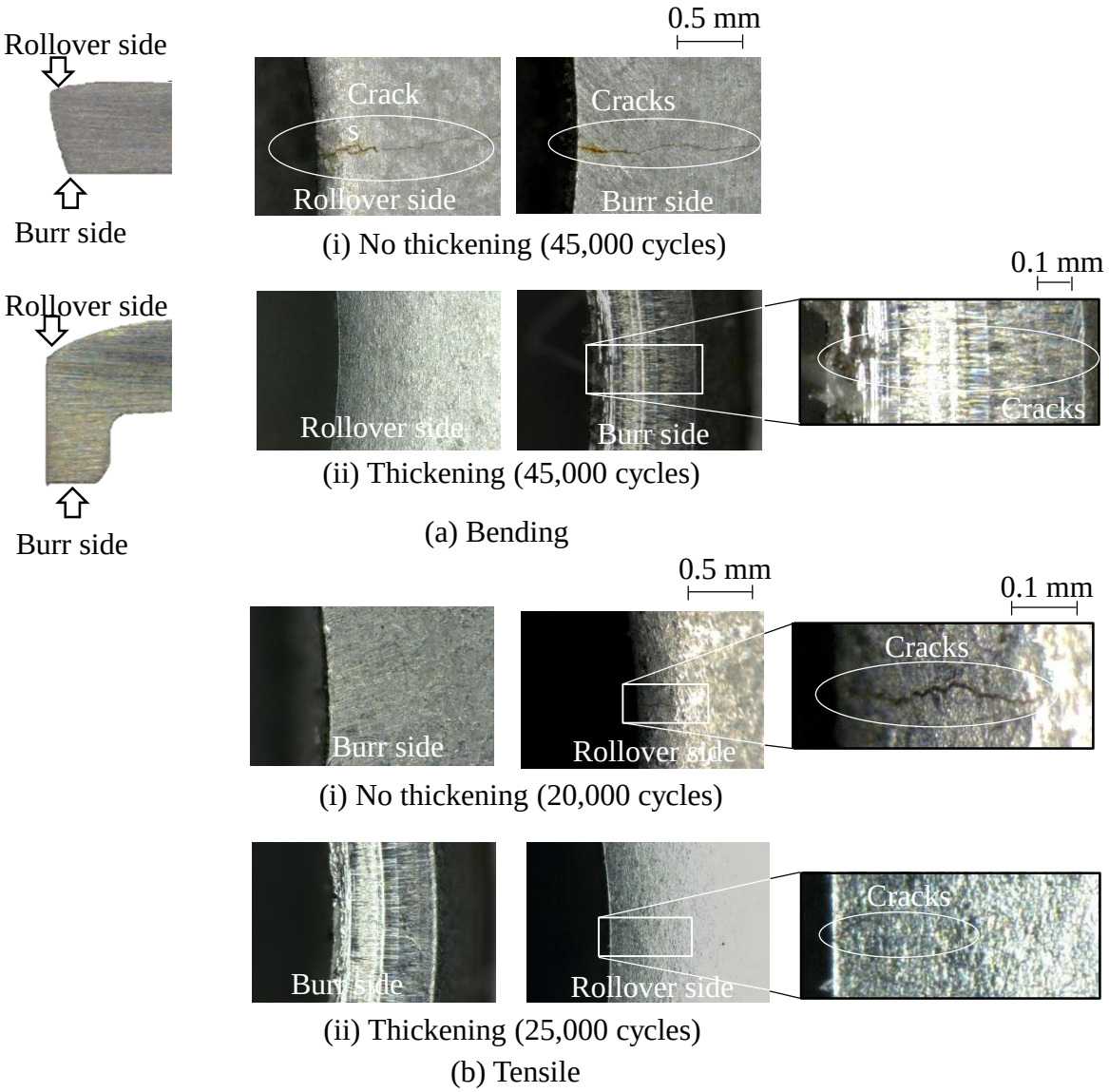

Fig. 4.20. Cracks around hole edge in fatigue tests with and without thickening for (a) bending and (b) tensile, h = 0.9 mm and JSC980.

4.4.2. Delayed fracture

Punched high strength steel sheets have the risk of delayed fracture, particularly for JSC980. The effect of the thickening of hole edge on the delayed fracture was examined by keeping the punched sheets in 35% concentration hydrochloric acid at room temperature. The procedure for delayed fracture test is shown in Fig. 4.21. The occurrence of delayed fracture was accelerated with the high concentration of the acid.

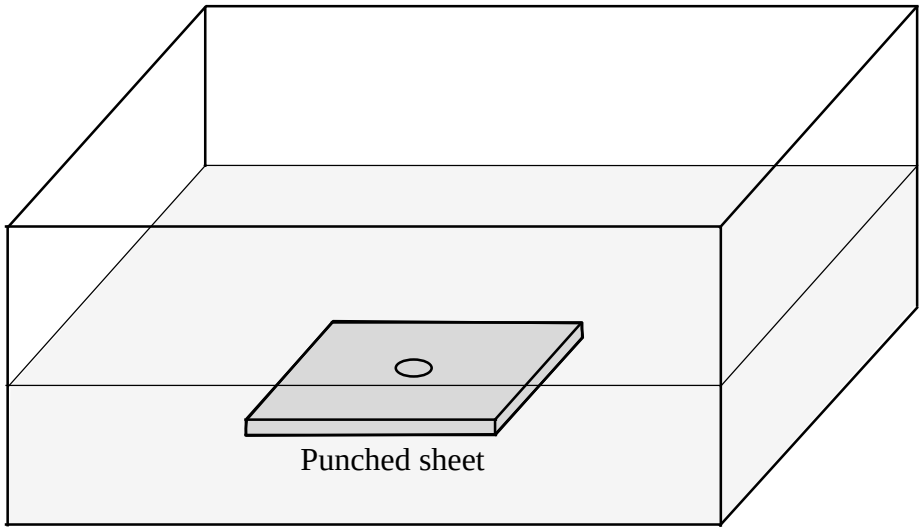

Fig. 4.21. Procedure for delayed fracture test by 35% concentration of hydrochloric acid.

The effect of thickening of the hole edge on the delayed fracture time for h = 0.9 mm and JSC980 is given in Fig. 4.22, where the delayed fracture time is the time from the soak of the sheet in the acid. The occurrence of cracks was visually observed. Although the cracks were observed after 2.5 hour for the punched sheet with no thickening, no cracks were observed up to 48 hour for the thickening. . For no thickening, the rough fracture surface in the sheared edge containing microcracks becomes large, and thus the hydrogen tends to diffuse. Moreover, the tensile residual stress in the sheared edge accelerates the occurrence of the delayed fracture. The delayed fracture for the thickening was prevented due to the large compressive stress and the small surface roughness.

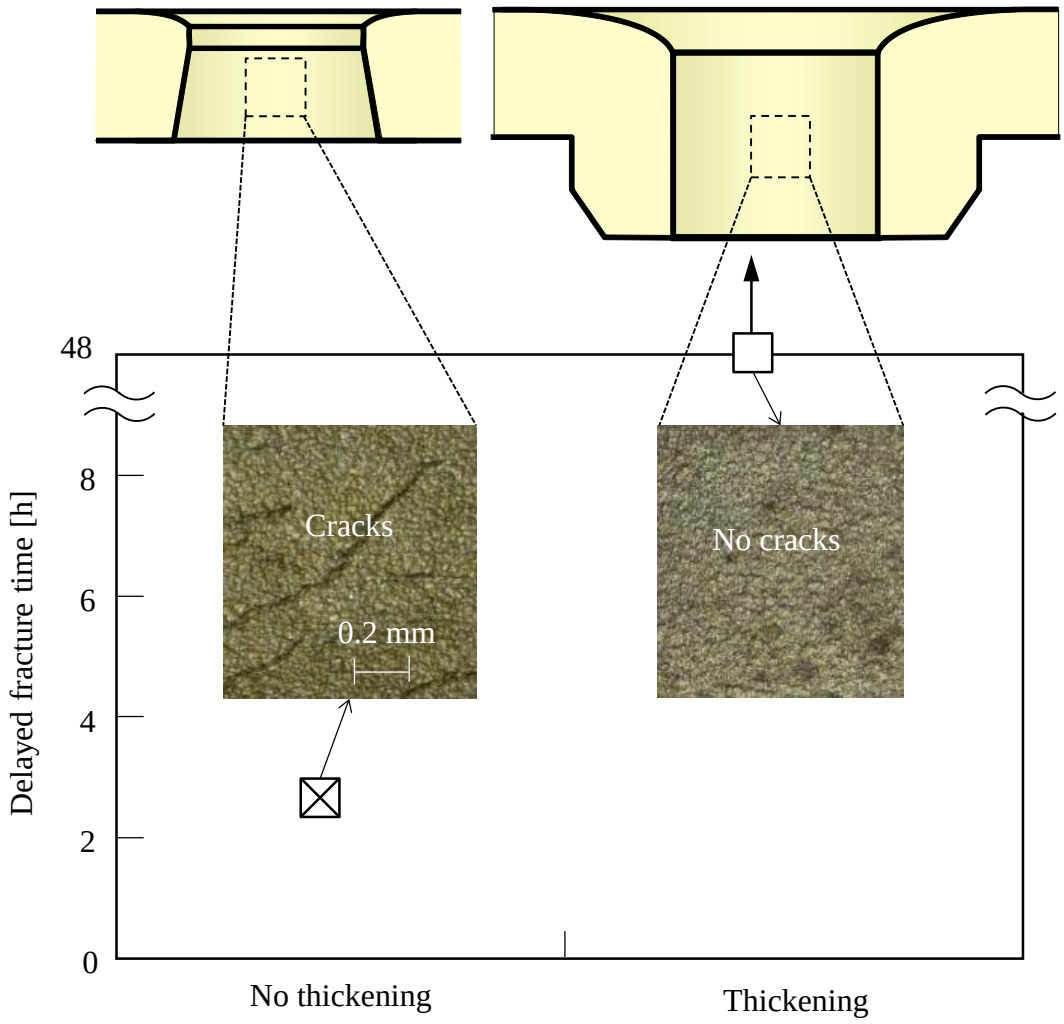

Fig. 4.22. Effect of thickening of hole edge on delayed fracture time for h = 0.9 mm and JSC980.

4.4.3. Static strength

To investigate the effect of the thickening on the static strength of the punched sheets, the static tensile test were carried out. The procedure and dimensions of specimen for the static test were shown in Fig. 2.20.

The maximum loads in the static tensile test of the punched sheets with and without thickening for h = 0.9 mm is shown in Fig. 4.23. The increase in the static strength for the thickening for both JSC590 and JSC980 was comparatively small due to the small increase in area, only 5% increase.

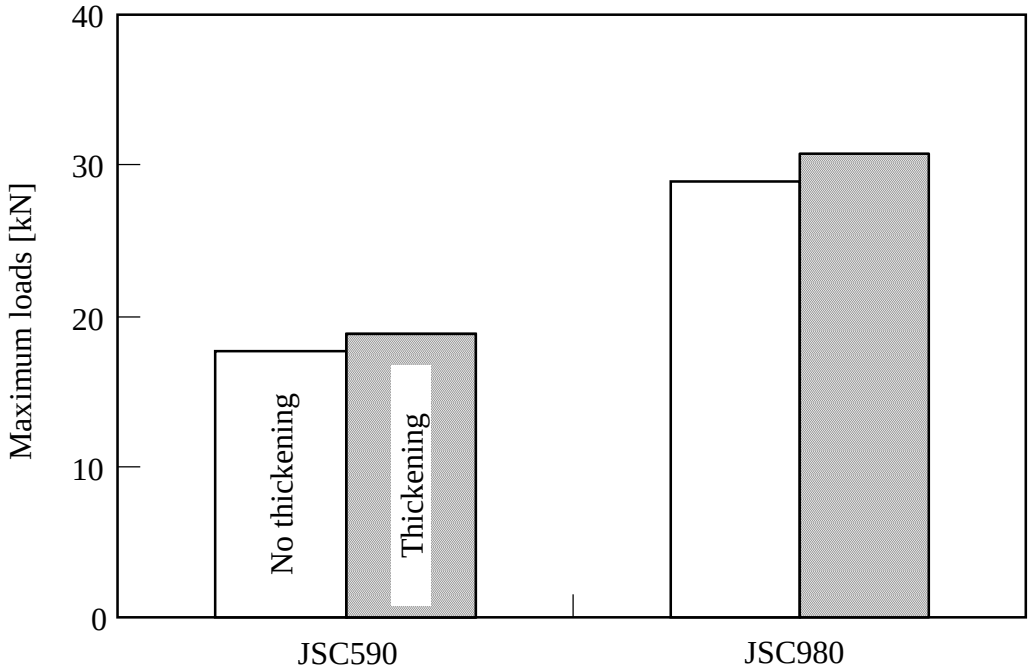

Fig. 4.23. Maximum loads in static tensile test of punched sheets with and without thickening for h = 0.9 mm.

4.5. Repeated punching including thickening of hole edge

Since the above mentioned results were obtained for a slow punching speed of 0.08 mm/s, repeated punching was carried out under a realistic punching speed of 100 mm/s to check the applicability of the present punching process to actual stamping operations. The tool used for the repeated punching of the ultra-high strength steel sheet is shown in Fig. 4.24.

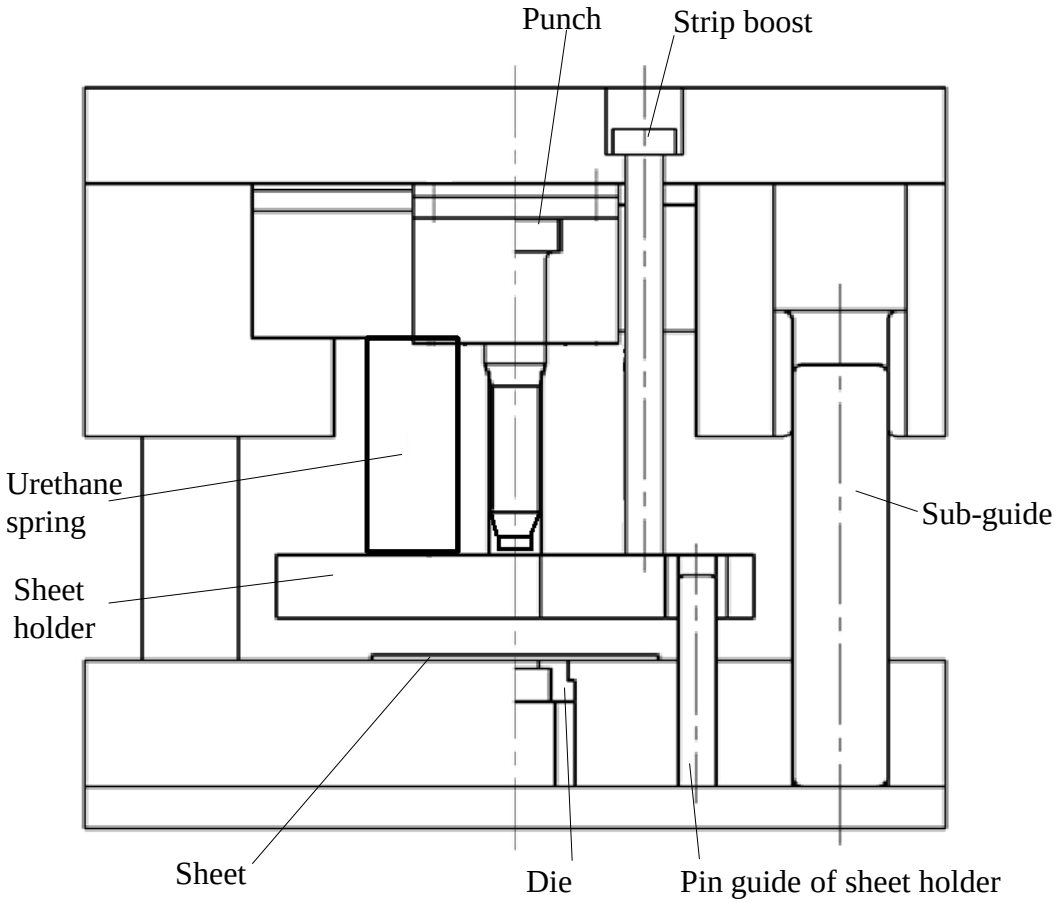

Fig. 4.24. Tools used for repeated punching of ultra-high strength steel sheet.

The conditions for the repeated punching of the ultra-high strength steel sheets are given in Table 4.3. The ultra-high strength steel sheet JSC980 was punched for $\theta = 10^{o}$ and h = 0.9 mm with a CNC servo press having a capacity of 800 kN. The dimension of the specimen for the repeated punching of the ultra-high strength steel sheets is shown in Fig. 4.25.

Table 4.3.

Conditions for repeated punching of ultra-high strength steel sheet.

Sheet	JSC980
Punching speed (mm/s)	100
Lubricant	No

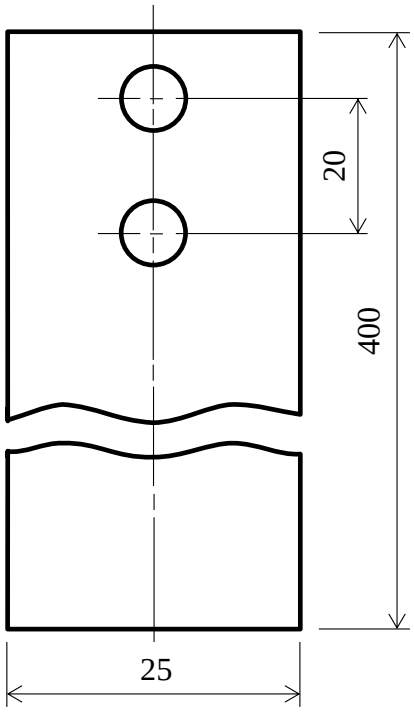

Fig. 4.25. Dimension of specimen for repeated punching of ultra-high strength steel sheet.

The punch was VC-coated by Toyota diffusion coating process and the hardness was 3500 HV. The wear and seizure resistances of this coating are very high and thus the required amount of lubricant could be reduced. The coating properties used for the repeated punching of the ultra-high strength steel sheet is shown in Table 4.4.

Table 4.4.
Coating properties used for repeated punching of ultra-high strength steel sheet.

Material	Deposition method	Vickers hardness (HV)
No coating	—	—
VC coating	PVD	3500

The surface and cross-section of the sheared edge in repeated punching of JSC980 are shown in Fig. 4.26, where *n* is the number of strikes. The surface quality of the sheared edge is high even for *n* = 100.

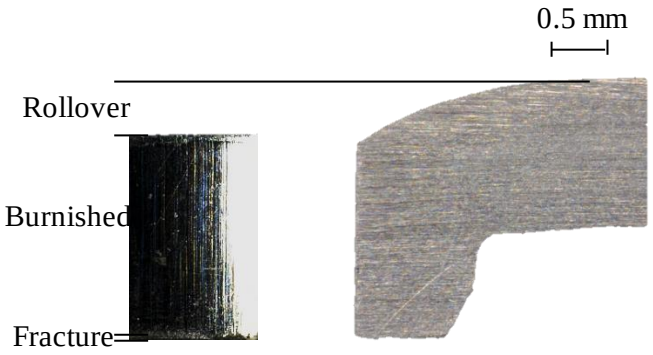

(a) n = 1

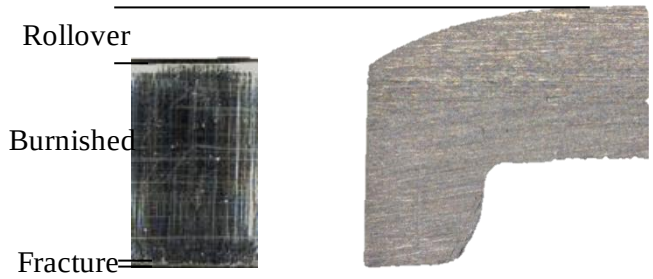

(b) n = 100

Fig. 4.26. Surface and cross-section of sheared edge in repeated punching of JSC980 for (a) n = 1 and (b) n = 100.

The side wall, taper and bottom portions of the punches were observed, as shown in Fig. 4.27. The surface of the punch in repeated punching of JSC980 is given in Fig. 4.28. The surface of the VC-coated punch hardly changed even for n = 100, whereas galling occurred due to severe shear deformation for the non-coated punch. It was found that the VC-coated punch is useful for the actual operations of punching including thickening of hole edge of ultra-high strength steel sheet.

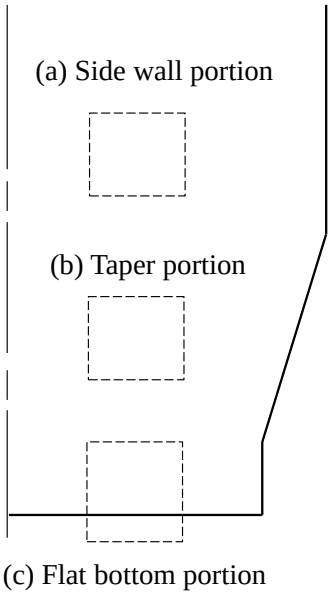

Fig. 4.27. Observation portion of punch in repeated punching of JSC980.

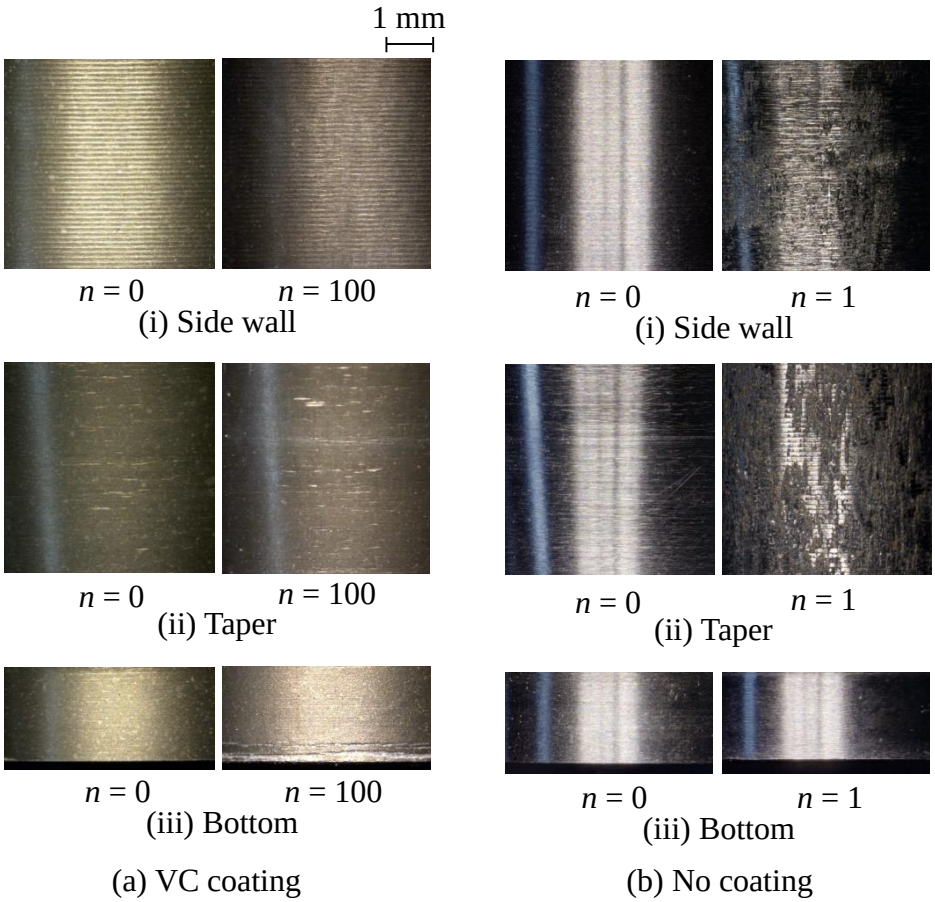

Fig. 4.28. Surface of punch for repeated punching of JSC980 with (a) VC coating and (b) no coating.

4.6. Conclusions

A punching process including thickening of a hole edge of ultra-high strength steel sheet was developed to improve fatigue strength of the punched sheet. A pair of taper punch and step die was designed to include thickening of the hole edge in the punching process and easily installed in conventional die sets. The results are summarised as follows:

1. The sheet was punched in the former stage by the bottom of the punch, and then the hole edge was thickened by the taper of the punch and the corner step of the die.
2. The surface quality of the sheared edge with thickening was improved due to ironing with the taper of the punch during the thickening stage.
3. The fatigue strength of the punched sheets with thickening was considerably higher than that without thickening due to the large compressive stress, the small surface roughness and the large hardness around the sheared edge.
4. The delayed fracture was prevented by thickening due to the large compressive residual stress and the small surface roughness.
5. Seizure on the surface of the punch was prevented by VC-coating for repeated punching and realistic punching speed.

4.7. References

[1] M. Kleiner, M. Geiger, A. Klaus, Manufacturing of lightweight components by metal forming, CIRP Annals - Manufacturing Technology 52 (2) (2003) 521-542.

[2] K. Mori, K. Akita, Y. Abe, Springback behaviour in bending of ultra-high-strength steel sheets using CNC servo press, International Journal of Machine Tools & Manufacture 47 (2) (2007) 321–325.

[3] J. Eriksson, M. Olssson, Tribological testing of commercial CrN, (Ti,Al)N and CrC/C PVD coatings – Evaluation of galling and wear characteristics against different high strength steels, Surface & Coating Technology 205 (16) (2011) 4045-4051.

[4] K. Mori, T. Maeno, S. Fuzisaka, Punching of ultra-high strength steel sheets using local resistance heating of shearing zone, Journal of Materials Processing Technology, 212-2 (2012), 534- 540.

[5] K. Inoue, M. Suzuki, S. Nishino, K. Ohya, Y. Tomota, Effect of coating microstructure of press-working dies on sliding damage, Steel Research International 81 (9) (2010), Supplement Metal Forming 2010, 849–852.

[6] Y. Murakami, S. Kodama, S. Konuma, Quantitative evaluation of effects of non-metallic inclusions on fatigue strength of high strength steels. I: Basic fatigue mechanism and evaluation of correlation between the fatigue fracture stress and the size and location of non-metallic inclusions, International Journal of Fatigue 11 (5) (1989) 291-298.

[7] D.J. Thomas, M.T. Whittaker, G. Bright, Y. Gao, The influence of mechanical and CO_2 laser cut-edge characteristics on the fatigue life performance of high strength automotive steels, Journal of Material Processing Technology 211 (2) (2011) 263-274.

[8] T. Matsuno, Y. Kuriyama, H. Murakami, S. Yonezawa, H. Kanamaru, Effects of punch shape and clearance on hole expansion ratio and fatigue properties in punching of high strength steel sheets, Steel Research International 81 (9) (2010), Supplement Metal Forming 2010, 853-856

Chapter 5

Punching of ultra-high strength steel sheets by punch having small round edge

5.1. Introduction

The reduction in weight of automobiles is in great demand for improving the fuel consumption. For the reduction, the use of high strength steel sheets for body-in-white parts sharply increases. Since the rise in strength of the sheet is required to satisfy the safety standards for protecting passengers in automobiles, the application of ultra-high strength steel sheets having a tensile strength above 1 GPa expands. Although parts made of ultra-high strength steels have superior mechanical properties, the stamping operation becomes difficult with the increase in strength of the sheet. The forming load and springback become very large, and the formability is considerably small [1-3].

Body-in-white parts are generally punched to make many holes for joining, paint removing, attachment, reduction in weight, etc. In punching of ultra-high strength steel sheets, tools tend to wear and chip due to large punching load, and thus the tool life is short [4-6]. The quality of the sheared edge in punching of ultra-high strength steel sheets deteriorates. Since the onset of cracks in the shearing is early due to the small ductility, the rough fracture surface increases [7-12]. Although shaving is generally used to improve the quality of the sheared edge, it is not easy to shave ultra-high strength steel sheets having large strength.

In the present study, ultra-high strength steel sheets were punched under a slight clearance with a punch having a small round edge to improve the quality of the sheared edge. The onset of cracks in the sheet during the punching was delayed by the small round edge of the punch and the slight clearance.

5.2. Punching of ultra-high strength steel sheets by punch having small round edge

To improve the quality of the sheared edge, ultra-high strength steel sheets were punched under a slight clearance between a punch and die. By the slight clearance, the tensile stress during the punching is reduced, and thus the onset of cracks is delayed for ultra-high strength steel sheets having small ductility. In the slight clearance punching, however, sharp edges of the punch and die tend to chip. The punch having a small round edge shown in Fig. 5.1 was developed to prevent the chipping of the tools, where R is the radius of the round edge measured from a laser displacement sensor, and R = 0 mm is equivalent to the conventional punch having a shape edge. The small round edge has the functions of avoiding the contact between the punch and die in the slight clearance punching and of delaying the onset of cracks. In addition, the side surface of the punch has the curved relief. The radius of the round edge was changed in the present study.

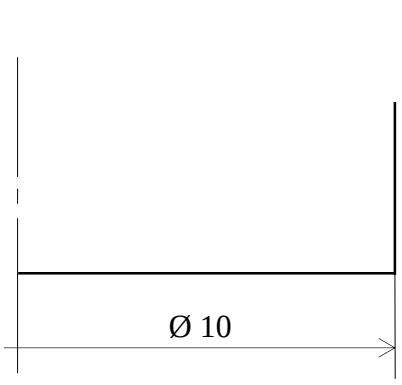

(a) R = 0 mm

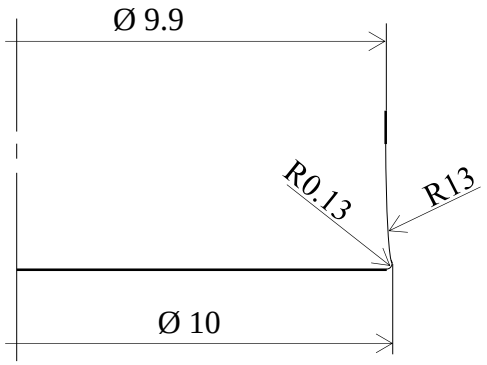

(b) R = 0.13 mm

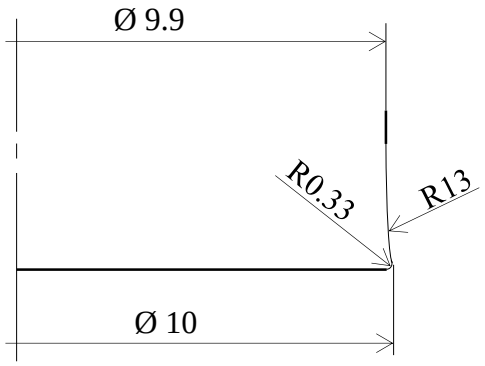

(c) R = 0.33 mm

Fig. 5.1. Punches having small round edge for punching of ultra-high strength steel sheets.

The mechanical properties of the ultra-high strength steel sheets used for the punching are given in Table 5.1. The sheets are cold-rolled ones generally used for automobile parts, and are made of dual-phase steel. The mechanical properties of the sheets were measured from the tensile test. The specimens were cut in the 0, 45 and 90º directions with respect to the rolling direction of the sheet, and the averages of the measured values are shown. The ultra-high strength steel sheets JSC980Y and JSC1180Y have the tensile strengths above 1 GPa. The dimensions of the sheets are shown in Fig. 5.2. The length and width of the punched sheet were 50 and 40 mm, respectively, and the center of the sheet was punched.

Table 5.1.

Mechanical properties of ultra-high strength steel sheets used for punching.

Sheet	Thickness (mm)	Tensile strength (MPa)	Elongation (%)	*n*-value	Reduction in area (%)
JSC780Y	1.4	769	20.0	0.15	38.2
JSC980Y	1.22	1051	12.8	0.09	37.4
JSC1180Y	1.21	1215	8.2	0.10	26.6

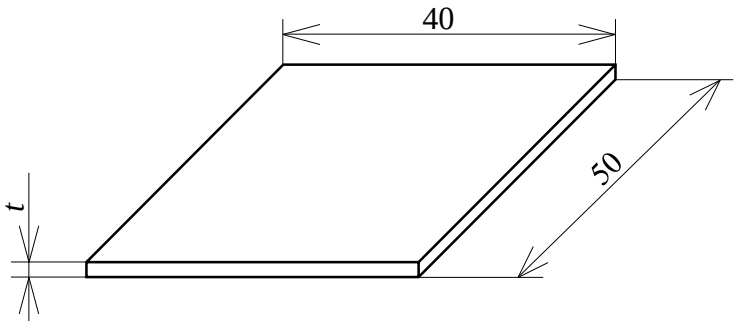

Fig. 5.2. Dimension of specimen for punching of ultra-high strength steel sheets.

The conditions of the punching of the ultra-high strength steel sheets are given in Table 5.2. The sheets were punched by a 250 kN screw driven type universal testing instrument. The ratio of clearance between the punch and die to the thickness was fixed to 0.8%, and the clearance ratio was changed above 20 % only for examination of effect of clearance. The very slow punching speed of 0.03 mm/s was chosen to avoid the chipping of the punch having a sharp edge for a clearance ratio of 0.8% between the punch and die.

A realistic punching speed was employed for repeated punching operations in Chapter 5.5. Each punching test was performed at least two times to prevent the scatter of results.

Table 5.2.

Conditions of punching of ultra-high strength steel sheets.

Die material	SKD11
Punch material	SKH51
Punch diameter (mm)	10
Ratio of clearance between punch and die to thickness, *c* (%)	0.8
Punching speed (mm/s)	0.03
Lubricant	Rust prevention oil

Finite element simulation of the punching process using the commercial software ABAQUS was performed under an assumption of axi-symmetric deformation. The die, sheet holder and punch were assumed to be rigid, and the cross-section of the sheet was divided into quadrilateral ring elements. To examine the concentration of deformation during the indentation of the punch, the calculation was performed until onset of crack without special treatment of occurrence of fracture. The conditions used for the simulation of ultra-high strength steel sheet JSC980Y are given in Table 5.3.

Table 5.3.

Conditions used for finite element simulation of ultra-high strength steel sheet JSC980Y.

Flow stress (MPa)	$\sigma = 1391\varepsilon^{0.09}$
Young`s modulus (MPa)	210000
Poisson`s ratio	0.3
Yield stress (MPa)	838
Coefficient of friction	0.05

5.3. Results of single punching of ultra-high strength steel sheets

5.3.1. Deformation behaviour

The effect of the edge radius of the punch on the deformation behaviour of the sheet during the punching for JSC980Y is shown in Fig. 5.3, where *s* is the punch stroke. For *R* = 0 mm, the cracks are caused from both edges of the punch and die, whereas the crack is initiated only from the edge of the die for *R* = 0.13 and 0.33 mm. The concentration of deformation around the edge of the punch was relaxed by the small round edge, and thus the onset of the crack from the edge of the punch was prevented.

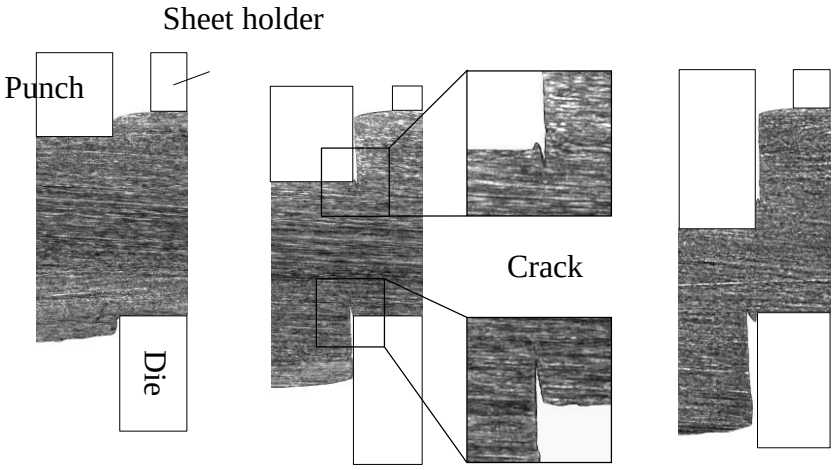

(a) *R* = 0 mm

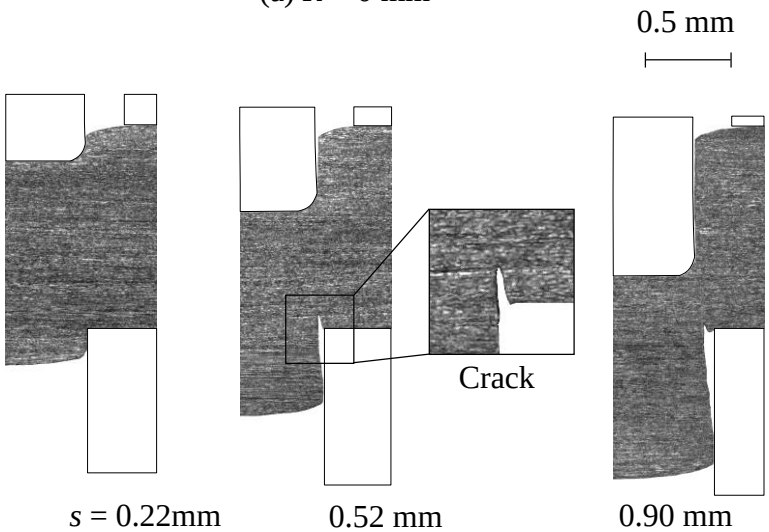

(b) *R* = 0.13 mm

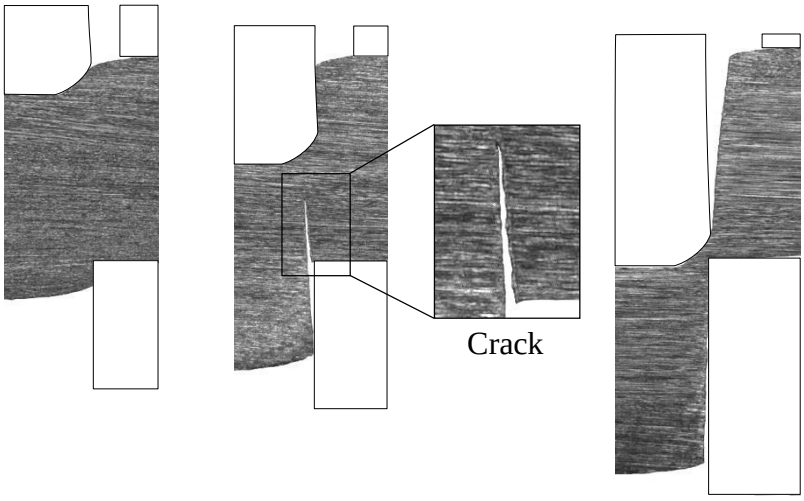

s = 0.23 mm 0.64 mm 1.26 mm

(c) *R* = 0.33 mm

Fig. 5.3. Effect of edge radius of punch on deformation behaviour of sheet during punching for JSC980Y.

The deformation behaviour during the punching was observed from the finite element simulation using the commercial software ABAQUS in detail. The distribution of equivalent strain just before the onset of crack calculated by the finite element simulation for JSC980Y is illustrated in Fig. 5.4. Although deformation concentrates at both edges of the punch and die for R = 0 mm, the concentration at the edge of the punch relaxes for R = 0.13 and 0.33 mm, and thus the crack is generated only from the edge of the die as shown in Fig. 5.3.

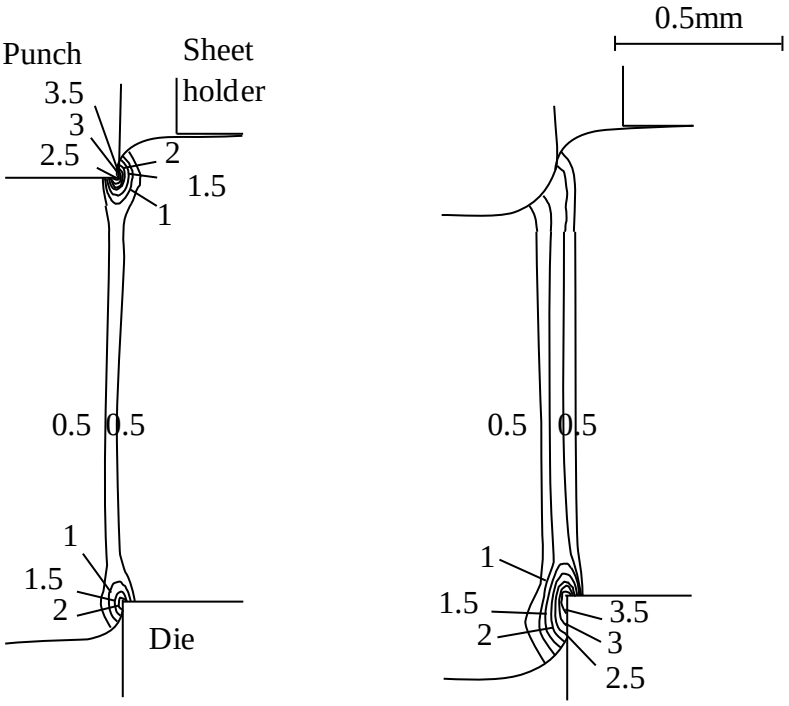

(a) R =0 mm, s = 0.13 mm (b) R = 0.13 mm, s =0.21 mm

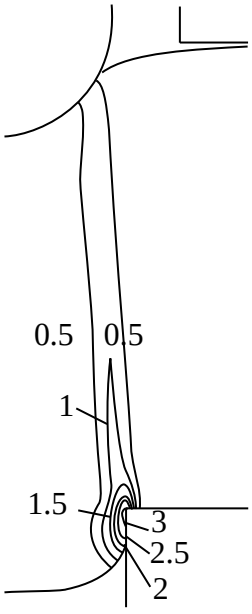

(c) R = 0.33 mm, s = 0.24 mm

Fig. 5.4. Distribution of equivalent strain just before onset of crack calculated by finite element simulation for JSC980Y.

The punching load-stroke curves for the different edge radii of the punch and JSC980Y are illustrated in Fig. 5.5. The maximum punching load for R = 0 mm occurs around 0.2 mm of punching stroke, then the curve become flat since the secondary burnished is formed. The punching load stroke curve for R = 0.15 mm is almost similar with that for R = 0 mm, however the stroke is longer due to the delayed cracks initiation. The stroke for PW is longer due to the taper shape of the bottom of the punch.

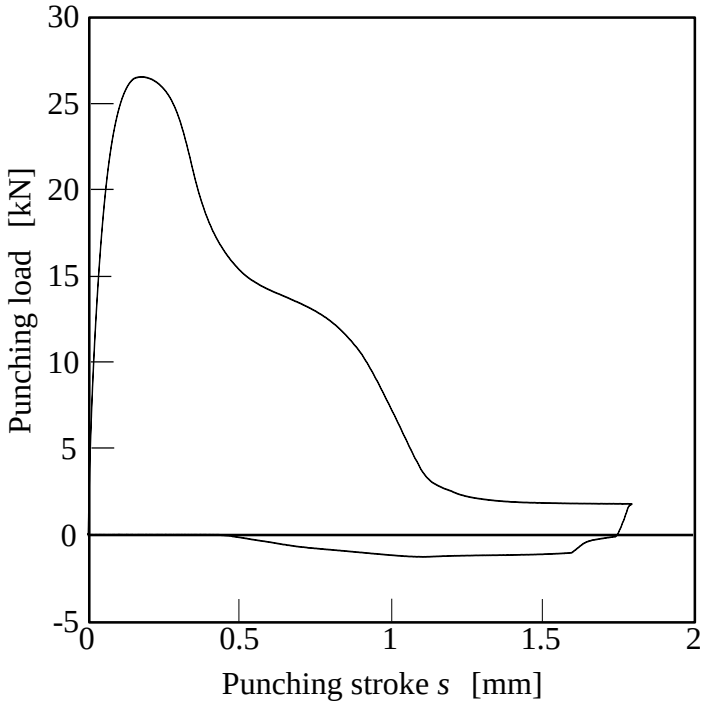

(a) R = 0 mm

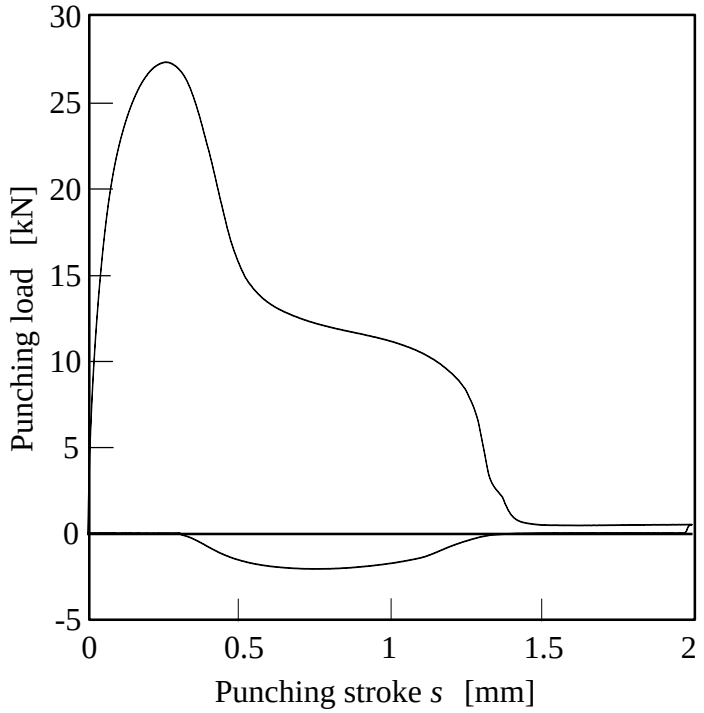

(b) R = 0.13 mm

Fig. 5.5. Punching load-stroke curves for different edge of radii of punch and JSC980Y.

The punching loads for the different edge radii of the punch are illustrated in Fig. 5.6. As the strength of the sheet increases, the punching load increases, whereas the loads for the three punches are similar due to the small edge radius.

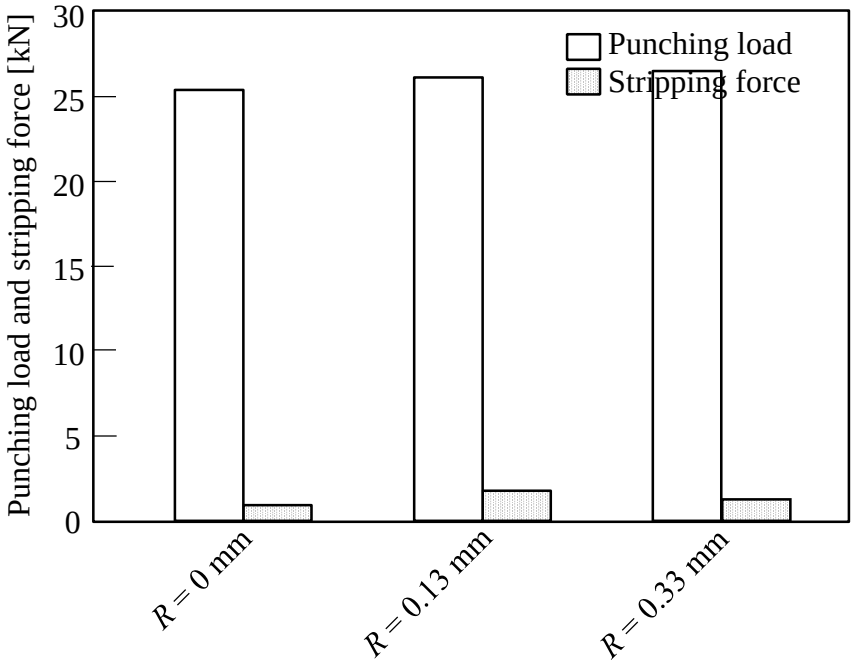

(a) JSC780Y

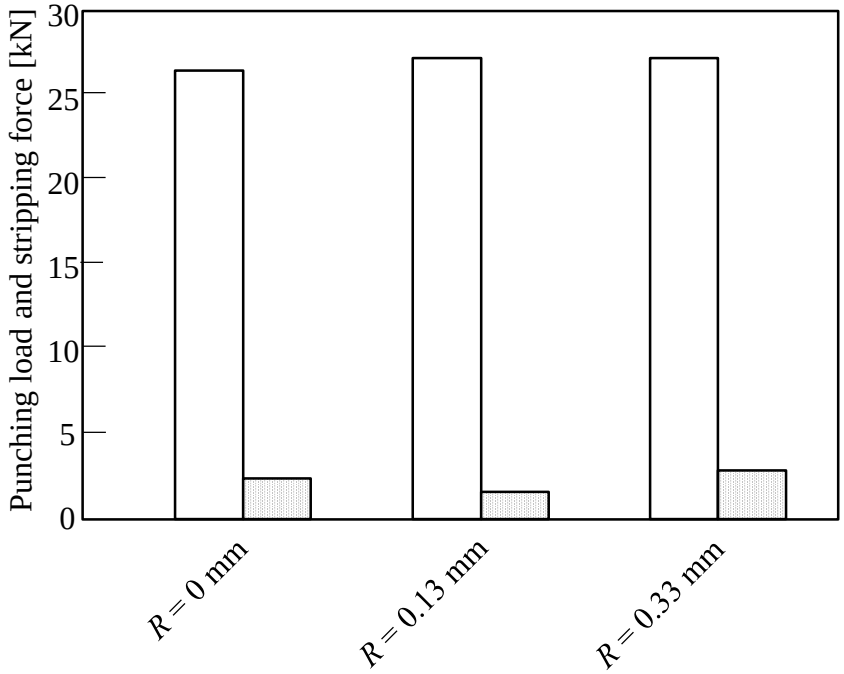

(b) JSC980Y

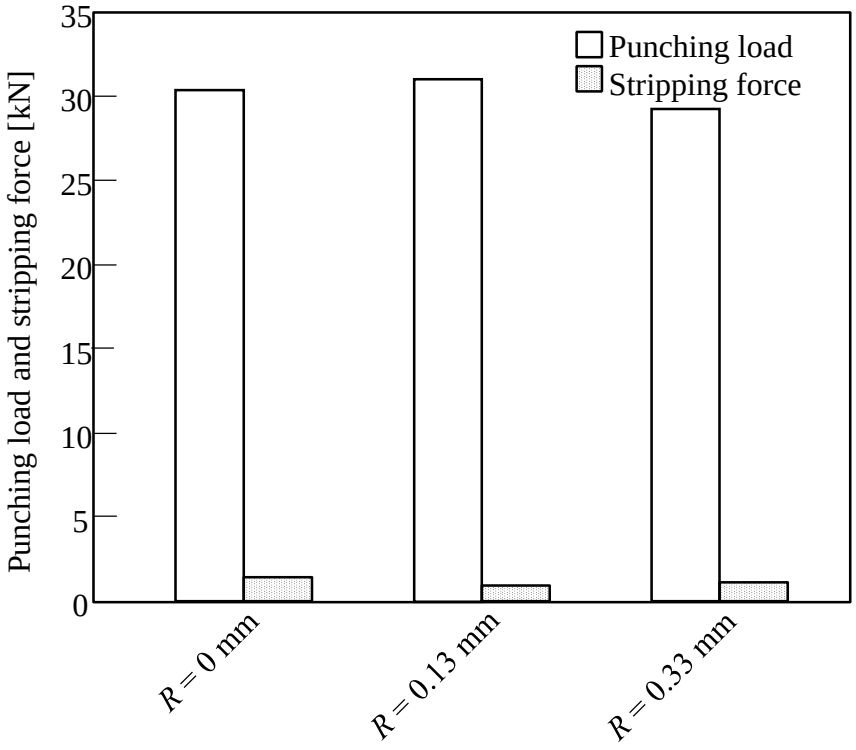

(c) JSC1180Y

Fig. 5.6. Punching load for different edge radii of punch.

5.3.2. Quality of sheared edge

The surface and cross-section of sheared edge for JSC780Y, JSC980Y and JSC1180Y are illustrated in Fig. 5.7, 5.8 and 5.9, respectively. Since the linkage of the cracks initiated from both edges of the punch and die for R = 0 mm is not smooth, the secondary burnished surface is caused, and the boundary with the fracture surface has a difference in level. For R = 0.13 and 0.33 mm, the smooth surface is obtained by propagating the crack only from the edge of the die, and the secondary burnished surface does not appear.

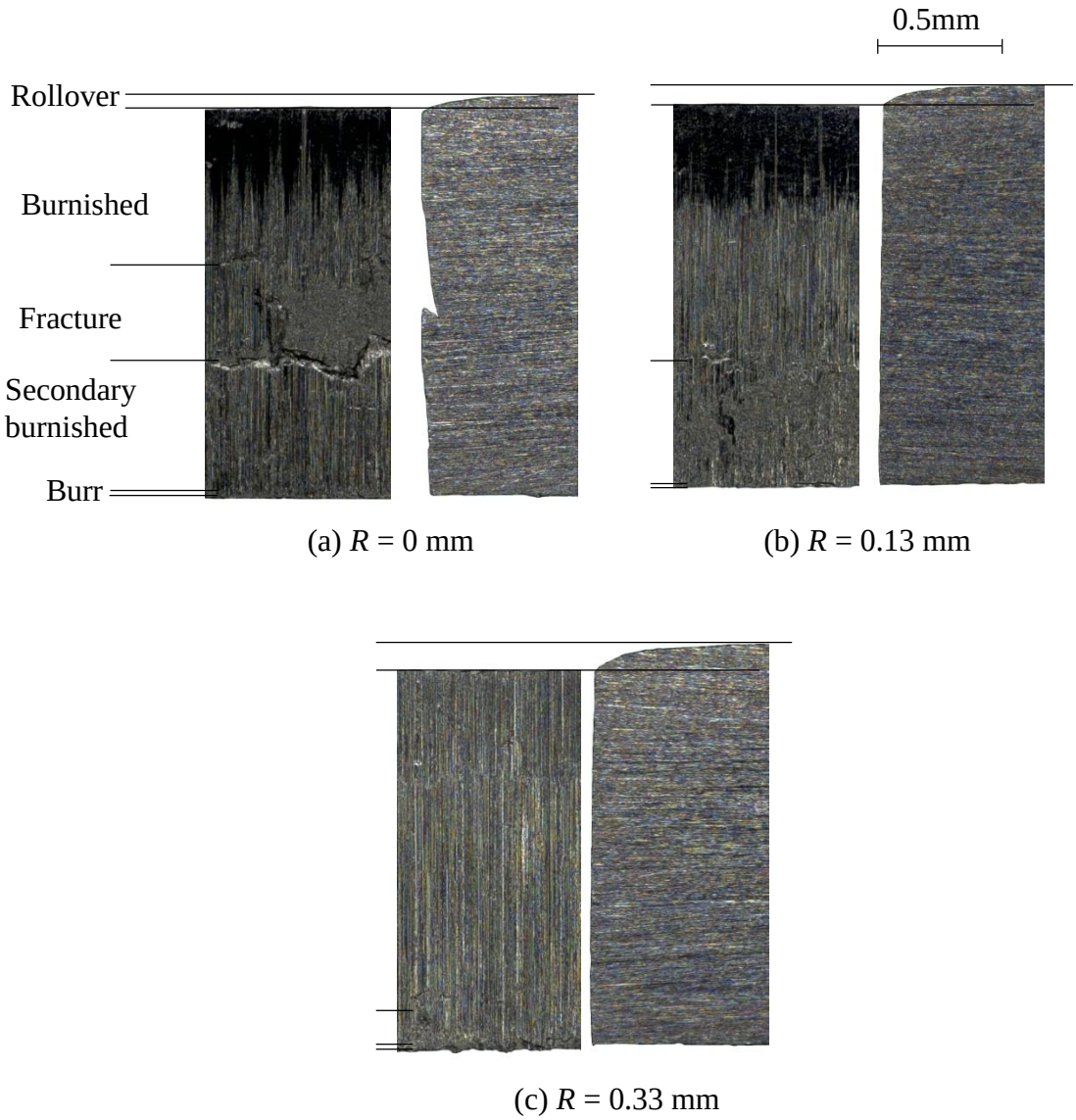

(a) R = 0 mm (b) R = 0.13 mm

(c) R = 0.33 mm

Fig. 5.7. Surface and cross-section of sheared edge for JSC780Y.

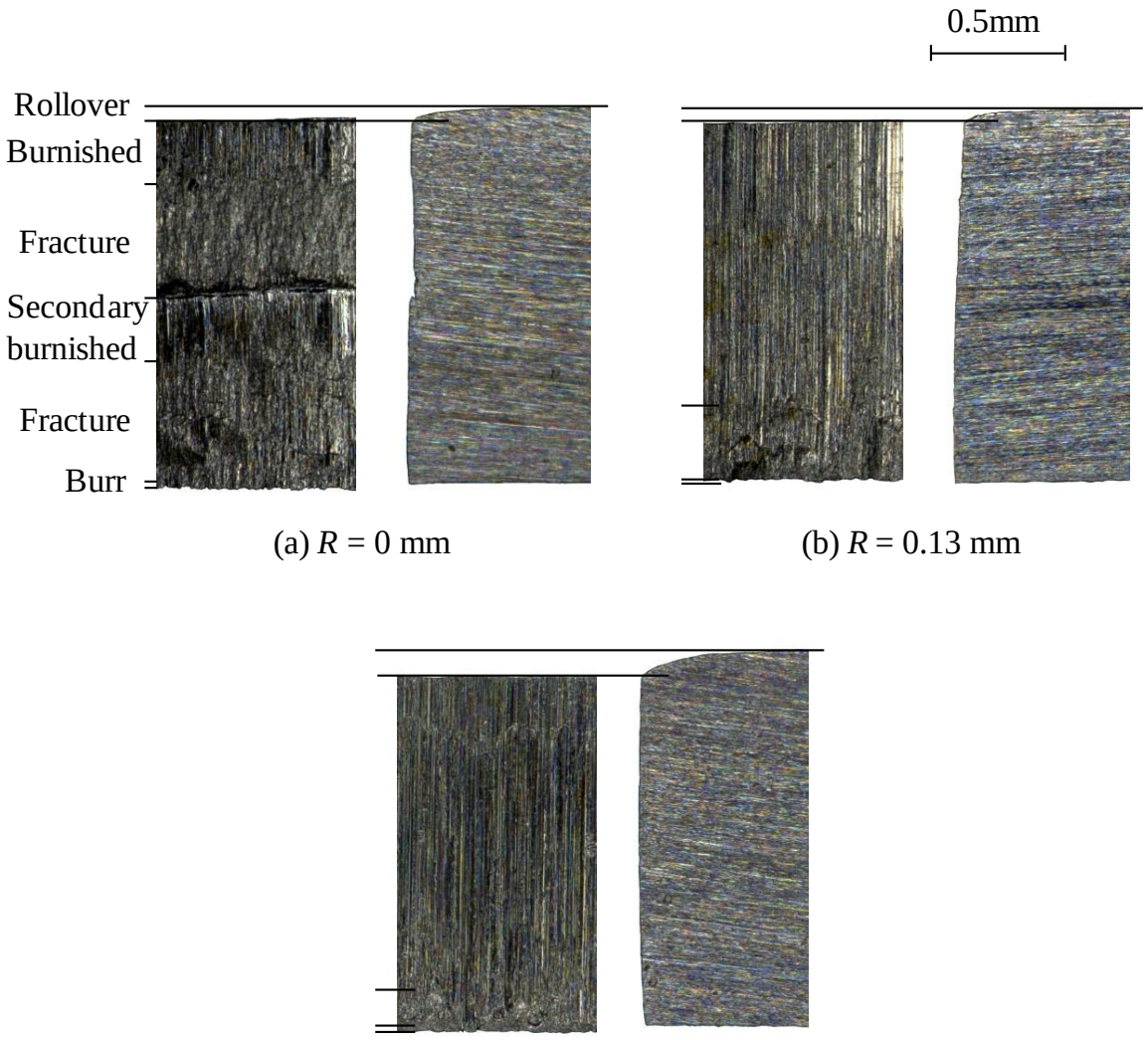

(a) R = 0 mm (b) R = 0.13 mm

(c) R = 0.33 mm

Fig. 5.8. Surface and cross-section of sheared edge for JSC980Y.

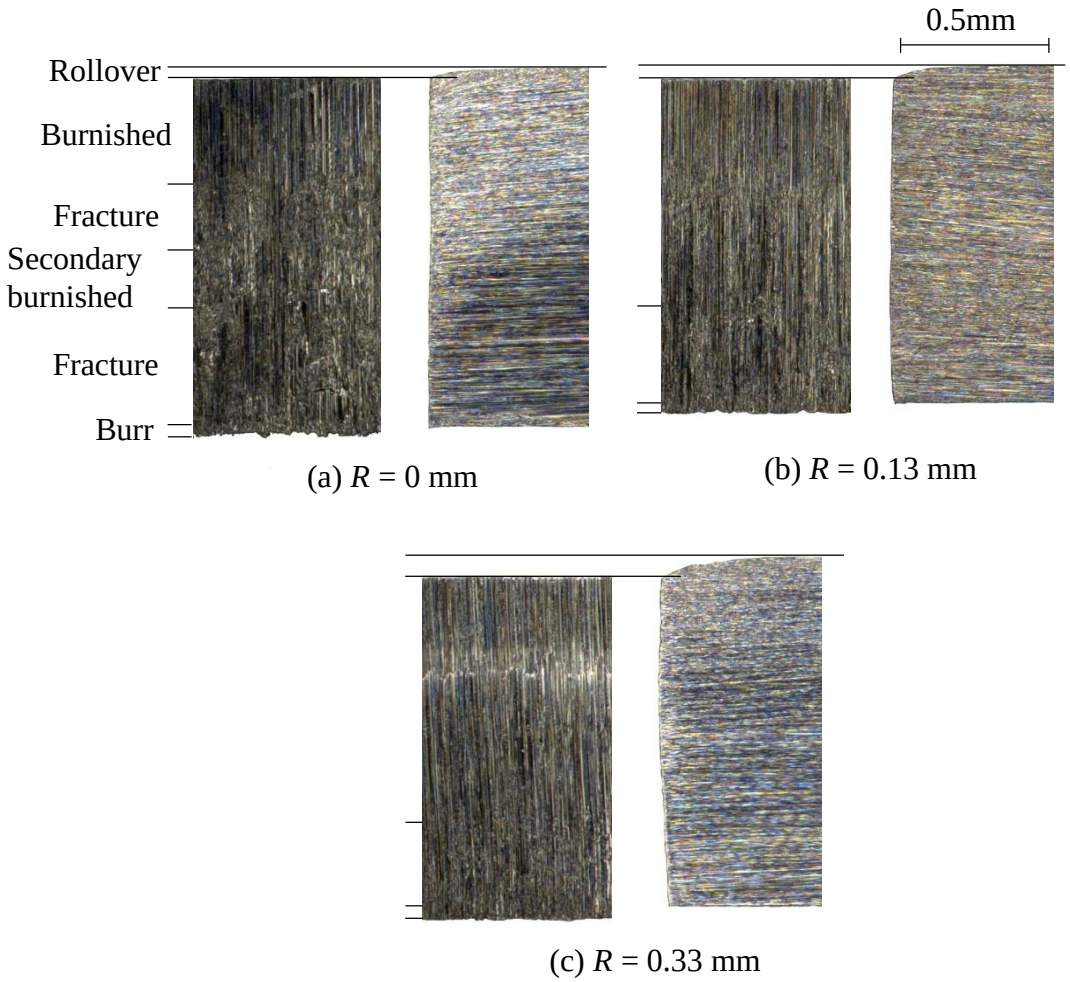

Fig. 5.9. Surface and cross-section of sheared edge for JSC1180Y.

The percentages of the rollover, burnished and fracture depths and the burr height on the sheared edge for the different edge radii are given in Fig. 5.10. For the small round edges of the punch, the burnished surfaces become considerably large, whereas the rollover and burr for R = 0.33 mm increase. It was found that the very small radius of R = 0.13 mm is effective for high quality of the sheared edge of the ultra-high strength steel sheets.

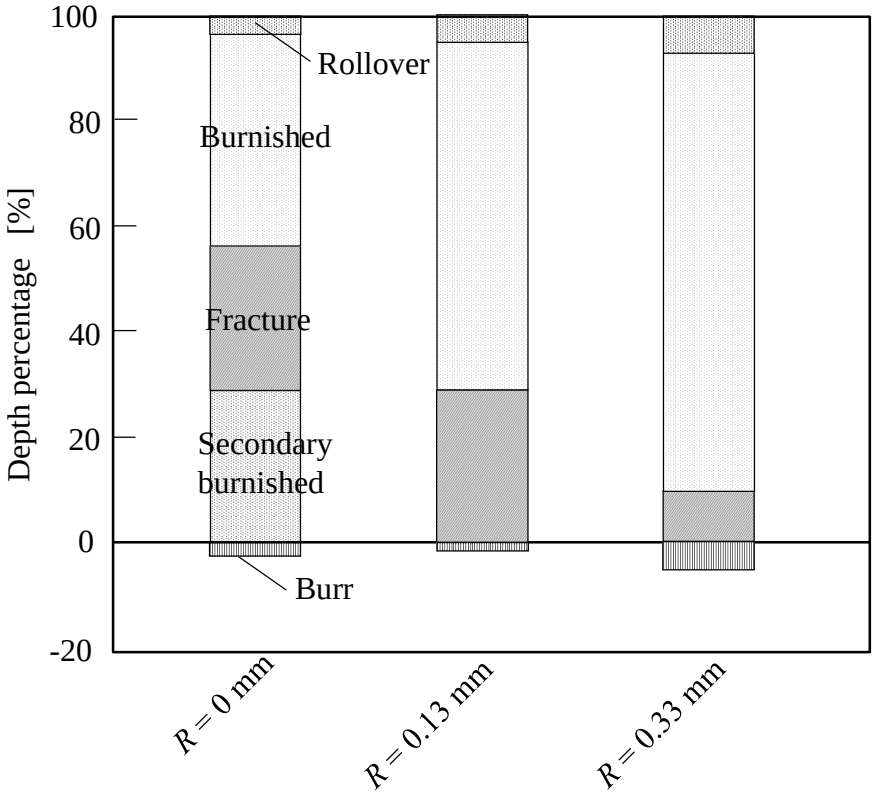

(a) JSC780Y

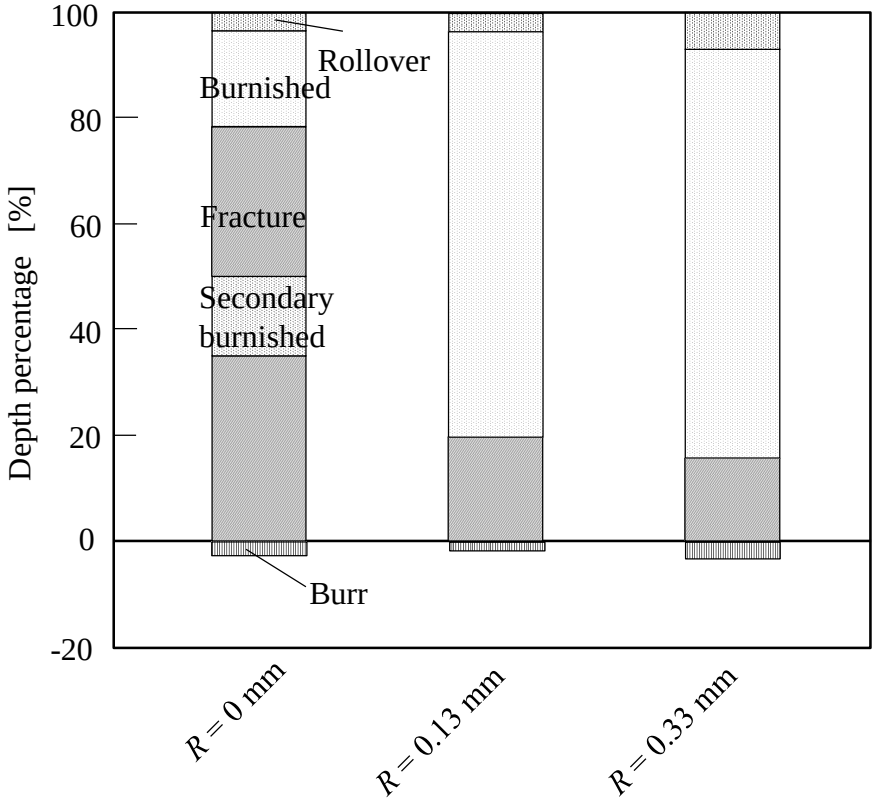

(b) JSC980Y

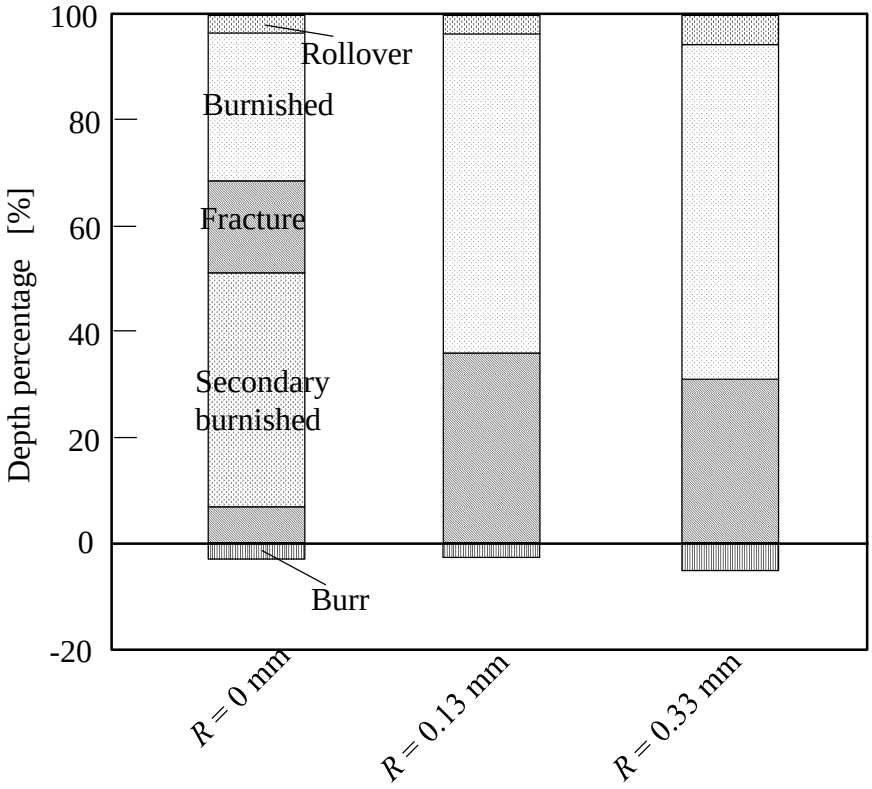

(c) JSC1180Y

Fig. 5.10. Percentages of rollover, burnished and fracture depths and burr height on sheared edge for (a) JSC780Y, (b) JSC980Y and (c) JSC1180Y.

The above-mentioned results are obtained for the slight clearance between the punch and die, c = 0.8%. The relationship between the percentage of rollover, burnished and fracture depths and burr height on the sheared edge and the clearance ratio for JSC980Y and R = 0.13 mm is shown in Fig. 5.11. As the clearance ratio increases, the burnished surface decreases, and the fracture surface and rollover increase. This is due to early onset of cracks induced by the increase in tensile stress around the edge of the die with the clearance as shown in Fig. 5.12. For R = 0.13 mm, the sheared edge of high quality is limited to the slight clearance. Since the ultra-high strength steel sheets have low ductility, both small round edge and slight clearance are indispensable, i.e. the relaxation of concentration of deformation around the punch edge and reduction in tensile stress around the die edge.

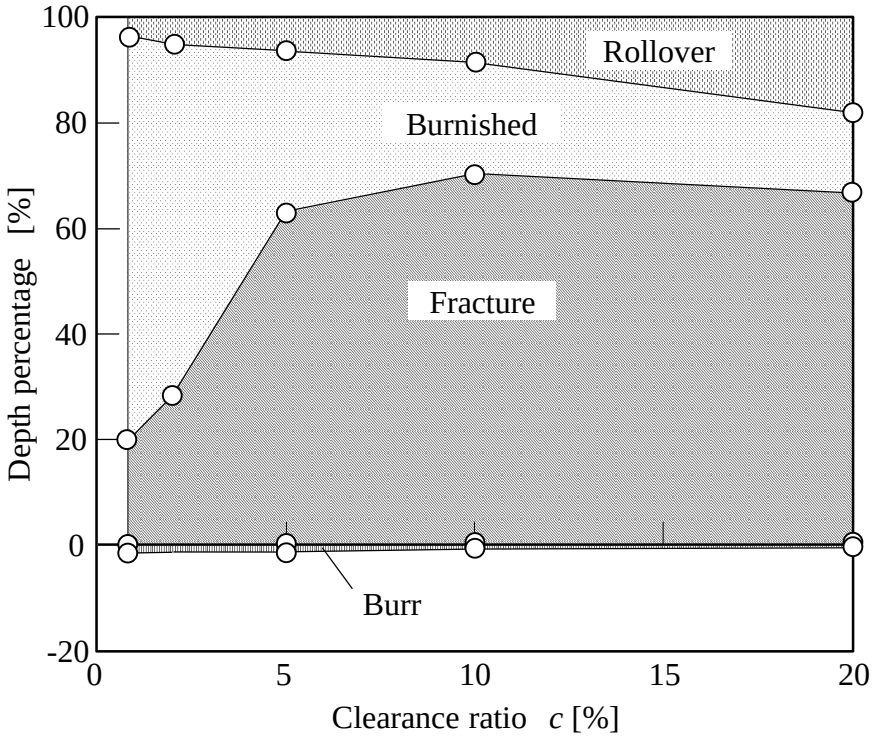

Fig. 5.11. Relationship between percentage of rollover, burnished and fracture depths and burr height on sheared edge and clearance ratio for JSC980Y and R = 0.13 mm.

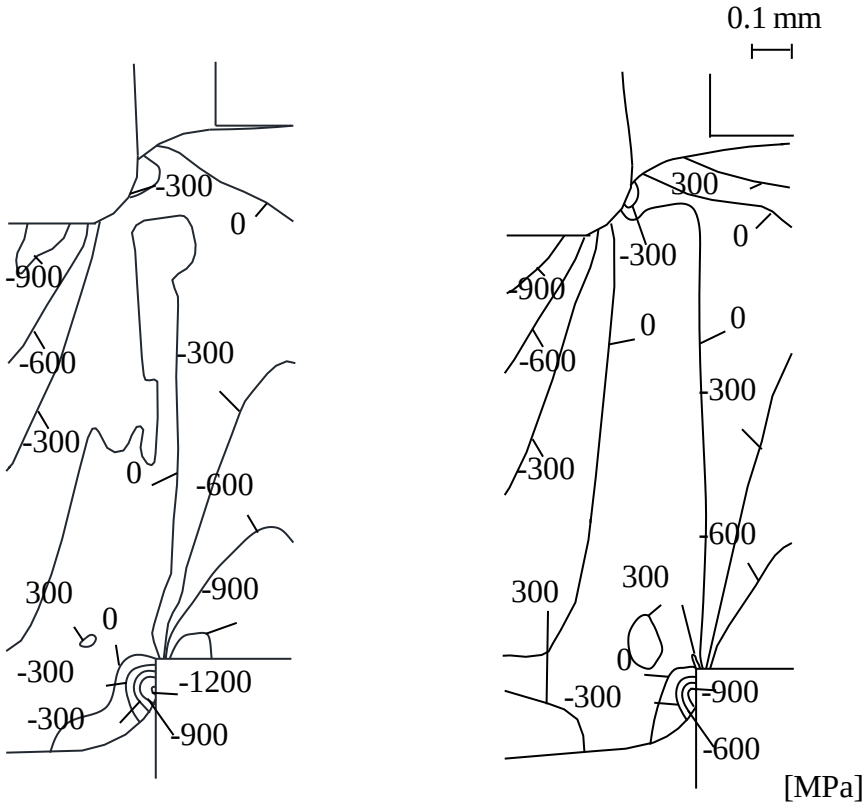

(a) c = 0.8% (b) c = 10%

Fig. 5.12. Distribution of mean stress calculated by finite element simulation for JSC980Y, R = 0.13 mm and s = 0.21 mm.

5.4. Mechanical properties of punched sheets

5.4.1. Delayed fracture

Punched ultra-high strength steel sheets have the risk of delayed fracture, particularly for JSC1180Y. The effect of the small round edge of the punch on the delayed fracture was examined by keeping the punched sheets in 35% concentration hydrochloric acid at room temperature. The occurrence of delayed fracture was accelerated with the high concentration of the acid.

The effect of the edge radius of the punch on the delayed fracture time for JSC1180Y is given in Fig. 5.13, where the delayed fracture time is the time from the soak of the sheet in the acid. The occurrence of cracks was visually observed. Although the cracks were observed after 2.5 h for c = 0.8% and R = 0 mm, no cracks were observed up to 24 h for R

= 0.13 and 0.33 mm. On the other hand, the cracks early occur for the large clearance of *c* = 10%.

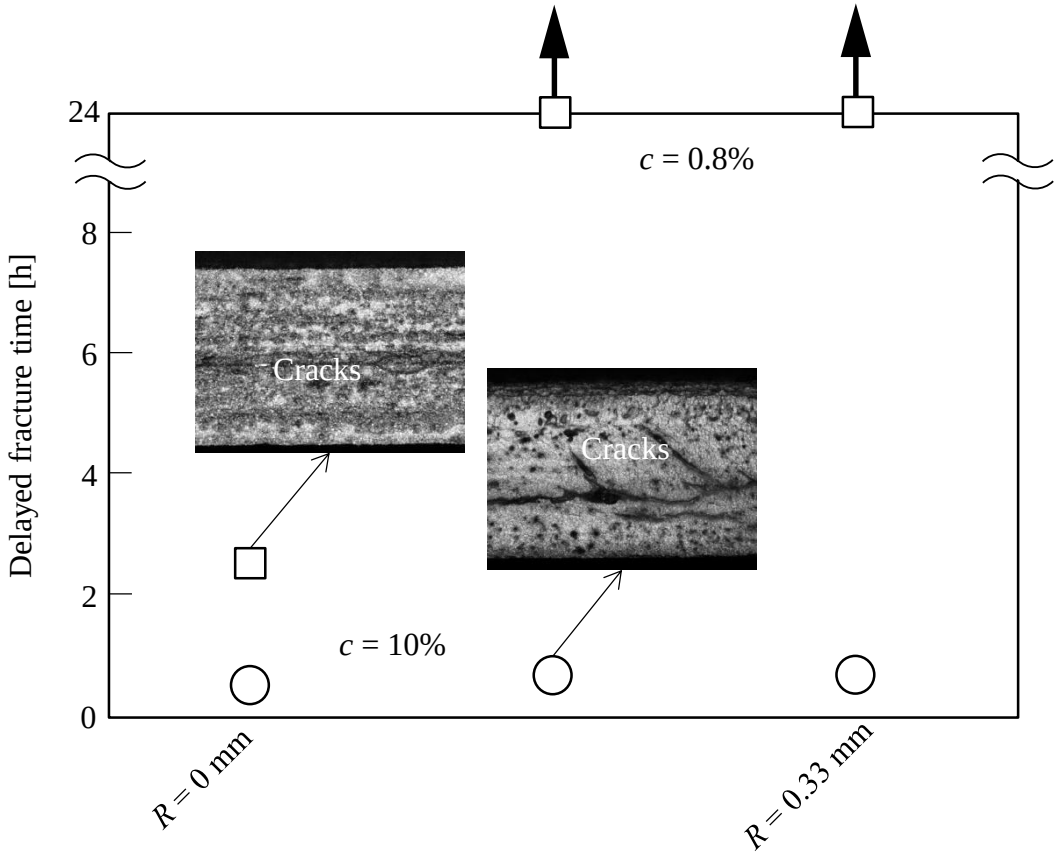

Fig. 5.13. Effect of edge radius of punch on delayed fracture time for JSC1180Y.

The effect of the edge radius of the punch on the residual stress in the thickness direction of the sheared edge measured by the X-ray diffraction for JSC1180Y is shown in Fig. 5.14. For the slight clearance, the compressive residual stress is increased by the small round edge, and the delayed fracture was prevented as shown in Fig. 5.13. On the other hand, the tensile residual stress becomes large for the large clearance.

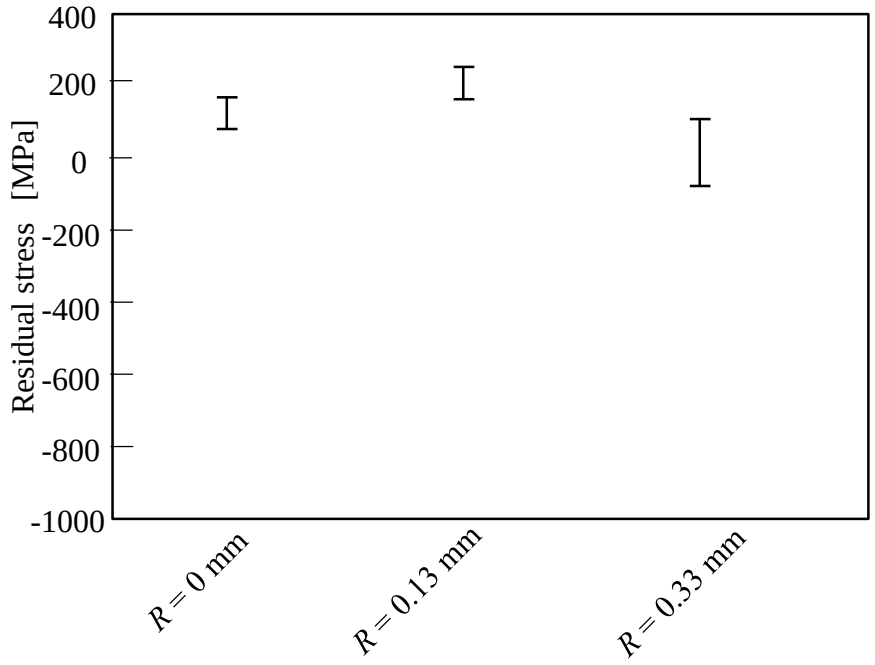

(a) c = 10%

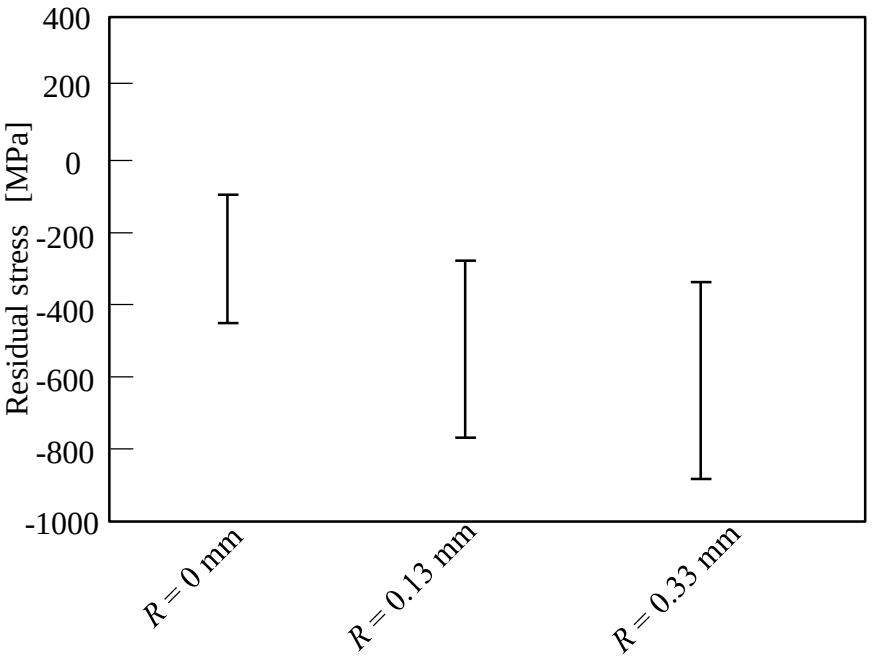

(b) c = 0.8%

Fig. 5.14. Effect of edge radius of punch on residual stress in sheared edge for JSC1180Y.

5.4.2. Limiting hole expansion

An expansion test of punched holes for the different edge radii of the punch was performed to examine the formability of the punched sheet. The procedure of expansion of

punched hole for evaluation of limiting hole expansion is shown in Fig. 5.15. The punched hole of the sheet was expanded with a conical punch having an angle of 60º. The expansion was stopped for just driving of cracks through the thickness, and the occurrence of cracks was visually observed as shown in Fig. 5.16. The burr of the sheet was set without touch of the punch on the opposite side.

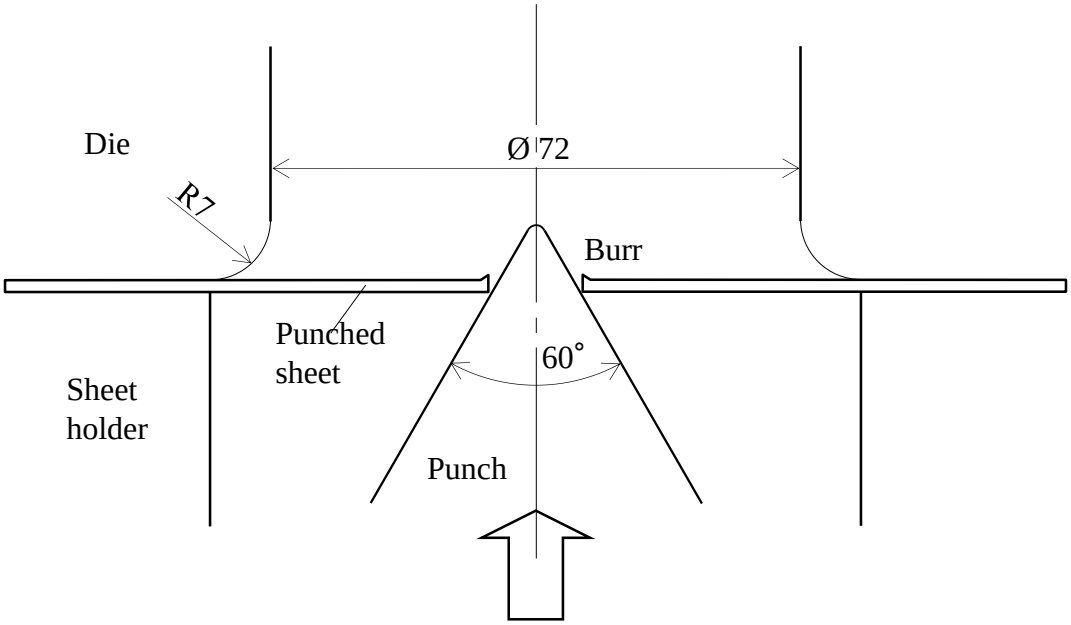

Fig. 5.15. Procedure of expansion of punched hole for evaluation of limiting hole expansion.

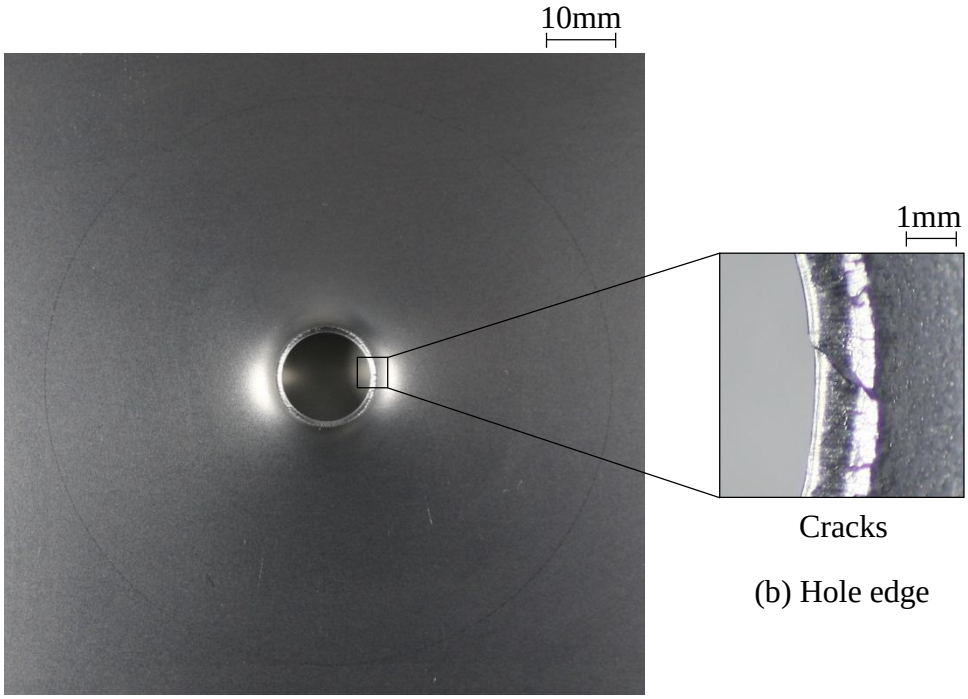

(b) Hole edge

(a) Punched sheet

Fig. 5.16. Cracks just driven though thickness caused by hole expansion at sheared edge for c = 0.8%, R = 0.15mm and JSC980Y.

A definition of limiting expansion ratio is illustrated in Fig. 5.17. The limiting expansion ratio is the change in diameter of the hole divided by the diameter before the expansion.

$$\text{Limiting expansion ratio } \lambda = \frac{d-d_0}{d_0}$$

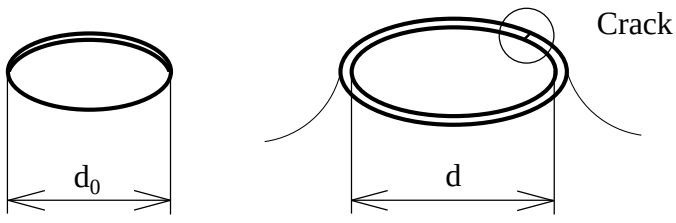

(a) Before expansion (b) After expansion

Fig. 5.17. Definition of limiting expansion ratio.

The relationship between the limiting expansion ratio and the average Vickers hardness of the sheared edge for JSC980Y is given in Fig. 5.18, where the hardness was measured in the cross-section at 0.05 mm from the sheared edge. As the hardness increases, the limiting expansion ratio decreases, and the ratio is the highest for R = 0 mm. The delay of the onset of the crack for the small round edges of the punch brings about increase in plastic deformation in the sheared edge as shown in Fig. 5.4, and thus the limiting expansion ratios for the small round edges are reduced by the increase. The hardness for R = 0.13 and 0.33 mm are almost the same, and thus the limiting expansion ratios are similar. The punch having the small round edge is inappropriate to burring processes of punched holes for forming a flange.

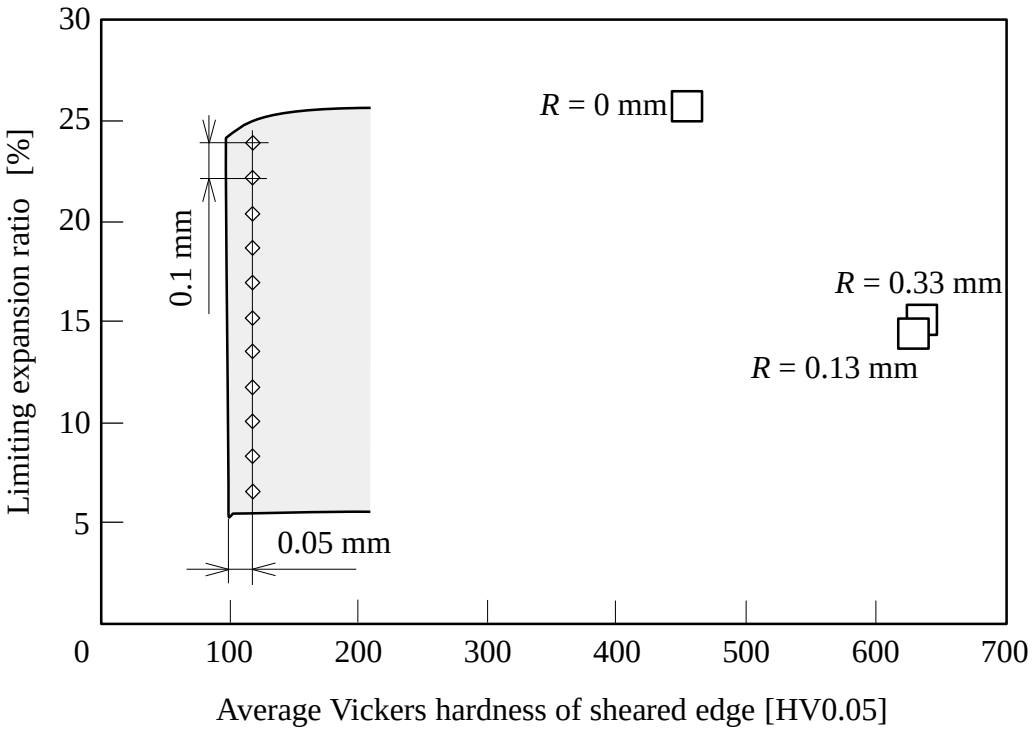

Fig. 5.18. Relationship between limiting expansion ratio and average Vickers hardness of sheared edge for JSC980Y.

5.4.3. Fatigue strength

To examine the effect of the edge radius of punch on the fatigue strength of the punched sheets, the plane bending fatigue test was performed. The frequency was set at 25Hz and the ratio of the minimum stress to maximum stress was -1.0. The loading for the

fatigue test was 3.78 N·m. The fatigue test was performed until separation induced by fracture occurred. Each fatigue test was performed at three times and the averages of the measured values are taken.

The number of cycles to failure in the plane bending fatigue test for the different punch shapes, c = 0.8% and JSC980Y is shown in Fig. 5.19. The fatigue strength for R = 0.13 and 0.33 mm is higher compare to that for R = 0 mm.

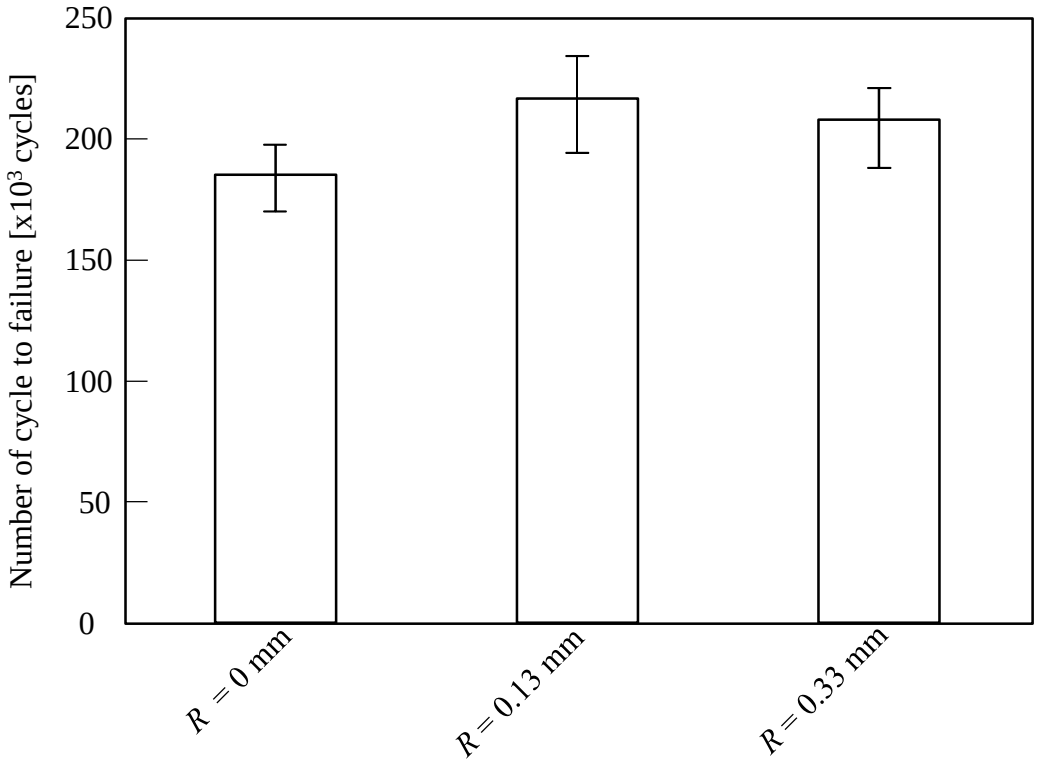

Fig. 5.19. Number of cycles to failure in plane bending fatigue test for different punch shapes, c = 0.8% and JSC980Y.

5.5. Repeated punching of ultra-high strength steel sheets

Since the punch having an edge radius of 0.13 mm exhibits high performance in the single punching operation, this punch was employed for repeated punching operation of the ultra-high strength steel sheet JSC1180Y. The tool used for the repeated punching of the ultra-high strength steel sheet is shown in Fig. 5.20. Three punches were installed in the

same time to investigate the different punch shape and punch coating in the repeated punching.

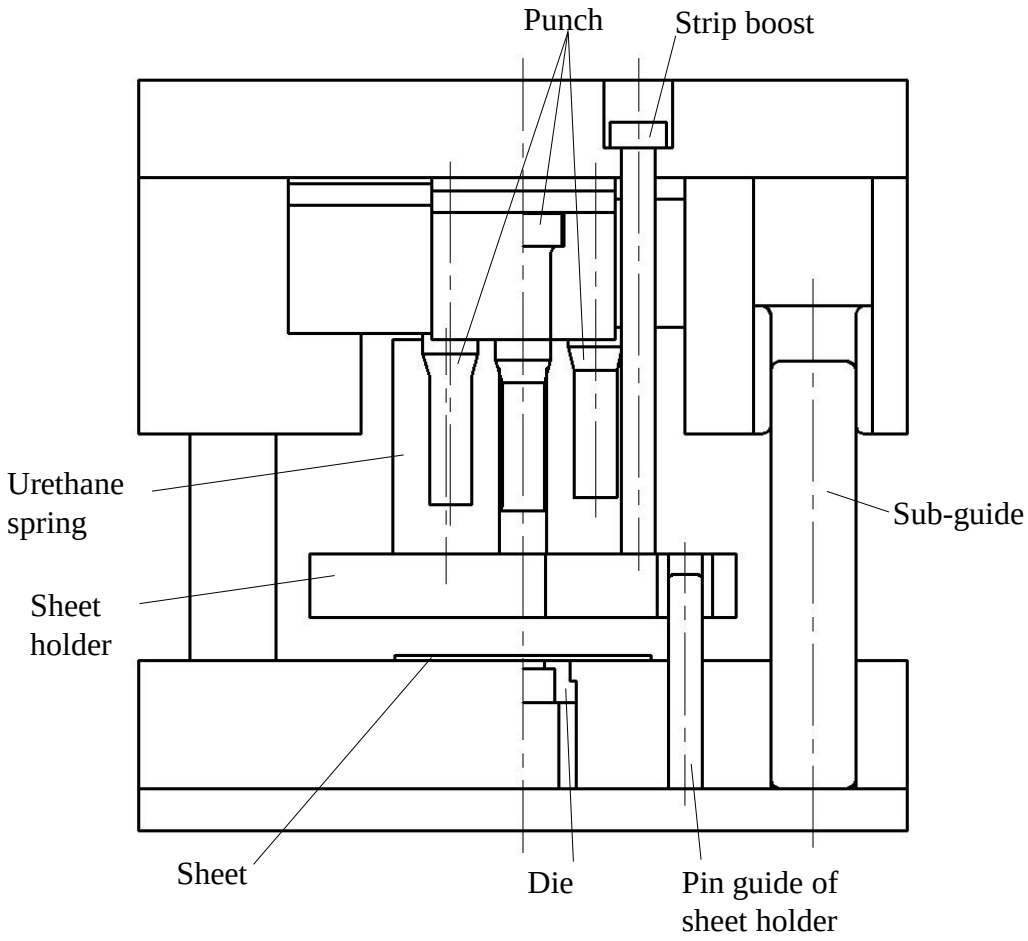

Fig. 5.20. Tools used for repeated punching of ultra-high strength steel sheets.

The conditions of the repeated punching of the ultra-high strength steel sheets are given in Table 5.4. A CNC servo press having a capacity of 800 kN was employed, and the punching speed was 75 mm/s. The ratio of clearance between the punch and die to the thickness was fixed to 1%. The dimension of the specimen for the repeated punching of the ultra-high strength steel sheets is shown in Fig. 5.21.

Table 5.4.

Conditions of repeated punching of ultra-high strength steel sheets.

Sheet	JSC1180Y
Clearance ratio *c* (%)	1.0
Punching speed (mm/s)	75
Lubricant	Rust prevention oil

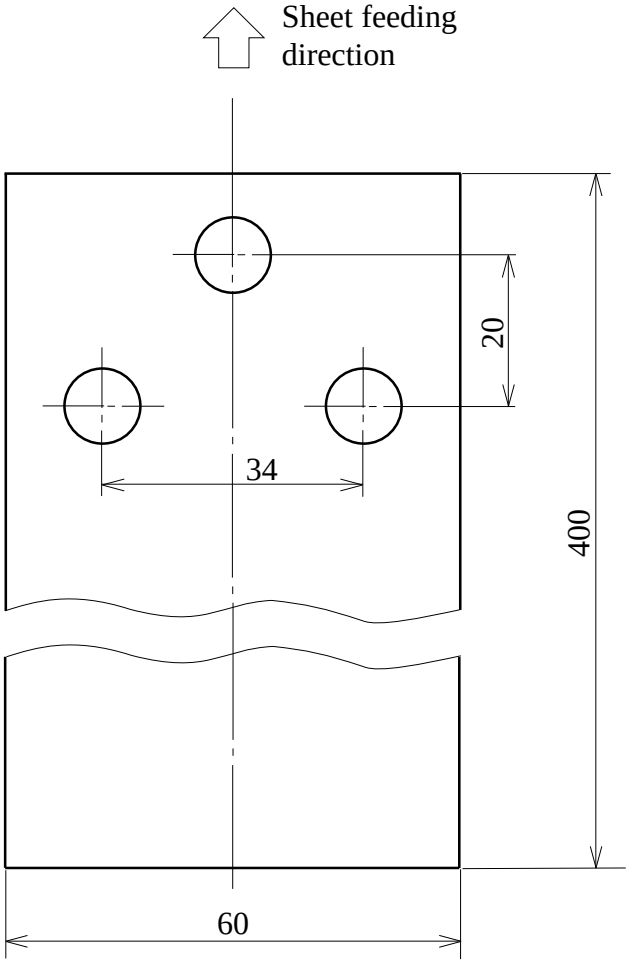

Fig. 5.21. Dimension of specimen for repeated punching of ultra-high strength steel sheets.

The tungsten carbide punch (1150HV) was treated by the TiN and TiAlN coatings having 2 μm in thickness. The coating properties used for the repeated punching of the ultra-high strength steel sheet is shown in Table 5.5.

Table 5.5.

Coating properties used for repeated punching of ultra-high strength steel sheets.

Material	Deposition method	Vickers hardness (HV)
TiN	PVD	2200
TiAlN	PVD	3500

The surface and cross-section of the sheared edge for the repeated punching of JSC1180Y are shown in Fig. 5.22. The surface of the sheared edge for the punch without the coating becomes rough after n = 100, whereas the quality of the surface for the TiN and TiAlN-coated punches is high even after n = 1000.

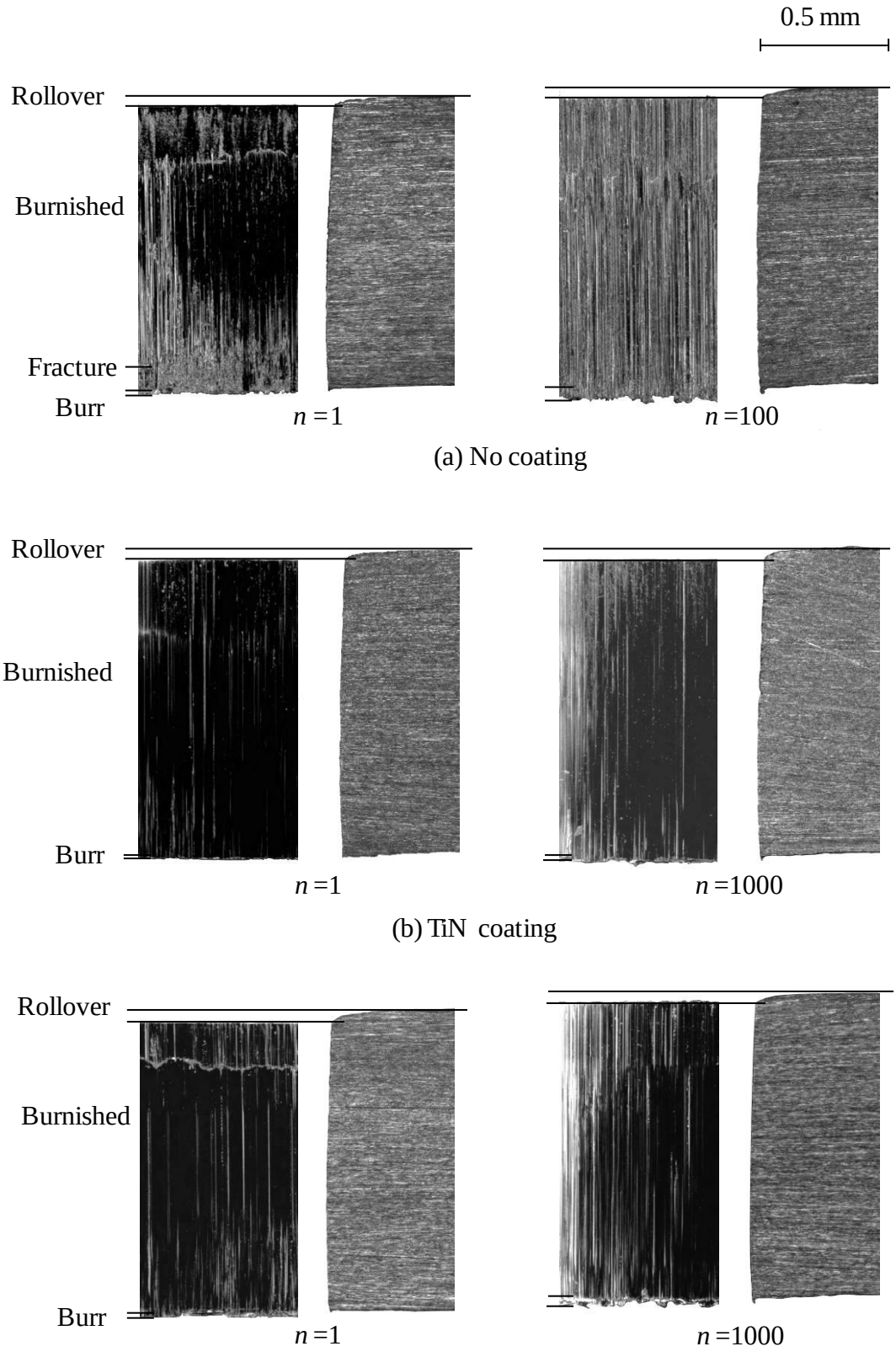

Fig. 5.22. Surface and cross-section of sheared edge for repeated punching of JSC1180Y.

The surface of the punch for the repeated punching of JSC1180Y is given in Fig. 5.23. The edge of the punch for R = 0 mm chipped from the early stage, and the chipping progressed. The chipping of the edge was prevented by the small round edge, and the wear of the round edges was not observed without change of the coating layer. Although the galling occurs around the punch edge after n = 100 for the punch without the coating, slight and no pick-ups appear after n = 1000 for the TiN and TiAlN-coated punches, respectively. It was found that the TiAlN-coated punch having a small round edge is useful for actual punching operations of ultra-high strength steel sheets.

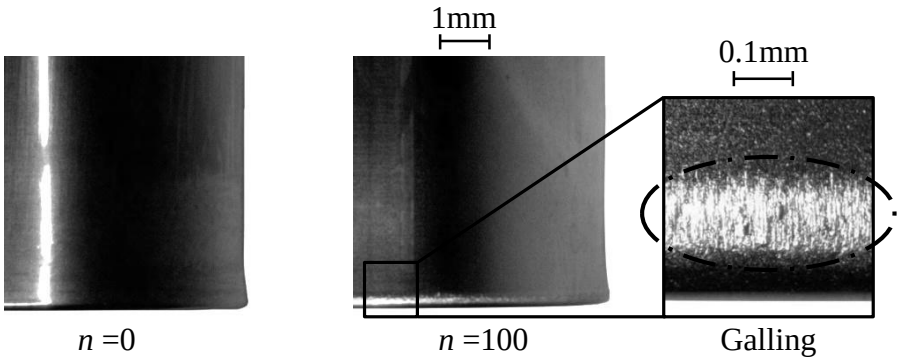

(a) R = 0.15 mm, no coating

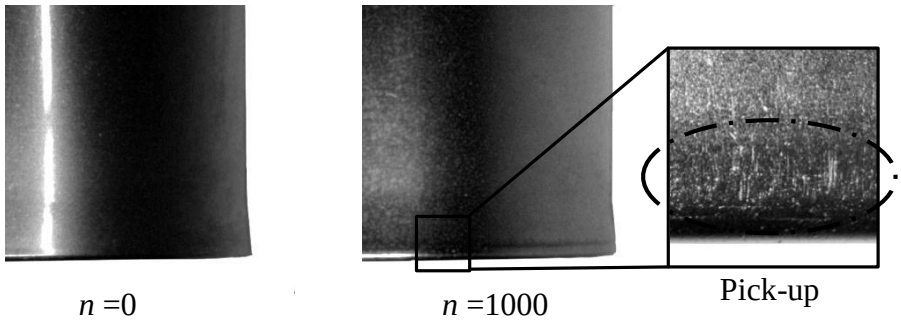

(b) R = 0.15 mm, TiN coating

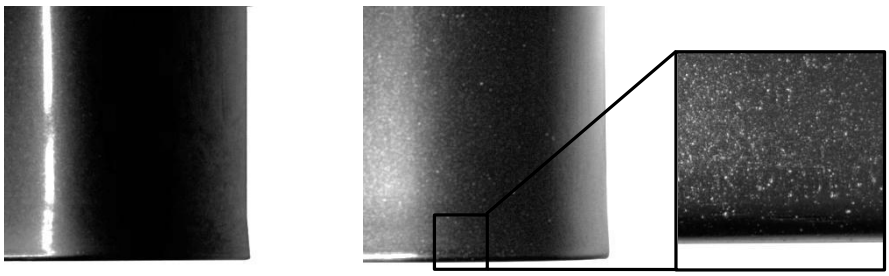

(c) R = 0.15 mm, TiAlN coating

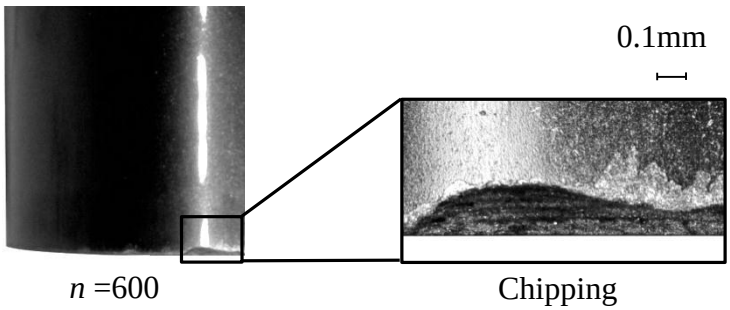

(d) R = 0 mm, TiAlN coating

Fig. 5.23. Surface of punch for repeated punching of JSC1180Y.

5.6. Conclusions

A slight clearance punching process using a punch having a small round edge was developed to improve the quality of the sheared edge for ultra-high strength steel sheets. The onset of cracks in the punching process was delayed by the small round edge of the punch. The following results were obtained;

1. The concentration of deformation around the edge of the punch was relaxed by the small round edge, the onset of a crack from the edge of the punch was prevented, and thus the burnished surfaces became considerably large.
2. A very small edge radius of 0.13 mm was effective for high quality of the sheared edge of ultra-high strength steel sheets.
3. The high quality of the sheared edge for the edge radius of 0.13 mm was limited to the slight clearance between the punch and die.
4. For the punched sheet with the punch having the small round edge, the delayed fracture was prevented and the fatigue strength was improved due to large compressive stress around the sheared edge.
5. The TiAlN-coated tungsten carbide punch having the small round edge had high galling resistance for the 1000 stroke punching.

5.7. References

[1] K. Mori, K. Akita, Y. Abe, Springback behaviour in bending of ultra-high-strength steel sheets using CNC servo press, International Journal of Machine Tools & Manufacture 47 (2) (2007) 321–325.

[2] K. Mori, S. Maki, Y. Tanaka, Warm and hot stamping of ultra high tensile strength steel sheets using resistance heating, CIRP Annals – Manufacturing Technology 54 (1) (2005) 209–212.

[3] K. Mori, T. Maeno, Y. Fukui, Spline forming of ultra-high strength gear drum using resistance heating of side wall of cup, CIRP Annals – Manufacturing Technology 60 (1) (2011) 299–302.

[4] K. Inoue, M. Suzuki, S. Nishino, K. Ohya, Y. Tomota, Effect of coating microstructure of press-working dies on sliding damage, Steel Research International 81 (9) (2010) Supplement Metal Forming 2010, 849–852.

[5] J. Eriksson, M. Olsson, Tribological testing of commercial CrN, (Ti,Al)N and CrC/C PVD coatings – Evaluation of galling and wear characteristics against different high strength steels, Surface and Coatings Technology 205 (16) (2011) 4045–4051.

[6] S. Sresomroeng, V. Premanond, P. Kaewtatip, A. Khantachawana, A. Kurosawa, N. Koga, Performance of CrN radical nitrided tools on deep drawing of advanced high strength steel, Surface and Coatings Technology 205 (17–18) (2011) 4198–4204.

[7] K. Mori, Y. Abe, Y. Suzui, Improvement of stretch flangeability of ultra high strength steel sheet by smoothing of sheared edge, Journal of Materials Processing Technology 210 (4) (2010) 653–659.

[8] K. Mori, Y. Abe, Y. Ikeda, Improvement of formability for expansion of punched hole of ultra-high strength steel sheets by smoothing of sheared edge, Steel Research International (2011) Special Edition, 604–609.

[9] T. Matsuno, Y. Kuriyama, H. Murakami, S. Yonezawa, H. Kanamaru, Effects of punch shape and clearance on hole expansion ratio and fatigue properties in punching of high strength steel sheets, Steel Research International 81 (9) (2010) Supplement Metal Forming 2010, 853–856.

[10] K. Mori, S. Saito, S. Maki, Warm and hot punching of ultra high strength steel sheet, CIRP Annals – Manufacturing Technology 57 (1) (2008) 321–324.

[11] K. Mori, T. Maeno, S. Fuzisaka, Punching of ultra-high strength steel sheets using local resistance heating of shearing zone, Journal of Materials Processing Technology 212 (2) (2012) 534–540.

[12] K. Mori, T. Maeno, Y. Maruo, Punching of small hole of die-quenched steel sheets using local resistance heating, CIRP Annals – Manufacturing Technology 61 (1) (2012) 255-258.

Chapter 6

Punching of inclined ultra-high strength steel sheet

6.1. Introduction

The reduction in weight of automobiles is in great demand for improving the fuel consumption. For the reduction, the use of high strength steel sheets for body-in-white parts sharply increases. Since the rise in strength of the sheet is required to satisfy the safety standards for protecting passengers in automobiles, the application of ultra-high strength steel sheets having a tensile strength above 1 GPa expands. Although parts made of ultra-high strength steels have superior mechanical properties, the stamping operation becomes difficult with the increase in strength of the sheet. The forming load and springback become very large, and the formability is considerably small [1-3].

Body-in-white parts are generally punched to make many holes for joining, paint removing, attachment, reduction in weight, etc. Since ultra-high strength steel sheets have large strength and low ductility, the punching becomes difficult due to the increases in punching load and tool wear [4-6]. Moreover, the quality of the sheared edge for the ultra-high strength steel sheet is lower than that for the mild steel sheets Since the onset of cracks in the shearing is early due to the small ductility [7-10]. Although punching of inclined portions is required for the automobile parts, it is not easy to punch these portions due to gradual contact between a sheet and a punch, and thus the quality of the sheared edge decreases, particularly for the ultra-high strength steel sheet [11].

In the present study, a punching process of an inclined ultra-high strength steel sheet using punches having different head shapes was developed to improve the quality of the sheared edge of an ultra-high strength steel sheet. The effects of clearance between the punch and die and a shape of the punch head on the quality of the sheared edges were investigated.

6.2. Punching of inclined ultra-high strength steel sheet

A punching process of the inclined ultra-high strength steel sheet is shown in Fig. 6.1. In this process, the contact between the sheet and a flat head punch becomes gradual because of touch from the bottom edge of the punch, and thus the sheared portion tends to bend in the latter half of punching. Therefore the quality of the sheared edge deteriorates.

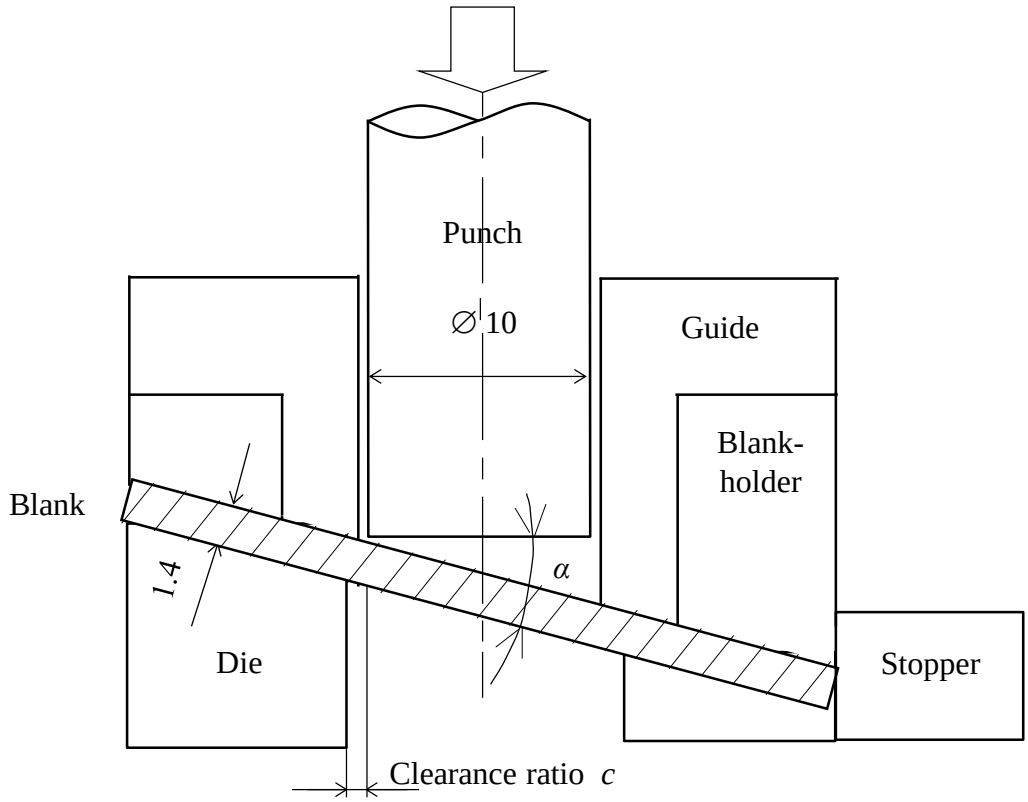

Fig. 6.1. Punching process of inclined ultra-high strength steel sheet.

To improve the quality of the sheared edge in the punching of inclined ultra-high strength steel sheet, the punches having different shapes of the head shown in Fig. 6.2 were employed. In the taper head punch, the head is in whole contact with the sheet. Although the bending moment is applied to the sheet due to the contact in one edge for the flat head punch, the moment is reduced by the contact in both edges for the curved head punch.

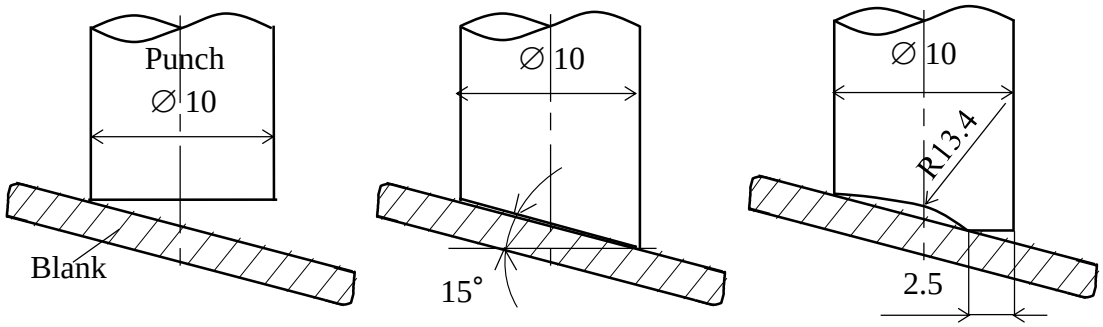

(a) Flat head punch (b) Taper head punch (c) Curved head punch

Fig. 6.2. Punches used in punching process of inclined ultra-high strength steel sheet.

The ultra-high strength steel sheet JSC980Y was used in the experiment. The mechanical properties of this sheet measured from the tensile test are given in Table 6.1. The dimension of the sheet is shown in Fig. 6.3. The thickness, length and width of the sheet are 1.4, 80 and 50 mm, respectively.

Table 6.1.

Mechanical properties of ultra-high strength steel sheet.

Sheet	Yield stress	Tensile strength	Elongation
JSC980Y	620 MPa	1027 MPa	18.7 %

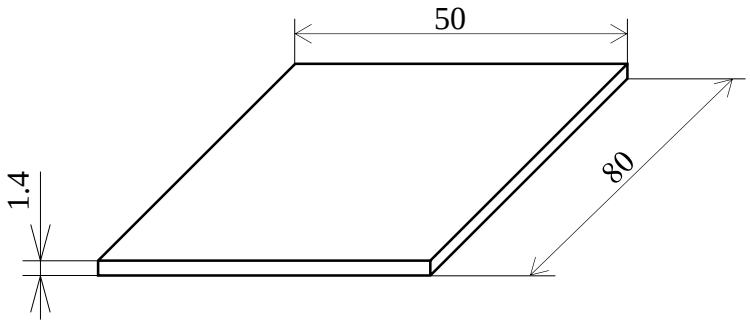

Fig. 6.3. Dimension of specimen for punching of inclined ultra-high strength steel sheets.

6.3. Results of punching of inclined ultra-high strength steel sheet

6.3.1. Deformation behaviour

The effect of the inclined angle to the deformation behaviour of the blank in the punching of ultra-high strength steel sheet was examined using the flat head punch. The deformation behaviours of the blank for different inclined angle and c = 20% are shown in Fig. 6.4, where s is the punching stroke. For α = 15^o, the crack has appeared in θ = 0 and 180^o for punching stroke s = 1.0 and 3.1 mm, respectively. Whereas, the crack has initiated in the whole surface of the blank for s = 0.7 mm and α = 0^o.

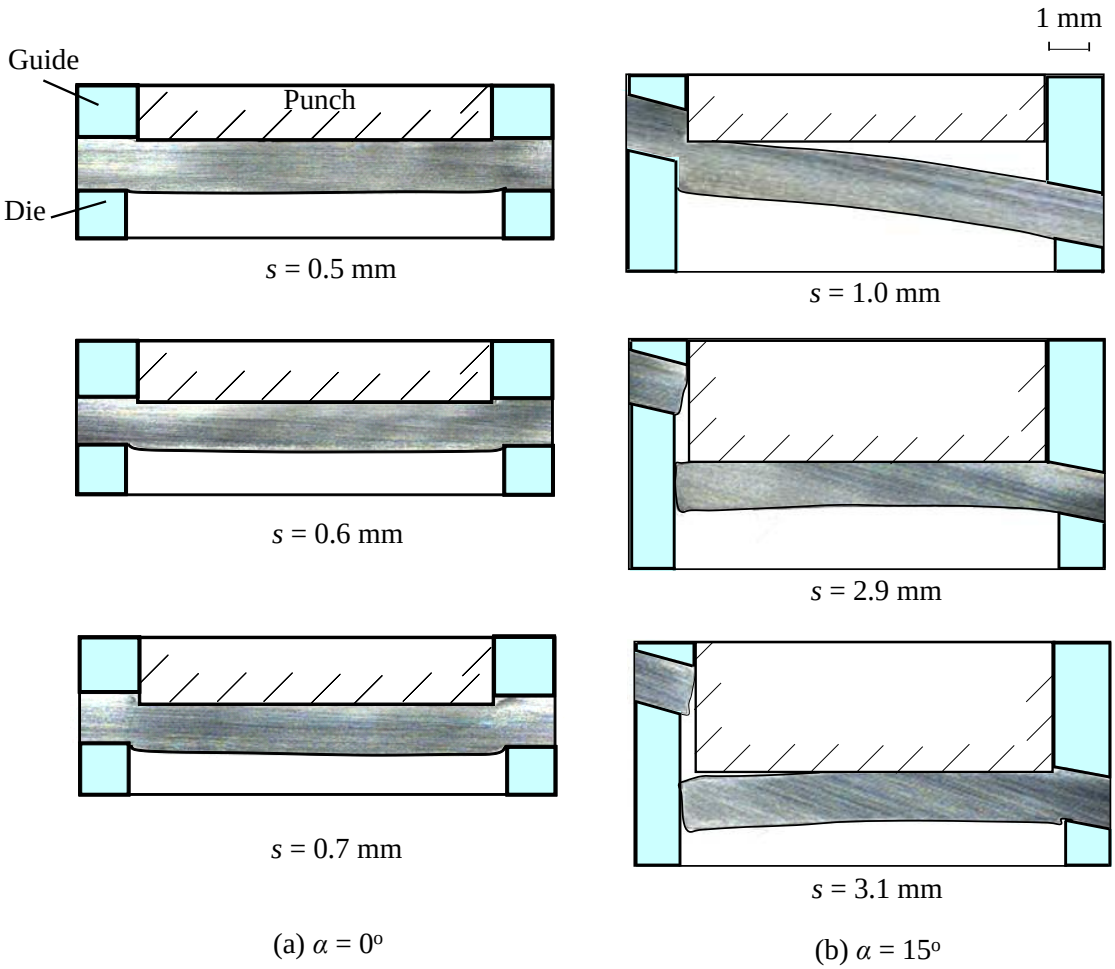

Fig. 6.4. Deformation behaviour of blank for flat head punch, c = 20%, (a) α =0^o and (b) α =15^o.

The punching load-stroke curves for the different inclined angle, flat head punch and c = 20% are shown in Fig. 6.5. The punching load for α = 0^o was larger than that for α = 15^o,

whereas the punching stroke was smaller. The punching load for $\alpha = 15^o$ has the two small peaks due to different time of crack initiation during punching.

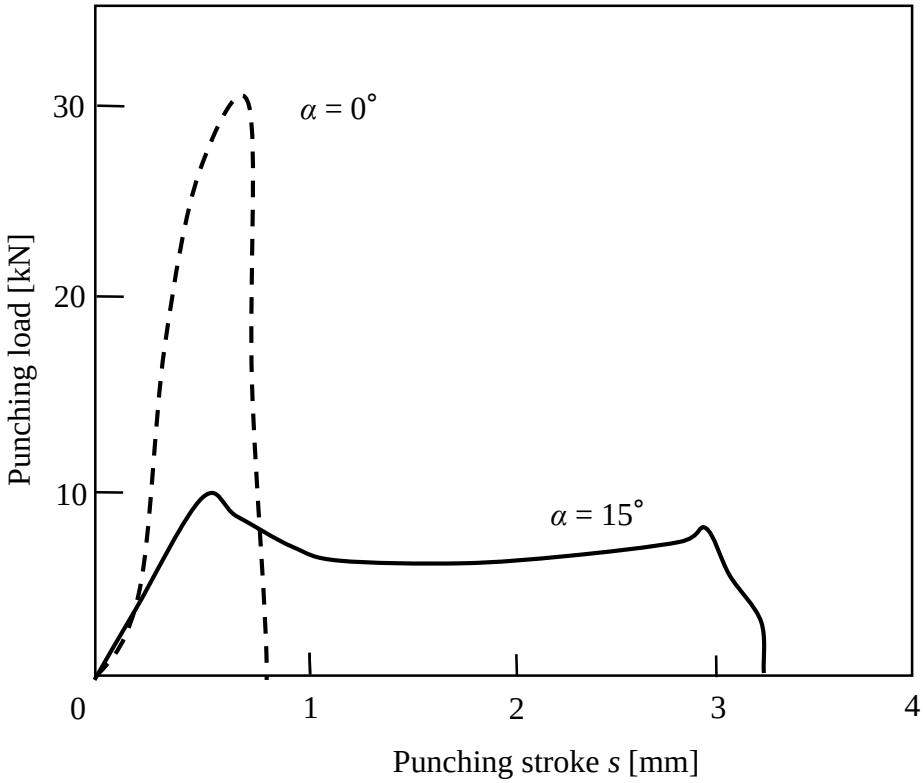

Fig. 6.5. Punching load stroke-curves for different inclined angle, flat head punch and c = 20%.

6.3.2. Quality of sheared edge

The surface and cross-section of the sheared edge for $\alpha = 0^o$ and 15^o, flat head punch and c = 20% are shown in Fig. 6.6, where θ is the measured angle. The rollover, burnished surface, fracture surface and burr are formed on the sheared edge. The quality of sheared edge for $\alpha = 0^o$ is uniform, whereas for $\alpha = 15^o$ is not similar for the different measured angle θ. Moreover, the burr is formed for $\alpha = 15^o$ in $\theta = 135^o$.

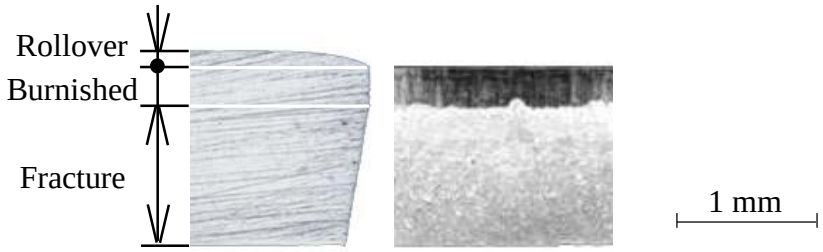

(a) $\alpha = 0^{\circ}$

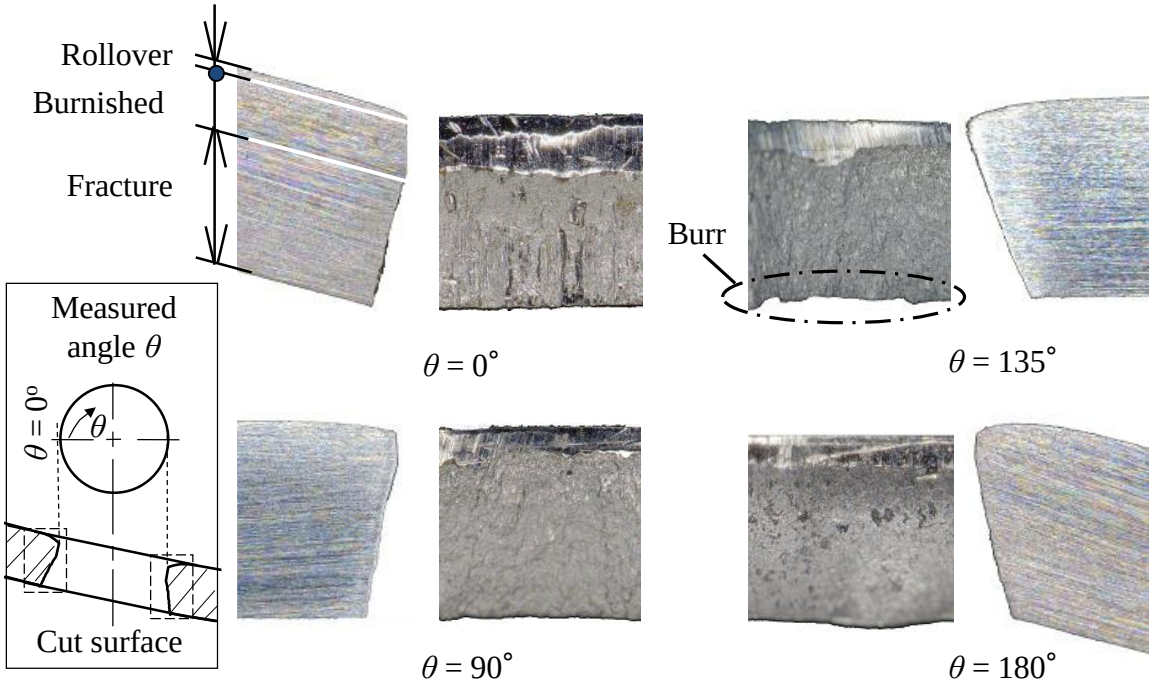

(b) $\alpha = 15^{\circ}$

Fig. 6.6. Surface and cross-section of sheared edge for flat head punch, c = 20%, (a) $\alpha = 0^{o}$ and (b) $\alpha = 15^{o}$.

The percentage of the depths of rollover, burnished surface, and fracture surface on the sheared edge for $\alpha = 0^{o}$ and 15^{o}, flat head punch and c = 20% is illustrated in Fig. 6.7. The quality of sheared edge for $\alpha = 0^{o}$ is uniform, whereas for $\alpha = 15^{o}$ is not similar for the different measured angle θ.

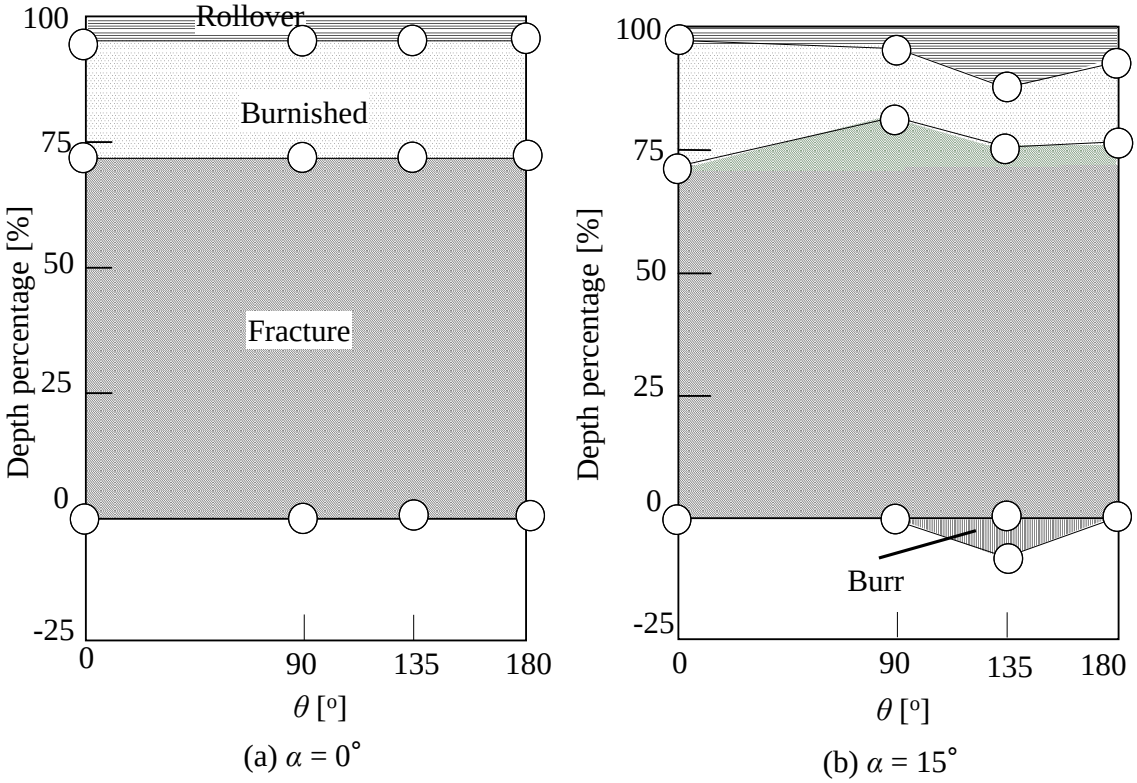

Fig. 6.7. Percentage of depths of rollover, burnished surface, and fracture surface on sheared edge for flat head punch, c = 20%, (a) α =0^o and (b) α =15^o.

6.4. Improvement of quality of sheared edge in inclined punching

6.4.1 Effect of punching clearance

The effect of the clearance between the punch and die to the quality of sheared edge in the inclined punching of ultra-high strength steel sheet was examined using the flat head punch. The deformation behaviour of the blank for the flat head punch, α = 15^o, c = 7 and 12% is shown in Fig. 6.8.

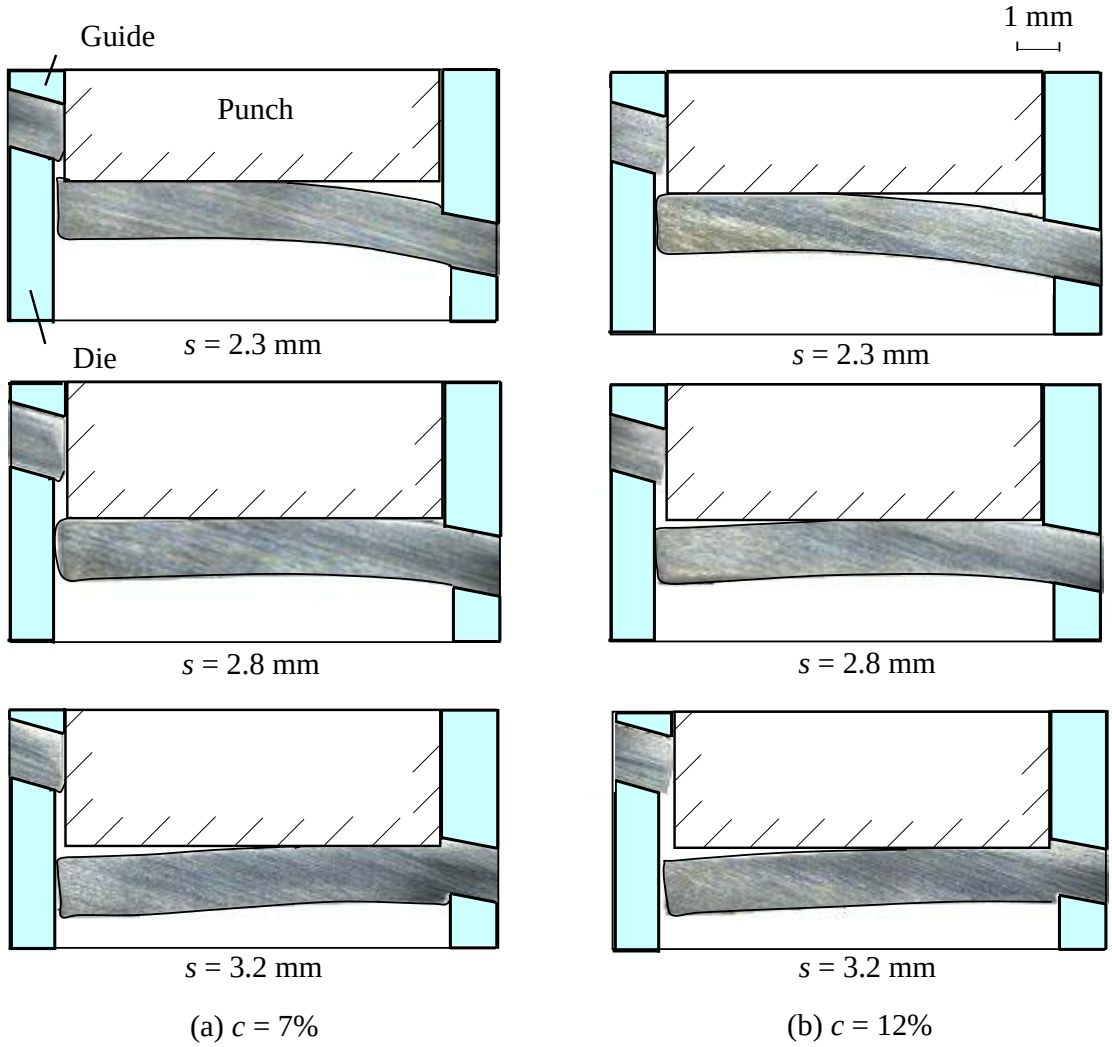

Fig. 6.8. Deformation behaviour of blank for flat head punch, α =15^o, (a) c = 7% and (b) c = 12%.

The surface and cross-section of the sheared edge for c = 7 and 12%, flat head punch and α = 15^o are shown in Figs. 6.9(a) and (b), respectively. The burnished surface in θ = 0 and 90^o for c = 7% are larger than those for c = 12%. However, the secondary burnished is formed in θ = 135 and 180^o for c = 7%, while for c = 12% the secondary burnished surface occurs only in θ = 180^o.

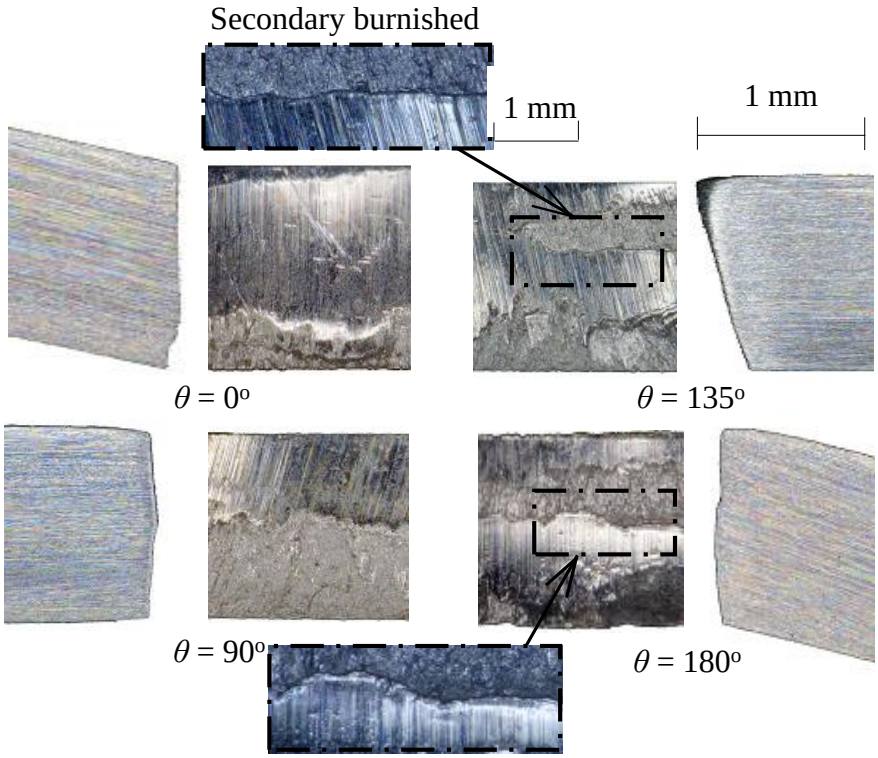

(a) c = 7%

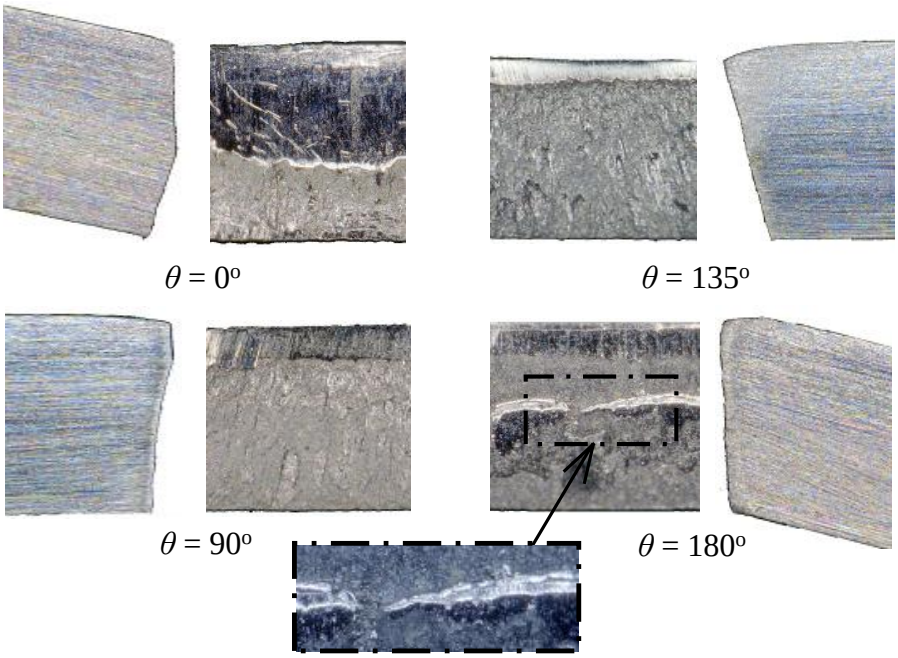

(b) c = 12%

Fig. 6.9. Surface and cross-section of sheared edge for flat head punch, α =15°, (a) c = 7% and (b) c = 12%.

Then the asymmetric clearance was implemented in the punching of inclined ultra-high strength steel sheet for improving the quality of the sheared edge. The procedure of the punching process for the asymmetric clearance is shown in Fig. 6.10. For the blank in the measured angle θ = 0 and 180^o, c = 12 and 20% were applied, respectively.

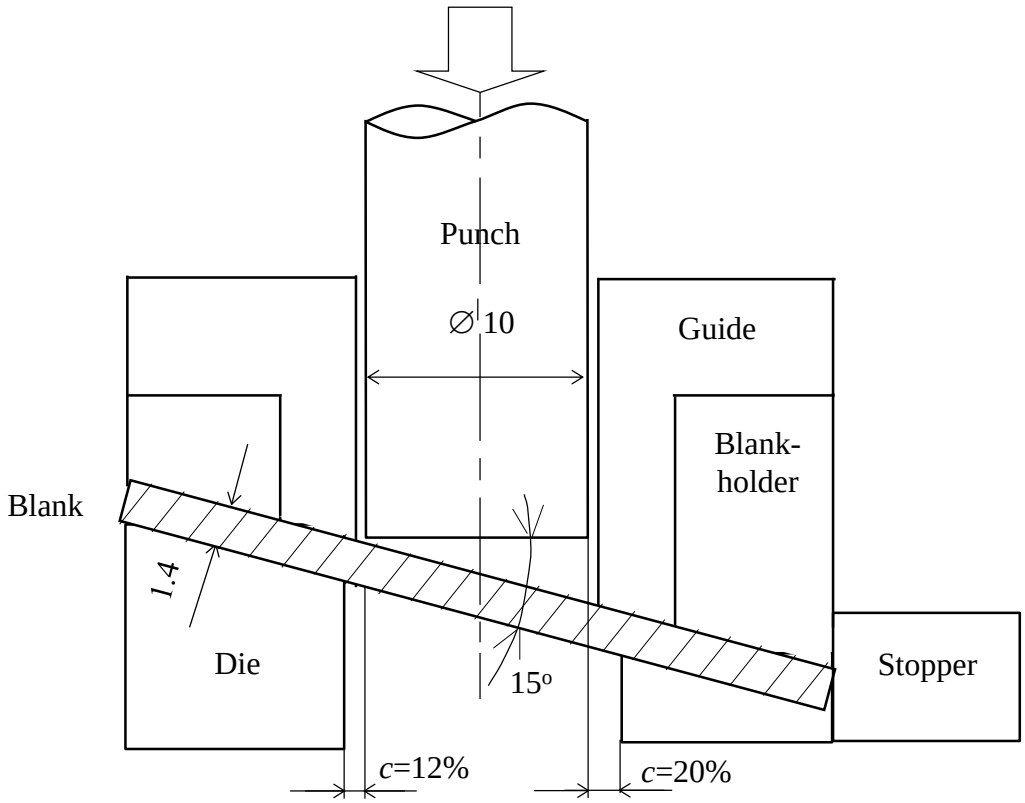

Fig. 6.10. Procedure of punching process for asymmetric clearance.

The surface and cross-section of the sheared edge for the asymmetric clearance of c = 12 and 20%, flat head punch and α = 15^o is shown in Fig. 6.11. For the asymmetric clearance, the secondary burnished surface not appears in θ = 180^o and the burnished surface in θ = 0^o as large as that for the symmetric c = 12%.

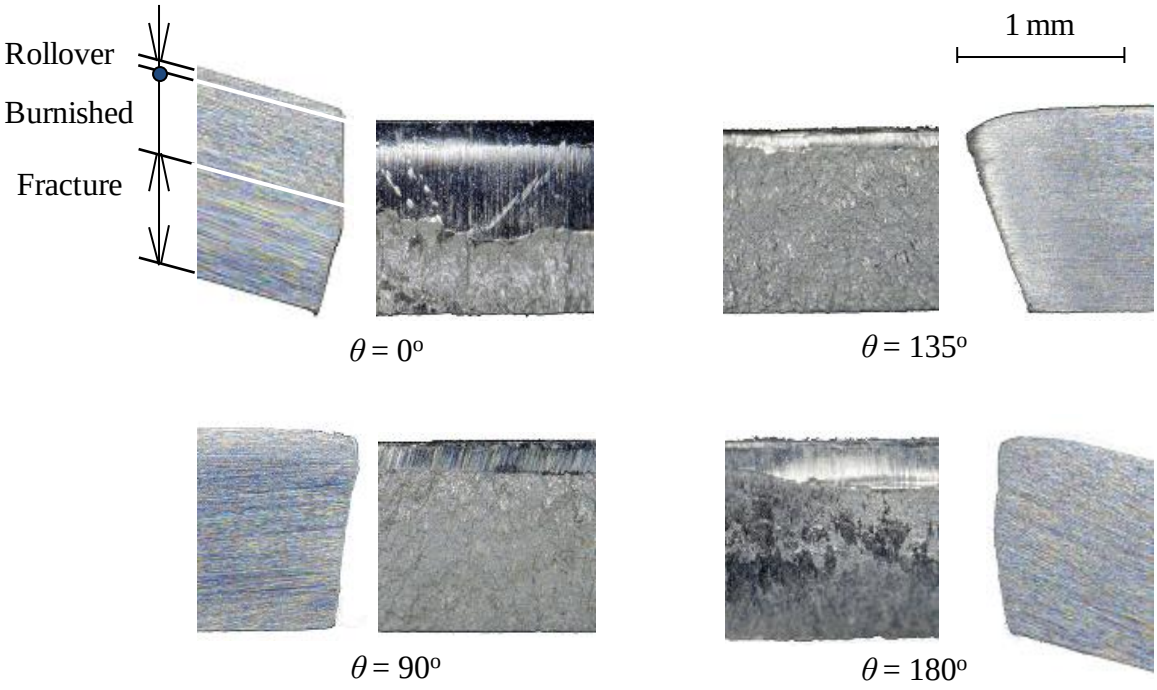

Fig. 6.11. Surface and cross-section of sheared edge for asymmetric clearance of c = 12 and 20%, flat head punch and $\alpha = 15^{o}$.

The punching load-stroke curves for the different clearance ratio c, flat head punch and $\alpha = 15^{o}$ are shown in Fig. 6.12. As the clearance ratio c decreases, the punching load and punching stroke increase. The maximum punching load for asymmetric clearance of c = 12 and 20% is between c = 12 and 20%.

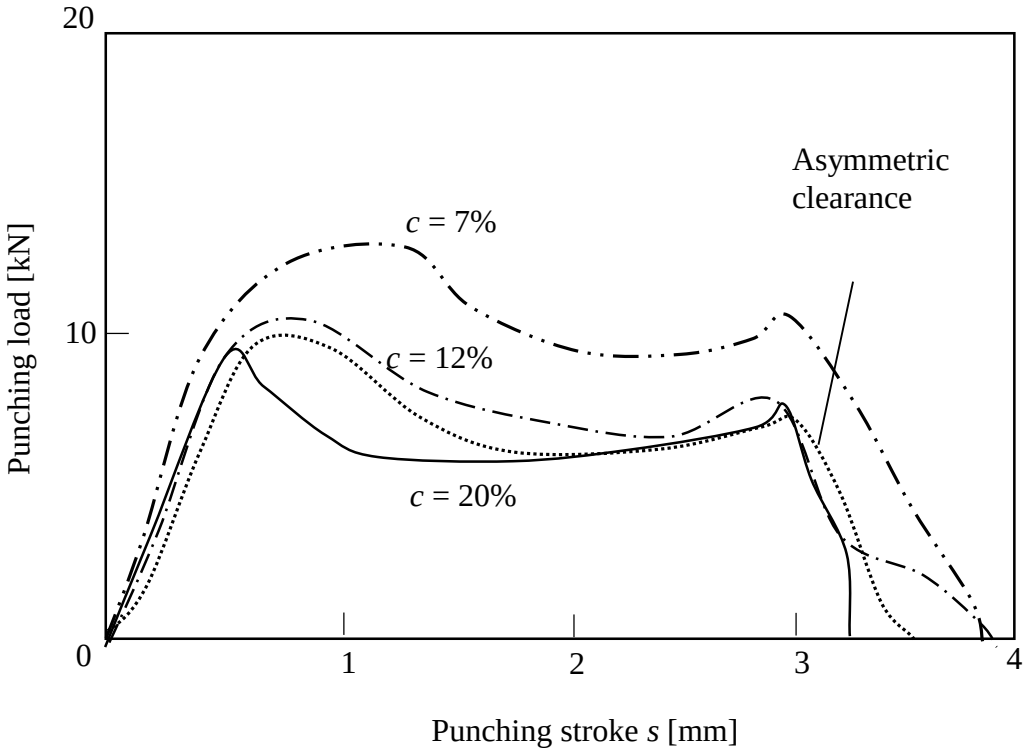

Fig. 6.12. Punching load stroke-curves for different clearance ratio *c*, flat head punch and α =15^{o}.

The percentage of the depths of rollover, burnished surface, and fracture surface on the sheared edge for the different clearance ratio, flat head punch and α = 0^{o} and 15^{o} are illustrated in Fig. 6.13. The sheared edge for the asymmetric clearance has the smallest burnished area, however the secondary burnished surface does not appear.

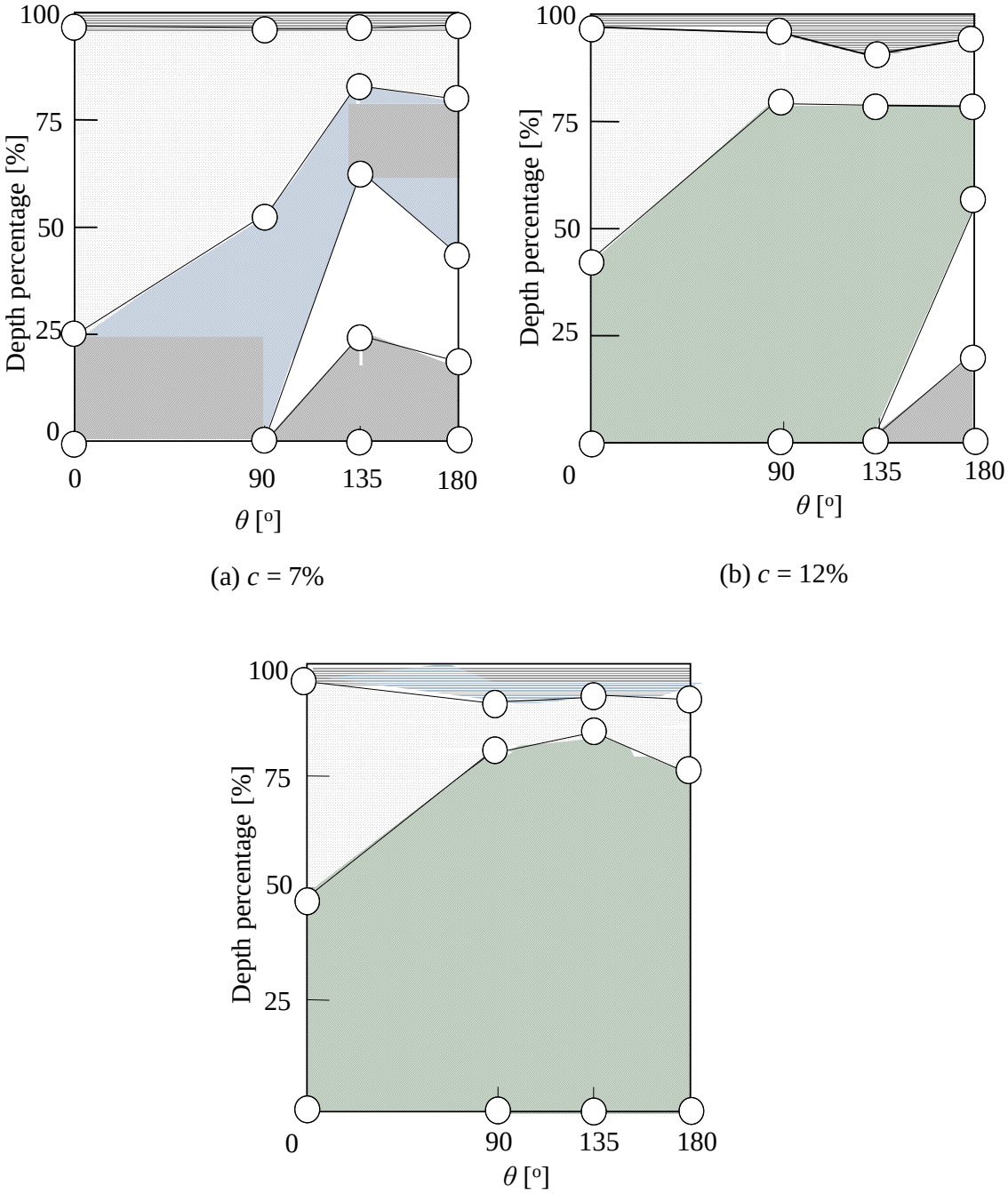

(a) c = 7%

(b) c = 12%

(c) Asymmetric clearance of c = 12 and 20%

Fig. 6.13. Percentage of depths of rollover, burnished surface, and fracture surface on sheared edge for flat head punch, α =15°, (a) c = 7%, (b) c = 12% and (c) Asymmetric clearance of c = 12 and 20%.

The relationship between the diameter of the punched hole and the measured angle for the flat head punch and the different clearance ratio is shown in Fig. 6.14. The hole

diameter was measured in $\theta = 0$, 45 and 90^o. The measured diameter of the punched hole for $\alpha = 15^o$ is not uniform as that for $\alpha = 0^o$ due to the inclined angle of the blank. As the clearance ratio increases, the different measurement of hole diameter in measured angle increases.

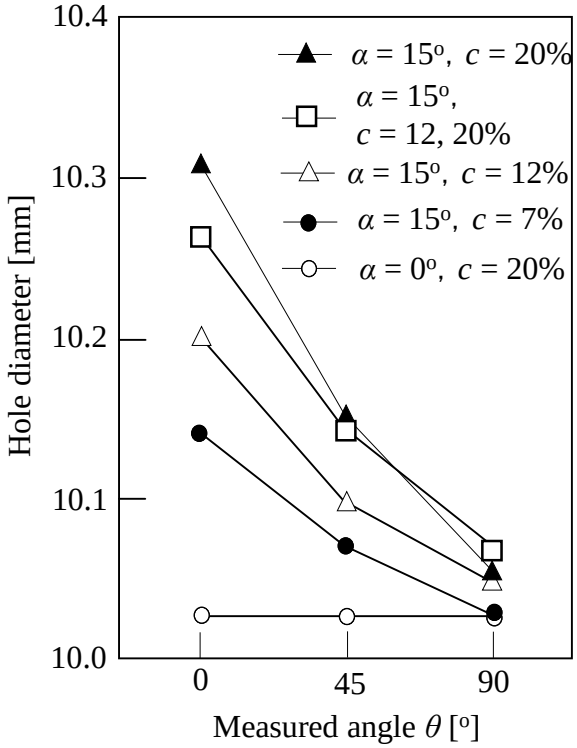

Fig. 6.14. Relationship between diameter of punched hole and measured angle for flat head punch and different clearance ratio.

6.4.2. Effect of punch head shape

The deformation behaviour of the blank for the different punches during punching process for $\alpha = 15^o$ and $c = 12\%$ are shown in Fig. 6.15. For $s = 0.7$ mm, the crack has initiated in the whole surface of the blank for the taper head punch, while for the curved head punch the crack initiates in $\theta = 0^o$ only.

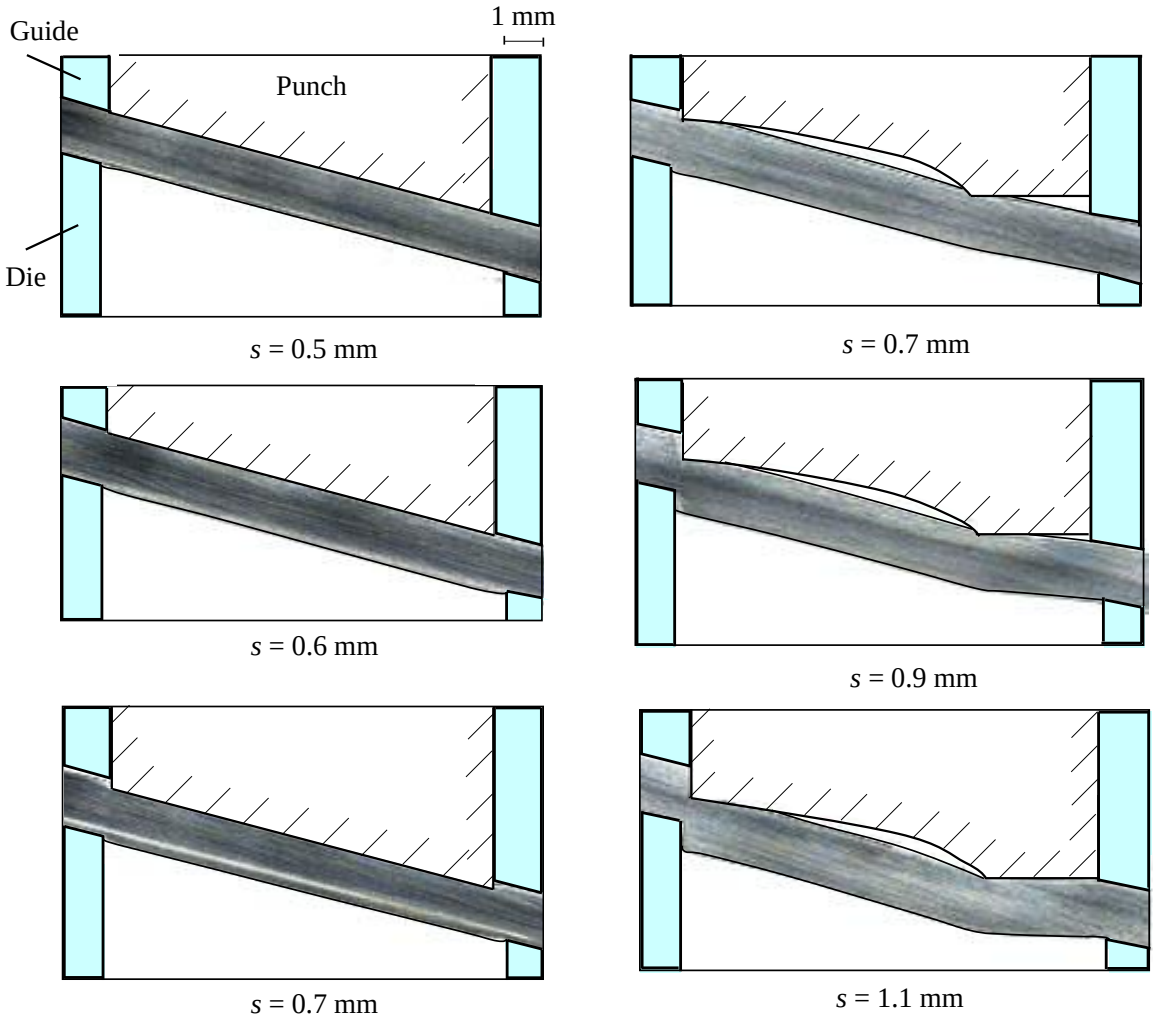

Fig. 6.15. Deformation behavior of blank for $\alpha = 15^{o}$, c = 12%, and (a) taper and (b) curved head punch.

The punching load-stroke curves for the flat head punch, taper head punch and curved head punch for $\alpha = 15^{o}$ and c = 12% are shown in Fig. 6.16. The punching load for the flat head punch has the two small peaks. The load for the taper head punch is the highest since the crack occurs in the blank simultaneously. The punching load for the curved head punch is 30% smaller than that for the taper head punch.

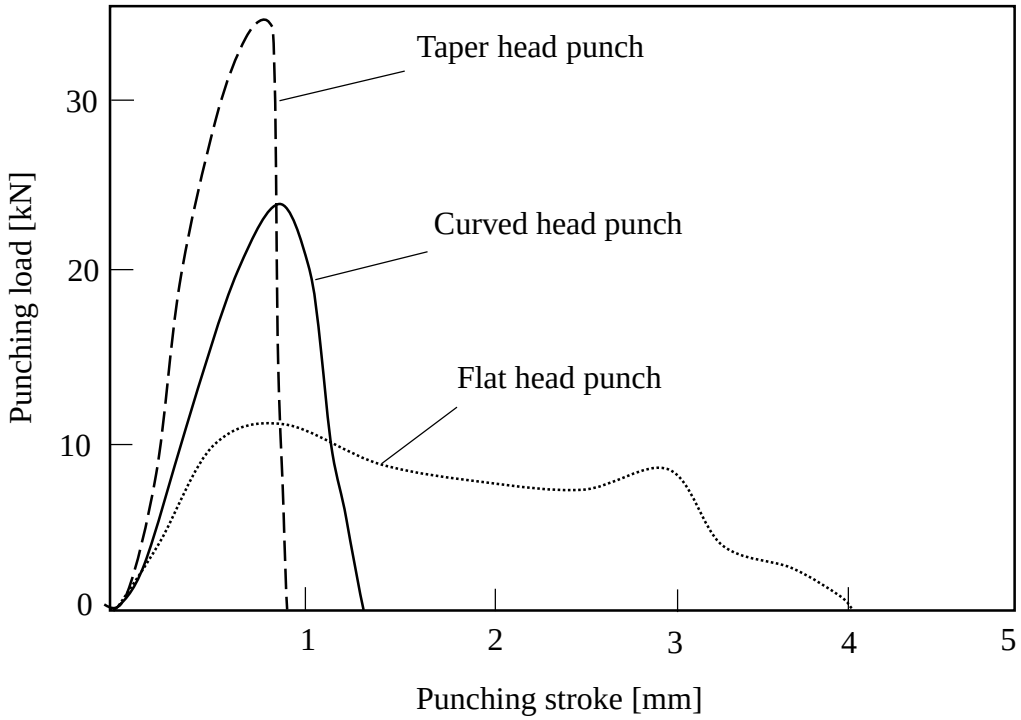

Fig. 6.16. Punching load stroke-curves for flat, taper and curved head punch for α =15^o and c = 12%.

A comparison of the punching load and energy among the punch shapes for α =15^o and c = 12% is shown in Fig 6.17. Although the punching loads for taper and curved head punches are larger than that for the flat head punch, the punching energy is smaller due to shorter punching stroke. The curved head punch has the smallest punching energy among the punches.

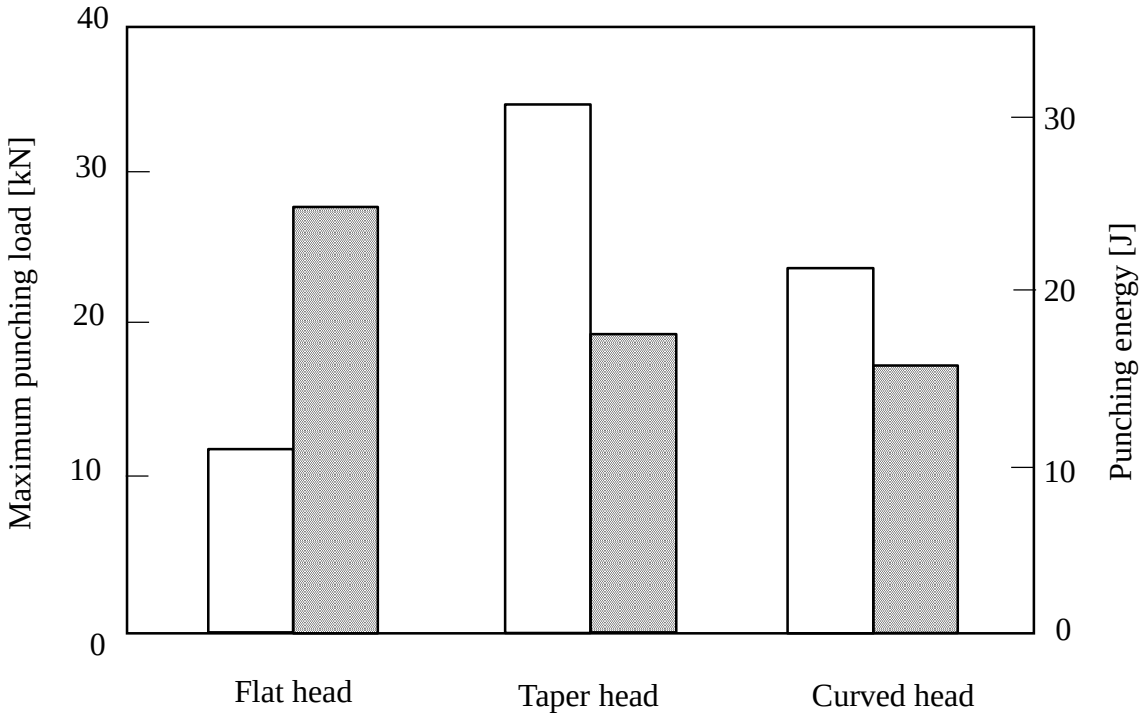

Fig. 6.17. Comparison of punching load and energy among punch shapes for α =15^{o} and c =12%.

The surface and cross-section of the sheared edge for the taper and curved head punch, α =15^{o} and c = 12% are shown in Fig. 6.18. It is found that there are no burr and secondary burnished surface formed in the both sheared edges. For the curved head punch, burnished surface area in θ = 0^{o} is almost twice of the burnished area of the taper head punch. However, in θ = 135 and 180^{o}, the burnished area is smaller than that for the taper head punch.

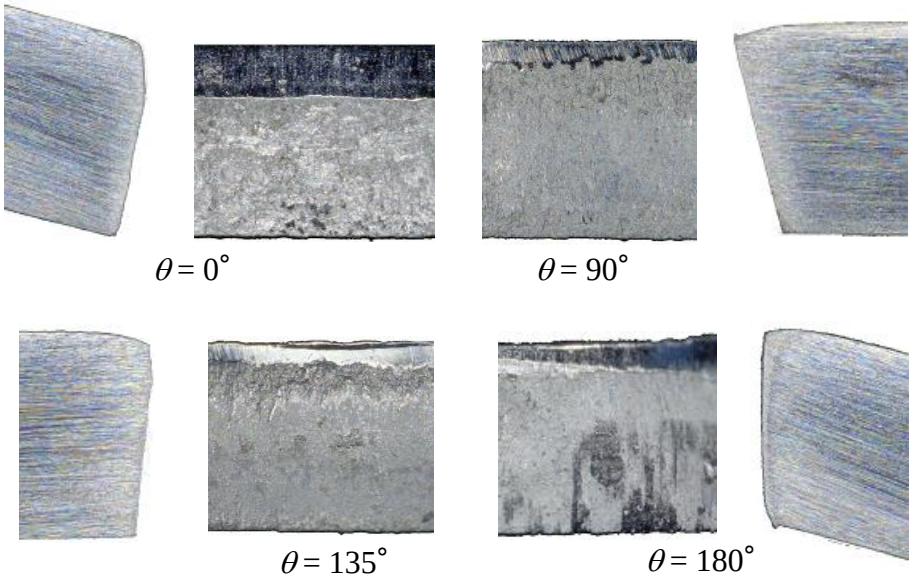

(a) Taper head punch

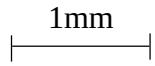

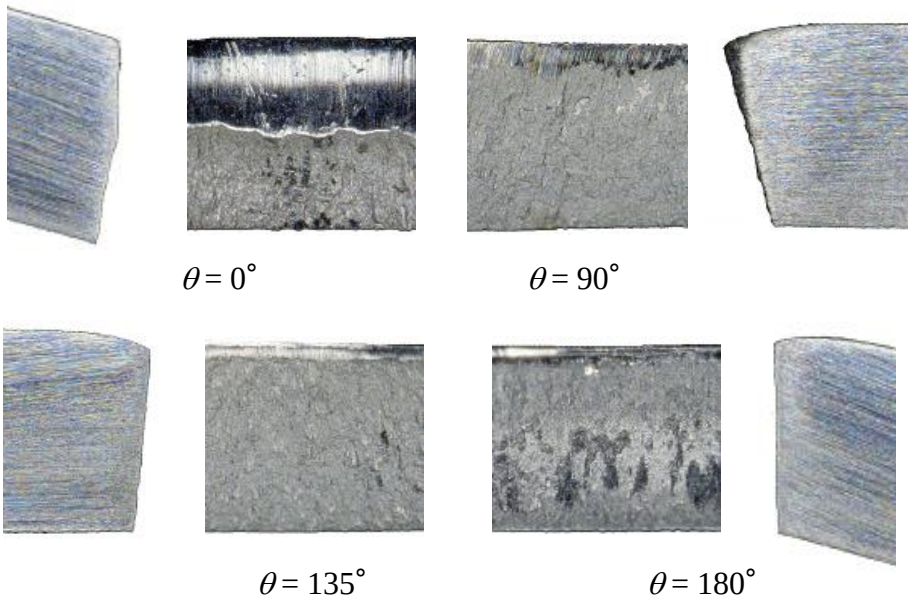

(b) Curved head punch

Fig. 6.18. Surface and cross-section of sheared edge for (a) taper and (b) curved head punch, α = 15^{o} and c = 12%.

The percentage of the depths of rollover, burnished surface, and fracture surface on the sheared edge for the taper and curved head punch, α =15^{o} and c = 12% are shown in Fig.

6.19. The composition of the sheared edge in the hoop direction for the taper head punch is more uniform than that for curved head punch.

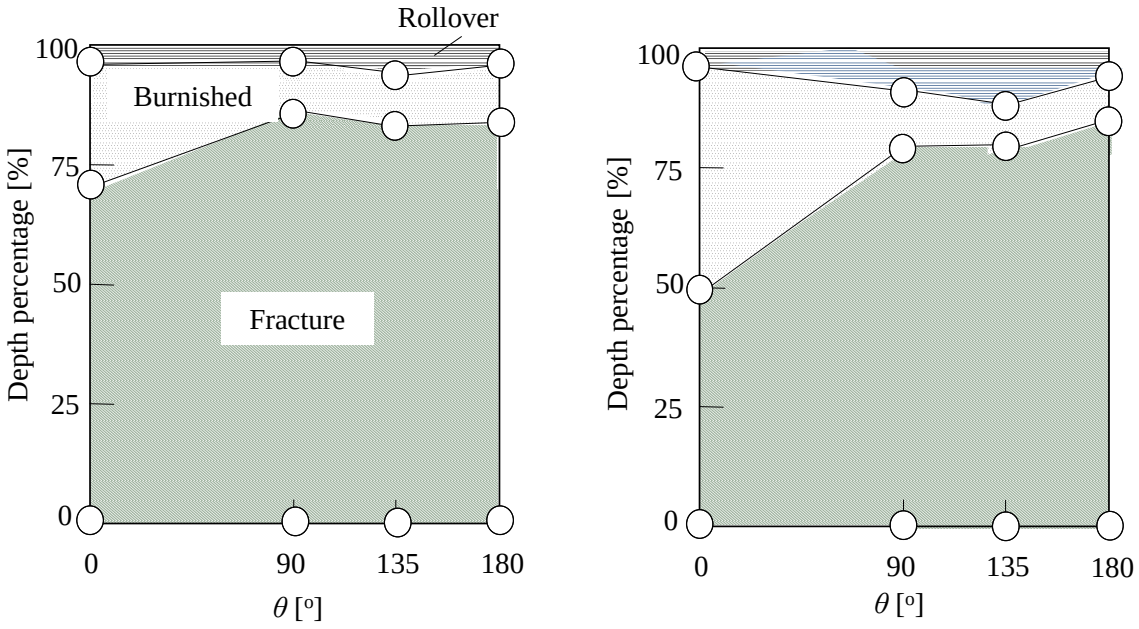

(a) Taper head punch

(b) Curved head punch

Fig. 6.19. Percentage of depths of rollover, burnished surface, and fracture surface on sheared edge for taper and curved head punch, α =15^{o} and c = 12%.

6.5. Conclusions

The effects of the punch head shape and clearance on the quality of the sheared edge in the punching process of inclined ultra-high strength steel sheet were investigated. The results are summarized as follows:

1. The burr and the secondary burnished surface in the punching process of inclined ultra-high strength steel sheet were eliminated by adjusting the punching clearance ratio and the eccentricity of the punch.
2. Applying the taper head punch improved the sheared edge quality, however the punching load increased. The maximum punching load reduced by about 30% by using the curved head punch.
3. The burnished surface in the sheared edge was almost uniform in the hoop direction for the taper head punch.

4. The measured diameter of the punched hole for the punching of inclined ultra-high strength steel sheet was not uniform due to the inclined angle of the blank.

6.6. References

[1] K. Mori, K. Akita, Y. Abe, Springback behaviour in bending of ultra-high-strength steel sheets using CNC servo press, International Journal of Machine Tools & Manufacture 47 (2) (2007) 321–325.

[2] K. Mori, S. Maki, Y. Tanaka, Warm and hot stamping of ultra high tensile strength steel sheets using resistance heating, CIRP Annals – Manufacturing Technology 54 (1) (2005) 209–212.

[3] K. Mori, T. Maeno, Y. Fukui, Spline forming of ultra-high strength gear drum using resistance heating of side wall of cup, CIRP Annals – Manufacturing Technology 60 (1) (2011) 299–302.

[4] K. Inoue, M. Suzuki, S. Nishino, K. Ohya, Y. Tomota, Effect of coating microstructure of press-working dies on sliding damage, Steel Research International 81 (9) (2010) Supplement Metal Forming 2010, 849–852.

[5] J. Eriksson, M. Olsson, Tribological testing of commercial CrN, (Ti,Al)N and CrC/C PVD coatings – Evaluation of galling and wear characteristics against different high strength steels, Surface and Coatings Technology 205 (16) (2011) 4045–4051.

[6] S. Sresomroeng, V. Premanond, P. Kaewtatip, A. Khantachawana, A. Kurosawa, N. Koga, Performance of CrN radical nitrided tools on deep drawing of advanced high strength steel, Surface and Coatings Technology 205 (17–18) (2011) 4198–4204.

[7] K. Mori, Y. Abe, Y. Suzui, Improvement of stretch flangeability of ultra high strength steel sheet by smoothing of sheared edge, Journal of Materials Processing Technology 210 (4) (2010) 653–659.

[8] T. Matsuno, Y. Kuriyama, H. Murakami, S. Yonezawa, H. Kanamaru, Effects of punch shape and clearance on hole expansion ratio and fatigue properties in punching of high strength steel sheets, Steel Research International 81 (9) (2010) Supplement Metal Forming 2010, 853–856.

[9] K. Mori, T. Maeno, S. Fuzisaka, Punching of ultra-high strength steel sheets using local resistance heating of shearing zone, Journal of Materials Processing Technology 212 (2) (2012) 534–540.

[10] K. Mori, T. Maeno, Y. Maruo, Punching of small hole of die-quenched steel sheets using local resistance heating, CIRP Annals – Manufacturing Technology 61 (1) (2012) 255-258.

[11] Y.Abe, S. Nakanoshita, K. Mori, Effects of inclined angle on sheared edge quality in inclined punching of ultra-high strength steel sheet, Proceedings of 2010 Japanese Spring Conference for Technology of Plasticity (2010), 121-122.

Chapter 7
Concluding remarks

7.1. Summary

7.1.1. Thickening of hole edge of punched high strength steel sheets by hole flanging

A hole edge of punched high strength steel sheets was thicken to improve the strengths of the punched sheets. A hole flanging process was performed to thickened one side of the hole edge, and a step die was employed to eliminate a sharp edge in the thickened edge. To thicken the both sides of the hole edge, a two-stage plate forging process was developed. In the 1st stage, the edge of the punched hole was flanged with the upper punch. In the 2nd stage, both sides of the edge of the hole were thickened by forming the flanged edge with the lower punch. The increase in total thickness for both sides and one side thickening of the hole edge was 31% and 42% of the initial sheet thickness, respectively. The fatigue strength for the punched sheet with the thickened hole edge was improved by the thickness increases, the smooth sheared surface and the harder the surface around the hole edge. Both sides thickening of the hole edge was effective in the improvement of fatigue life of punched sheet for tensile fatigue test, while one side thickening for plane bending fatigue test.

7.1.2. Punching including thickening of hole edge of high strength steel sheet

A punching process including thickening of a hole edge of high strength steel sheets was developed to improve fatigue strengths of the punched sheets. Conventionally, a hole flanging operation is performed as a next stage after the punching operation, and thus the number of stages increases. In the developed process, the pair of punch and die was designed so as to have both functions of punching and thickening in one stroke process and easily installed in conventional die sets. The height of burnished surface of the hole edge and the width of the thickened edge for the taper step punches were larger than that for the taper punch. Although the cross-section of the sheared edge for the taper step punch was

almost similar with that for the round step punch, the fatigue strength for the taper step punch was higher than that for the round step punch.

7.1.3. Optimization of tools shape in punching including thickening of hole edge of ultra-high strength steel sheet

The punching process including thickening of a hole edge of an ultra-high strength steel sheet with a taper punch and step die was employed to improve fatigue strength of the punched sheet. The taper angle of the punch and the step height of the die were optimised to increase the amount of thickening. As the step height of the die increases, the fatigue strength increases. The fatigue strength of the punched sheets with thickening was considerably higher than that without thickening due to the large compressive stress, the small surface roughness and the large hardness around the sheared edge. The delayed fracture was prevented by thickening due to the large compressive residual stress and the small surface roughness. Seizure on the surface of the punch was prevented by VC-coating for repeated punching and realistic punching speed.

7.1.4. Punching of ultra-high strength steel sheets by punch having small round edge

A slight clearance punching process of ultra-high strength steel sheets using a punch having a small round edge was developed to improve the quality of the sheared edge. No crack from the edge of the punch was generated by relaxing concentration of deformation with the punch having a small round edge, and the fracture was delayed. A small edge radius of 0.13 mm was effective for improving the quality of the sheared edge of ultra-high strength steel sheets. The delayed fracture was prevented and the fatigue strength was improved by the increase in compressive residual stress for the punch having the small round edge. The TiAlN-coated tungsten carbide punch having the small round edge had high galling resistance for the 1000 stroke punching. In addition, the chipping of the punch edge was prevented even for a slight clearance by the small round edge.

7.1.5. Punching of inclined ultra-high strength steel sheet

A punching process of an inclined ultra-high strength steel sheet using punches having different head shapes was developed to improve the quality of the sheared edge. In the punching of the inclined sheet, the contact between the sheet and punch becomes gradual

because of touch from the bottom edge of the punch, and thus the sheared portion tends to bend in the latter half of punching. To improve the quality of the sheared edge in the punching of inclined ultra-high strength steel sheet, punches having taper and curved head were developed. In these punches, the contact with the sheet was changed, full contact with the taper and contact of both edges with the curved head. In addition, the asymmetric punching clearance ratio was applied to eliminate the burr and the secondary burnished in the sheared edge. It was found that the quality of the sheared edge in the punching process of inclined ultra-high strength steel sheet was improved by adjusting the punching clearance ratio and the eccentricity of the punch.

7.2. Future perspectives

The use of the ultra-high strength steel sheets for automobile parts is increasing, whereas the applicable range is still limited to the fatigue strength. The fatigue strength of the ultra-high strength steel sheets is not increased as much as the static strength. Although microstructure in the ultra-high strength steel sheets is controlled in steel making industry to heighten the fatigue strength, forming of products having high fatigue strength is an alternative approach. The fatigue strength can be increased by relieving concentration of tensile stress during loading, particularly relieving around sheared edges such as the thickening around the hole edge is considerably effective.

Currently, the ultra-high strength steel sheets are not applied to automobile wheels subjected to cyclic loading due to insufficient fatigue strength. Since the thickening around the hole edge is effective to heighten the fatigue strength of the punched ultra-high strength steel sheet, this method could be promising to apply on the forming of wheels made by ultra-high strength steel sheets. However, the surface of the wheels for the punched hole has a curved shape, as shown in Fig. 7.1, thus the projection of the thickened edge is not uniform. The punching process and the shape of the tools should be designed to punch the hole in the inclined or curved surface to apply this punching process to the automobile wheels.

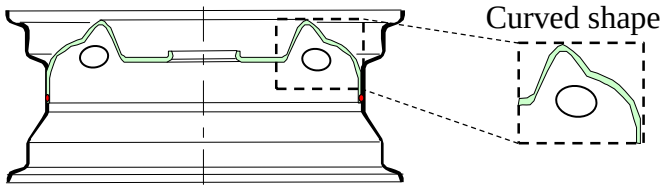

Fig. 7.1. Disk of automobile wheels.

List of Publications

1. **Purwo Kadarno**, Ken-ichiro Mori, Yohei Abe and Tatsuro Abe, Punching process including thickening of hole edge for improvement of fatigue strength of ultra-high strength steel sheet, *Manufacturing Review* 1, 4, pp. 1-12, 2014.

2. Ken-ichiro Mori, Yohei Abe, Yoshinori Kidoma and **Purwo Kadarno,** Slight clearance punching of ultra-high strength steel sheets using punch having small round edge, *International Journal of Machine Tools & Manufacture* 65, pp. 41-46, 2013.

3. 安部 洋平, 中野下 茂広, 森 謙一郎, **Purwo Kadarno**, 傾斜した超高張力鋼板の直接穴抜き加, *Journal of Japan Society for Technology of Plasticity* 54 (627), pp. 348-352, 2013.

4. **Purwo Kadarno**, Ken-ichiro Mori and Yohei Abe, Two stage plate forging for thickening hole edge of punched high strength steel sheet, *Proc. 14th International Conference on Metal Forming*, Krakow, Poland, pp. 899-902, 2012.

5. **Purwo Kadarno**, Ken-ichiro Mori, Yohei Abe and Tatsuro Abe, Flanging using step die for improving fatigue strength of punched high strength steel sheet, *Procedia Engineering* (Accepted).

List of Presentations

1. **Purwo Kadarno,** Yohei Abe, Ken-ichiro Mori, Tatsuro Abe. Effect of thickening of hole edge on fatigue strength of punched ultra-high strength steel sheets. *The 2013 Japanese Spring Conference for the Technology of Plasticity*, Daido University, Nagoya, Japan, 7-9 June 2013.

2. **Purwo Kadarno**, Ken-ichiro Mori, Yohei Abe, Tatsuro Abe. Punching and thickening of hole edge for improvement of strength of punched high strength steel sheets. *The 63rd Japanese Joint Conference for the Technology of Plasticity*, Kitakyushu International Conference Center, Kitakyushu, Japan, 4-6 November 2012.

3. **Purwo Kadarno**, Ken-ichiro Mori, Yohei Abe. Two stage plate forging for thickening hole edge of punched high strength steel sheet. *The 14th International Conference on Metal Forming*, AGH University of Science and Technology, Krakow, Poland, 16-19 September 2012.

4. **Purwo Kadarno,** Yohei Abe, Ken-ichiro Mori, Tatsuro Abe. Thickening of hole edge in punching of high strength steel sheets. *The 2012 Japanese Spring Conference for the Technology of Plasticity*, Komatsu Way Comprehensive Learning Centre, Komatsu, Japan, 7-9 June 2012.

5. **Purwo Kadarno**, Yohei Abe, Tatsuro Abe, Ken-ichiro Mori. Thickening of edge of punched hole of high strength steel sheets by flanging. *The 62nd Japanese Joint Conference for the Technology of Plasticity*, Nikko Hotel, Toyohashi, Japan, 27-29 October 2011.

6. Yohei Abe, **Purwo Kadarno,** Yoshinori Kidoma, Ken-ichiro Mori. Improving quality of sheared edge in punching of ultra-high strength steel sheet by optimizing punch head shape. *IRGTM Summer School 2011: The Environmentally Friendly Press Shop.* Arcadia Hotel, Limburg, Germany, 18-25 September 2011.

7. Yohei Abe, Shigehiro Nakanoshita, Ken-ichiro Mori, **Purwo Kadarno**. Effects of punch shape and clearance on sheared edge quality in inclined punching of ultra-high strength steel sheets. *The 2011 Japanese Spring Conference for the Technology of Plasticity*, Waseda University, Tokyo, Japan, 27-29 May 2011.